AD_____

Award Number: DAMD17-97-1-7204

TITLE: Role of IGFBP-3/IGFBP-3 Receptor Interaction In Normal And Malignant Mammary Growth: A Potential Diagnostic Parameter And A New Strategy for Endocrine Therapy

PRINCIPAL INVESTIGATOR: Youngman Oh, Ph.D.

CONTRACTING ORGANIZATION: Oregon Health Sciences University
Research Administration
Portland, Oregon 97201-3098

REPORT DATE: September 2001

TYPE OF REPORT: Final

PREPARED FOR: U.S. Army Medical Research and Materiel Command
Fort Detrick, Maryland 21702-5012

REPORT DOCUMENTATION PAGE

Form Approved
OMB No. 074-0188

1. AGENCY USE ONLY (Leave blank)	2. REPORT DATE	3. REPORT TYPE AND DATES COVERED
	September 2001	Final (1 Sep 97 - 31 Aug 01)

4. TITLE AND SUBTITLE
Role of IGFBP-3/IGFBP-3 Receptor Interaction In Normal And Malignant Mammary Growth: A Potential Diagnostic Parameter And A New Strategy for Endocrine Therapy

5. FUNDING NUMBERS
DAMD17-97-1-7204

6. AUTHOR(S)
Youngman Oh, Ph.D.

7. PERFORMING ORGANIZATION NAME(S) AND ADDRESS(ES)
Oregon Health Sciences University Research Administration
Portland, Oregon 97201-3098

E-Mail: ohy@ohsu.edu

8. PERFORMING ORGANIZATION REPORT NUMBER

9. SPONSORING / MONITORING AGENCY NAME(S) AND ADDRESS(ES)
U.S. Army Medical Research and Materiel Command
Fort Detrick, Maryland 21702-5012

10. SPONSORING / MONITORING AGENCY REPORT NUMBER

11. SUPPLEMENTARY NOTES

12a. DISTRIBUTION / AVAILABILITY STATEMENT
Approved for Public Release; Distribution Unlimited

12b. DISTRIBUTION CODE

13. ABSTRACT: This report will detail research accomplishments of the investigations of the biological actions of insulin-like growth factor binding protein 3 (IGFBP-3), which has been shown to exhibit activity in an IGF-independent manner. Data indicate that IGFBP-3 alone can bind to breast cancer cell surfaces, and subsequently exert inhibitory effects on cell growth. We have isolated, cloned, expressed, and purified a novel IGFBP-3 receptor, and demonstrated a specific interaction with IGFBP-3 in a human breast cancer cell system. To facilitate more detailed investigation into the interaction and functions of these two proteins, we have generated a polyclonal α4-33 antibody which is specific and functional in a variety of immunoassays. We have also generated IGFBP-3 stably transfected human breast cancer cell lines, in which expression of IGFBP-3 is inducible. Additionally, we have localized the IGFBP-3 receptor binding domain within the mid-region of the IGFBP-3 molecule, residues 88-148. Finally, we have characterized the IGF-independent actions of IGFBP-3 in breast cancer cells, cell cycle arrest in G1/S phase and induction of apoptosis. The potential mechanisms responsible for those effects were elucidated that
The IGFBP-3/IGFBP-3 receptor signaling pathway appears to cross-talk with MAPK signaling cascades, and thereby regulating cell cycle progression. Moreover, the IGFBP-3/IGFBP-3 receptor induces apoptosis through modulation of caspase activity. As completion of the proposed project, we believe that this project provides pivotal evidence for clinical significance and potential application of IGFBP-3 in the prevention and/or treatment of human neoplasia, particularly in conjunction with IGFBP-3 receptor.

14. SUBJECT TERMS
Breast Cancer

15. NUMBER OF PAGES
83

16. PRICE CODE

17. SECURITY CLASSIFICATION OF REPORT	18. SECURITY CLASSIFICATION OF THIS PAGE	19. SECURITY CLASSIFICATION OF ABSTRACT	20. LIMITATION OF ABSTRACT
Unclassified	Unclassified	Unclassified	Unlimited

Table of Contents

I. INTRODUCTION

The insulin-like growth factor binding proteins (IGFBPs) 1-6 bind IGF-I and IGF-II with high affinity and serve to transport the IGFs, prolong their half-lives, and modulate their proliferative and anabolic effects on target cells (1-9). The molecular mechanisms involved in the interaction of the IGFBPs with the IGFs and their receptors remain unclear, but these molecules appear, at least, to regulate the availability of free IGFs for interaction with IGF receptors (11-12). Recent studies from our laboratory and others demonstrated that some IGFBPs have ability to exert IGF-independent actions (13-17).

In this project, I proposed investigation of **the characterization of the IGFBP-3-specific receptor, the elucidation of the pertinent signal transduction pathways** and analysis of **structure-function relationships in the IGFBP-3** in the context of growth control in human breast cancer.

II. BODY

I. characterization of the IGFBP-3 receptor in human breast cancer cells (Tasks 1-7).

The proposal of my grant is to investigate the biological significance and mechanism of IGFBP-3 as well as identification and characterization of the IGFBP-3 receptor in human breast cancer cells. We have initially proposed to employ expression cloning by use of λ expression libraties for identification of IGFBP-3 receptor. The expression library, consisting of Hs578T-derived cDNAs cloned into the λgt11 expression vector, was generated and the resultants were screened by use of [^{125}I]IGFBP-3 or polyclonal IGFBP-3 receptor antibodies. However, We have faced technical difficulties during the experiments due to the nature of IGFBP-3 protein, showing that this protein binds to proteins in a non-specific manner. As an alternative approach, yeast two-hybrid screening was employed to identify IGFBP-3 interacting proteins. As a first year task, I initiated to identify IGFBP-3 receptor in human breast cancer cells by employing an yeast two-hybrid system. To date this approach has been successfully proceeded using total Hs578T breast cancer cell mRNA for cDNA library and cDNA encoding IGFBP-3 fragment (IGFBP-3$^{88-148}$) for a bait . We have successfully screened the IGFBP-3 interacting proteins including putative IGFBP-3 receptor in human breast cancer cells by employing the yeast two-hybrid system. One of the cDNAs, designated clone 4-33 represents a novel gene / protein. During the third year peroid, we have synthesized recombinant human 4-33 protein by use of a Glutathione S-Transferase fusion and generated polyclonal 4-33 antibodies. We characterized the specificity of the antibodies by showing immunoprecipitation of clone 4-33 protein with the antibodies. On an immunoblot of cell lysates from normal and cancerous human breast and prostate cell lines, the clone 4-33 antisera recognizes a species which migrates at roughly 32

kilodaltons. We have also demonstrated specificity of the clone 4-33 antisera in immunocytochemical staining of transiently transfected human breast cancer cell lines. Furthermore, in collaboration with Dr C. Corless, who is an associate professor of Pathology, we have successfully characterized our polyclonal anti-IGFBP-3 and IGFBP-3 receptor antibodies. As indicated in the Figure, the IGFBP-3 receptor was detected in ductal invasive carcinoma cells but not in stromal fibroblasts and fat bodies using IgG purified polyclonal IGFBP-3R antibody. No detectable staining was observed with IgG-purified preimmune serum. Furthermore, we have detected IGFBP-3R protein from in a variety of frozen-fresh tumor tissue samples by Western immunoblot.

Immunohistochemistry of IGFBP-3 Receptor in Human Breast Tumor (TB1980)

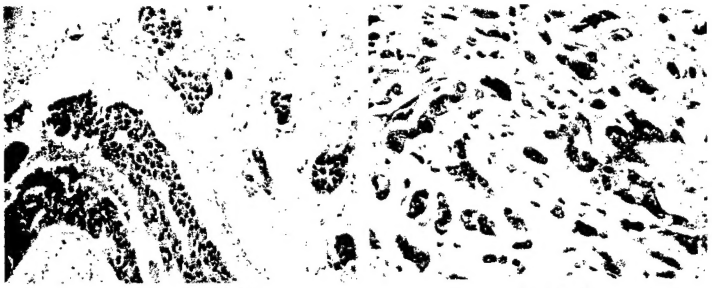

(x200) (x400)

Western innunoblot of IGFBP-3R in Breast Tumor Samples

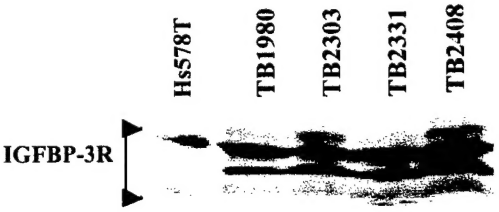

In our continuing investigation of the biological importance of IGFBP-3, we have characterized specificity of the IGFBP-3 receptor binding to IGFBP-3 and involvement of the IGFBP-3 receptor on the IGFBP-3-induced growth inhibition.

As IGFBP-3 has been previously reported to specifically bind to the surface of breast cancer cells and subsequently exhibit growth suppressing activity, I further determined whether the IGFBP-3 receptor might participate in this process. Hs578T and MCF-7 human breast cancer cells were transiently transfected with a construct encoding IGFBP-3 receptor FLAG-tagged at the C-terminus ($4\text{-}33^F$) or with vector alone. These cells were then subjected to a monolayer binding assay using ^{125}I-labelled IGFBP-3. The overexpression of 4-33 resulted in a 30-60% increase in IGFBP-3 binding to the cell surface relative to cells expressing endogenous levels of 4-33 (see Appendix 1). This result was greatly magnified when the same assay was done using Sf9 insect cells either uninfected or infected with virus harboring the $4\text{-}33^F$ cDNA, as the infected cells overexpress $4\text{-}33^F$ to a much greater degree compared to control cells. In these cells the increase in IGFBP-3 cell surface binding was nearly 3.5 fold over control. The increased IGFBP-3 binding was competed in a dose-dependent manner with the addition of cold IGFBP-3, and was unaffected by the presence of the FLAG-tag at the C-terminus of the 4-33 protein. Further, fragments of IGFBP-3 containing the putative binding region for 4-33 (amino acids 88-148) were able to successfully compete labelled full-length IGFBP-3 binding, but an N-

terminal fragment comprised of amino acids 1-97 was not. Additionally, other IGF binding proteins were unable to compete IGFBP-3 binding in this assay, demonstrating IGFBP-3 specificity.

The IGFBP-3 receptor involvement in IGFBP-3 biological function: cell cycle arrest and apoptosis.

To facilitate the study of the biological actions of 4-33 and IGFBP-3, we have generated a stably-transfected inducible IGFBP-3 MCF-7 breast cancer cell line using the ecdysone-inducible system (see Appendix 2). One of the sublines, designated MCF-7:BP-3 #3 (colony #3), inducibly produced IGFBP-3 at levels comparable to the endogenous levels produced by Hs578T cells. The induction of IGFBP-3 in these cells caused inhibition of growth and DNA synthesis as measured by incorporation of [^{3}H]thymidine, to a similar degree as has been described for treatment of MCF-7 cells with exogenous IGFBP-3. Induced expression of IGFBP-3 in these cells further leads to cell cycle arrest at G_1. We observed an increase in the percentage of cell in G_1 from 72.1% to 78.1%, with a concurrent decrease in cells in S and G2/M phases (see Appendix 2). Further, our data indicate that IGFBP-3 induces apoptosis in this cell system.

Studies of 4-33 in breast cancer cells which produce IGFBP-3 demonstrated that transient overexpression of 4-33 resulted in a significant increase in cell detachment / death over time, compared to little or no effect in cells which do not produce IGFBP-3. IGFBP-3-expressing Hs578T cells displayed fewer cells per field following transient overexpression of 4-33 compared to transfection with vector alone, while no such effect was seen in IGFBP-3-nonexpressing MCF-7 cells. We further investigated the effect of 4-33 and IGFBP-3 on cell proliferation as indicated by incorporation of [^{3}H]thymidine during DNA synthesis. We compared wild type MCF-7 cells with the MCF-7:BP-3 #3 subline, with and without incubation with ponasterone A. As expected, induction of IGFBP-3 by ponasterone A resulted in an inhibition of DNA synthesis to an average of 55% of control levels (see Appendix 2). With the additional overexpression of 4-33 in these cells, DNA synthesis was further inhibited down to an average of 35% of control levels (see Appendix 1). Overexpression of 4-33 had no significant effect on DNA synthesis in the absence of IGFBP-3 (either wild type MCF-7 or uninduced MCF-7:BP-3 #3 cells), and ponasterone A had no inhibitory effect in wild type MCF-7 cells.

Taken together, we have successfully executed the proposed tasks for identification and characterization of the IGFBP-3 receptor in human breast cancer cells.

2. Identification of the IGFBP-3/IGFBP-3 receptor-induced signal tansduction pathway (Tasks 8 and 9)

Induction of IGFBP-3 in inducible IGFBP-3 stably transfected human breast cancer cells showed dose-dependent inhibition of DNA synthesis as assessed by [^{3}H]-thymidine incorporation assays. This inhibitory effect was abolished by co-treatment with Y60L-IGF-I, an IGF analog which has significantly reduced affinity for the IGF receptor but retains high affinity for IGFBP-3, demonstrating specificity and IGF-independence. In addition, flow cytometry analysis showed that induced expression of IGFBP-3 led to an arrest of the cell cycle in G1-S phase. Induction of IGFBP-3 resulted in a significant decrease in the mRNA and protein levels of cyclin D, but not cyclin E, as well as concomitant decreases in the levels of cdk4, total-Rb, and phosphorylated-Rb, consistent with and presenting a possible mechanism for IGFBP-3-induced cell cycle arrest. Moreover, IGFBP-3 inhibited oncogenic Ras-induced phosphorylation of MAPKs, presenting the evidence for cross-talk of IGFBP-3 signaling with MAPK signal transduction pathway. IGFBP-3-expressing cells also displayed increased Annexin V binding compared to controls, exhibiting the IGFBP-3-induced apoptosis. Further studies demonstrated that IGFBP-3 caused an increase in caspase activities, suggesting a potential mechanism for the IGFBP-3-induced apoptosis. Taken together, present study shows that cellular production of IGFBP-3 leads to cell cycle arrest and induction of apoptosis, thereby inhibiting cell proliferation in these MCF-7 human breast cancer cells and suggesting that IGFBP-3 functions as a negative regulator of breast cancer cell growth, independent of the IGF axis.

Cell cycle arrest. We examined the effect of the IGFBP-3 receptor on these specific proteins known to be involved in cell cycle progression and the apoptotic process (see Appendix 2). Hs578T and MCF-7 cells, and the IGFBP-3-constitutively expressing MCF-7:BP-3 #1 cell line were either left untreated, treated with an apoptosis inducer (sodium butyrate, NaB), or transfected with vector alone or the IGFBP-3 receptor. At 24 hours post-transfection cell lysates were harvested, assayed for protein content, and equal amounts of protein per sample were immunoblotted. Examination of cell cycle proteins cyclin D1, cyclin E, and p21/Waf1 revealed a specific decrease in the level of cyclin D1 protein in the IGFBP-3 receptor-transfected cells in the presence of IGFBP-3. Control transfected cells, and the IGFBP-3 receptor-transfected cells in the absence of IGFBP-3 had no effect on cyclin D1 levels. Cyclin E and p21/Waf1 were unaffected by these treatments, while proper induction of p21/Waf1 was seen with NaB treatment. Additionally, when the IGFBP-3 receptor-transfected cells were examined by immunofluorescence with antibodies against Cyclin D1, Rb and the IGFBP-3 receptor, a significant reduction in both Cyclin D1 and Rb immunodetectable protein levels occurred in 4-33-transfected cells, but not in neighboring untransfected cells. A possible mechanism for this

effect may be perturbation of p44/42 mitogen-activated protein kinase (MAPK) signaling pathways. Our data indicate that levels of phosphorylated MAPK, Cyclin D1, and phosphorylated retinoblastoma (Rb) proteins are significantly reduced upon induction of IGFBP-3 expression in MCF-7:BP-3 #3 cells (see Appendix 2).

Apoptosis: We further investigated whether the IGFBP-3 receptor plays a role in IGFBP-3-induced apoptosis. Hs578T, MCF-7, and induced MCF-7:BP-3 #3 cells were either untreated or transfected with vector or 4-33 and the cell cycle profile was analyzed by propidium iodide staining of DNA content followed by flow cytometry detection (see Appendix 1). In each case, the IGFBP-3 receptor-transfected cells displayed an increase in the sub-G1 population and a concurrent decrease in the S/G2/M population compared to control cells. A peak in the sub-G1 range can be indicative of cells undergoing apoptosis. We investigated this further using an Annexin V assay, which is used to identify cells early in the apoptotic process. By incubating suspended cells with FITC-labelled Annexin V, coupled with concurrent propidium iodide staining without permeabilization of the plasma membrane, it is possible to discriminate between cells in early apoptosis and those in late apoptosis or necrosis using a two-color flow cytometric analysis. Hs578T cells were transfected with vector alone or the IGFBP-3 receptor, and subsequently harvested and assayed at 14, 24, 36, and 48 hours post-transfection. At each time point, the population of early apoptotic cells was significantly increased in the cells transfected with the IGFBP-3 receptor, compared to control-transfected cells.

As IGFBP-3 has been shown to potentiate caspase activity, we examined this phenomenon as a potential mechanism for IGFBP-3/IGFBP-3 receptor biological funtion. Caspases are a family of evolutionarily related cysteine-dependent proteases, with an universal specificity for Asp in the P_1 position, that play a prominent role during the progression of apoptosis. Activation of caspases and subsequent cleavage of critical cellular substrates are implicated in many of the morphological and biochemical changes associated with apoptotic cell death. Using an assay which detects activity of a broad range of caspases by incubating cell lysates with a mixture of purified fluorogenic peptide caspase substrates and measuring subsequent reaction kinetics, we demonstrated a measurable and reproducible increase in caspase activity (described as pmol substrate cleaved / min / mg protein) in Hs578T cells with transient overexpression of 4-33 compared to control-transfected cells (see Appendix 1).

Taken together, our data demonstrate that 4-33 is a functional IGFBP-3 receptor and required for the IGFBP-3-induced cell cycle arrest and apoptosis. The potential mechanisms appear to be both a cross-talk between the IGFBP-3/IGFBP-3 receptor axis and MAPK signaling pathway and induction of caspase activity.

3. Characterization of structure-function aspects of IGFBP-3 action in human breast cancer. (Tasks 10-13)

Previous studies have demonstrated that the effect of IGFBP-3 on IGF-induced mitogenic action can be modulated by IGFBP-3 proteases. It has been demonstrated that IGFBP-3 proteases appear to enhance mitogenic action of IGFs; proteolysis of IGFBP-3 results in significantly reduced affinity for IGF peptides, thereby facilitating IGF binding to its receptors. Several proteases have been identified in human breast cancer and normal mammary epithelial cells (18-23); some proteases, such as cathepsin D, prostate specific antigen (PSA) have been proposed as prognosis factors because of enhanced expression in breast cancer cells. Interestingly, these proteases, including plasmin (plasminogen activator), are capable of proteolyzing IGFBP-3 molecule. Therefore, it can be speculated that these proteases can modulate not only the IGFBP-3 effect on IGF binding to IGF receptors, but also IGFBP-3 binding to the IGFBP-3 receptor and its subsequent biological action. We have generated proteolytic fragments derived from plasmin-digested recombinant human IGFBP-3, synthetic fragments generated using the baculovirus expression system, and IGFBP-3 fragments in normal human urine (see Appendix 3). With each of these reagents we demonstrated retention of IGF binding of an N-terminal IGFBP-3 fragment, albeit with significantly reduced affinity as compared to the intact molecule. In addition, we demonstrated that these N-terminal fragments can bind specifically to insulin, and inhibit insulin receptor autophosphorylation (see Appendix 4). As further investigation, we identified differential effects of IGFBP-3 and those IGFBP-3 proteolytic fragments on ligand binding, cell surface association and IGF-I receptor signaling (see Appendix 5). We demonstrated that IGFBP-3 showed a dose-dependent inhibition of autophosphorylation of the beta-subunit of IGF-I receptor (IGFIR). The (1-97)NH2-terminal fragment inhibited IGFIR autophosphorylation at high concentrations and this effect appears largely due to sequestration of IGF-I. In contrast, no inhibition of IGF-I induced IGFIR autophosphorylation was detectable with the (98-264) and (184-264)COOH-terminal fragments, despite their ability to bind IGF. However, unlike the (1-97)NH2-terminal fragment, the COOH-terminal fragments of IGFBP-3 retained their ability to associate with the cell surface and this binding was competed by heparin, similar to intact IGFBP-3 (Appendix #5). In addition, we are in the progress to synthesize IGFBP-3 mutants which show no binding affinity to IGFs, but retain full affinity for the IGFBP-3 receptor.

Taken together, those IGFBP-3 fragments as well as a (88-149) mid-region fragment will provide more detailed information about how IGFBP-3 interacts with the IGFBP-3 receptor and how the IGFBP-3/IGFBP-3 receptor complex transmits its signaling to exert biological actions.

Our proposed project supports the hypothesis that 4-33 is a functional receptor for IGFBP-3 in the breast cancer system, and that the interaction of IGFBP-3 with 4-33 may be an important mechanism in the IGF-independent, growth-inhibitory actions of IGFBP-3. These studies firstly demonstrated the underlying mechanism for the IGF/IGFBP-3 receptor-induced biological function; the IGFBP-3/IGFBP-3 receptor axis arrests cell cycle progression through ablation of the MAPK signaling cascades, and induces apoptosis via potentiating caspase activities. Current findings under this grant support will provide pivotal evidence for clinical significance and potential application of the IGFBP-3/IGFBP-3 receptor axis in the prevention and/or treatment of human neoplasia, in particular, breast cancer.

III. KEY RESEARCH ACCOMPLISHMENTS

- Identification of a new gene product 4-33 as a functional IGFBP-3 receptor.
- Demonstration of the binding specificity of the IGFBP-3 receptor (4-33) to IGFBP-3 and other binding proteins.
- Characterization of the IGFBP-3-induced biological function in human breast cancer ells.
- Identification of the potential mechanisms for the IGFBP-3/IGFBP-3 receptor-mediated cell cycle arrest and induction of apoptosis.
- Characterization of IGFBP-3 proteolytic fragments on ligand binding, cell surface association and IGF-I receptor signaling.

IV. REPORTABLE OUTCOMES

- Vorwerk, P, et al., 1997. J. Clinic. Endocrinol. Metab., 82:2368-2370.
- U.S. Patent Application OHSU Serial # 490 (2000) Induction of Apoptosis and Cell Growth Inhibition by Protein 4-33.
- Oh, Y. 1998. Breast Cancer Research and Treatment, 47:283-293.
- Vorwerk, P, *et al.*, 1998. J. Clinic. Endocrinol. Metab., 83:1392-1395.
- Yamanaka, Y, *et al.*, 1999. Endocrinology, 140:1319-1328.
- Devi, GR, *et al.*, 2000. Endocrinology, 2000, 141:4171-4180.
- How, HK, *et al.*, 2001. Cancer Research, in submission.
- Kim, H-S, *et al.*, 2001. J. Biol. Chem, in preparation.
- Ingermann, AR and Oh, Y. 2001. Nature, Medicine. in preparation.
- Ingermann, AR and Oh, Y. 2000. 4th International Workhsop on IGF Binding Proteins, Sydney, Australia.
- Kim, H-S and Oh, Y. 2000. 4th International Workhsop on IGF Binding Proteins, Sydney, Australia.

V. CONCLUSIONS

We have successfully executed our third year tasks (DAMD17-97-1-7204) outlined in the Statement of Work. As mentioned in previous statements, we had difficulites to employ expression cloning techniques for identification of an IGFBP-3 receptor due to the nature of the IGFBP-3 protein, specifically its ability to bind proteins in a non-specific manner under these experimental conditions. As an alternative approach, yeast two-hybrid screening was employed to identify IGFBP-3 interacting proteins. Nevertheless, we have successfully screened the IGFBP-3 interacting proteins including putative IGFBP-3 receptor in human breast cancer cells by employing the yeast two-hybrid system. Two cDNA clones matched sequences in the GenBank database: (1) Eps8 - epidermal growth factor receptor kinase substrate, and (2) GRP78 / BiP - glucose regulated stress protein, or human immunoglobulin heavy chain binding protein. The third cDNA, designated clone 4-33, was not identified in the database and represents a novel gene / protein. Further investigation has proved that 4-33 protein is a functional IGFBP-3 receptor. Firstly, we characterized binding specificity of the IGFBP-3 receptor to IGFBP-3; Only IGFBP-3 and its fragment (aa88-148) bind the IGFBP-3 receptor with high affinity, whereas IGFBPs, -2, 4-, -5 and —6 did not interact with the IGFBP-3 receptor, demonstrating specificity of the IGFBP-3 receptor. We have also identified the IGFBP-3/IGFBP-3 receptor-mediated signal transduction pathway in human breast cancer cells. Further studies demonstrated that the IGFBP-3/IGFBP-3 receptor axis causes cell cycle arrest in G1 phase and induces apoptosis. The underlying mechanisms are ablation of MAPK signaling cascades and increase of caspase activity, respectively. As characterization of the structure-functional analysis of IGFBP-3 and the IGFBP-3 receptor, we demonstrated that these N-terminal fragments can bind specifically to insulin, and inhibit insulin receptor autophosphorylation. As further investigation, we identified differential effects of IGFBP-3 and those IGFBP-3 proteolytic fragments on ligand binding, cell surface association and IGF-I receptor signaling. Taken together, our findings under this grant support will provide pivotal evidence for clinical significance and potential application of the IGFBP-3/IGFBP-3 receptor axis in the prevention and/or treatment of human neoplasia, in particular, breast cancer.

IV. REFERENCES

1. Salmon WD, Daughaday WH: A hormonally controlled serum factor which stimulates sulfate incorporation by cartilage in vitro. J Laboratory Clinical Medicine 49:825-836, 1957.
2. Daughaday WH, Hall K, Raben MS, Salmon WD, Van den Brande JLV, and Van Wyk JJ: Somatomedin: Proposed designation for sulphation factor. Nature 235:107, 1972.
3. Daughaday WH, Rotwein P: Insulin-like growth factors I and II peptide messenger ribonucleic acid and gene structures serum and tissue concentrations. Endocrine Rev 10:68-91, 1989.
4. Rosenfeld RG, Lamson GL, Pham H, Oh Y, Conover C, DeLeon DD, Donovan SM, Ocrant I, Giudice LC: Insulin-like growth factor-binding proteins. Recent Progress in Hormone Res 46:99-159, 1991.
5. Baxter RC, Martin JL: Binding proteins for the insulin-like growth factors: structure, regulation and function. Progress Growth Factor Res 1:49-68, 1989.
6. Jones JL, Clemmons DR: Insulin-like growth factors and their binding proteins: biological actions. Endocrine Rev 16:3-34. 1995.
7. Oh Y, Muller HL, Neely EK, Lamson G, Rosenfeld RG: New concepts in insulin-like growth factor receptor physiology. Growth Regul 3:113-123, 1993.
8. Werner H, Woloschak M, Stannard B, Shen-Orr Z, Roberts CT Jr., LeRoith D: The insulin-like growth factor receptor: molecular biology heterogeneity and regulation. In: LeRoith (eds.) Insulin-like growth factors: Molecular and Cellular Aspects CRC Press Boca Rawton, 1991, pp. 17-47.
9. Lowe L: Biological actions of the insulin-like growth factors. In: LeRoith (eds.) Insulin-like growth factors: CRC Press Boca Rawton ,1991, pp. 49-85.
10. Kelley KM, Oh Y, Gargosky SE, Gucev Z, Matsumoto T, Hwa V, Ng L, Simpson D, Rosenfeld RG: Insulin-like growth factor-binding proteins (IGFBPs) and their regulatory dynamics. Int J Biochem Cell Biol 28:619-637, 1995.

11. Jones JI, Clemmons DR: Insulin-like growth factors and their binding proteins: biological actions. Endocrine Review 16:3-34, 1995.
12. Liu L, Delbe J, Blat C, Zapf J, Harel L. (1992) Insulin-like growth factor binding protein (IGFBP-3), an inhibitor of serum growth factors other than IGF-I and II. J Cell Physiol. 153: 15-21.
13. Oh Y, Muller HL, Lamson G, Rosenfeld RG. (1993) Insulin-like growth factor (IGF) independent action of IGF-binding protein-3 in Hs578 human breast cancer cells. J Biol Chem. 268: 14964-14971.
14, Cohen P, Lamson G, Okajima T, Rosenfeld RG. (1993) Transfection of the human insulin-like growth factor-binding protein-3 gene into Balb/c fibroblasts inhibits cellular growth. Mol Endocrinol. 7: 380-386.
14. Oh Y, Muller HL, Pham HM, Rosenfeld RG. (1993) Demonstration of receptors for insulin-like binding protein-3 on Hs578T human breast cancer cells. J Biol Chem. 268: 26045-26048.
15. Oh Y, Muller HL, Ng HM, Rosenfeld RG. (1995) Transforming growth factor-β induced cell growth inhibition in human breast cancer cells is mediated through IGFBP-3 action. J Biol Chem. 270: 13589-13592.
16. Gucev ZS, Oh Y, Kelley KM, Rosenfeld RG. (1995) Insulin-like growth factor binding protein 3 mediates retinoic acid- and transforming growth factor β2-induced growth inhibition in human breast cancer cells. Cancer Res. 56: 1545-1550.
17. Valentinis B, Bhala A, De Angelis T, Baserga R, Cohen P. (1995) The human insulin-like growth factor (IGF) binding protein-3 inhibits cell growth of fibroblasts with a target disruption of the IGF-I receptor gene. Mol Endocrinol. 9: 361-367.
18. Buckbinder L, Talbott R, Velasco-Miguel S, Takenata I, Faha B, Seizinger BR, Kley N. (1995) Induction of the growth inhibitor IGF-binding protein 3 by p53. Nature. 377: 646-649. Cohen P, Graves HCB, Peehl DM, Kamarei M, Giudice LC, Rosenfeld RG. (1992) Prostate-specific antigen (PSA) is an insulin-like growth factor binding protein-3 protease found in seminal plasma. J Clin Endocrinol Metab. 75: 1046-1053.
19. Campbell PG, Novak JF, Yanosick TB, McMaster JH. (1992) Involvement of the plasmin system in dissociation of the insulin-like growth factor binding-protein complex. Endocrinology. 130: 1401-1412.
20. Conover CA, Kiefer MC, Zapf J. (1993) Posttranslational regulation of insulin-like growth factor-binding protein-4 in normal and transformed human fibroblasts. J Clin Invest. 91: 1129-1137.

21. Cheung PT, Wu J, Banach W, Chernausek SD. (1994) Glucocorticoid regulation of an insulin-like growth factor-binding protein-4 protease produced by a rat neuronal cell line. Endocrinology. 135: 1328-1335.
22. Fowlkes JL, Enghild JJ, Suzuki K, Nagase H. (1994) Matrix metalloproteinases degrade the insulin-like growth factor binding protein-3 in dermal fibroblast cultures. J Biol Chem. 269: 25742-25746.
23. Conover CA, De Leon DD. (1994) Acid-activated insulin-like growth factor-binding protein-3 proteolysis in normal and transformed cells. Role of cathepsin D. J Biol Chem. 269: 7076-7080.

VI. APPENDICES

1. Ingermann AR, Kim, H-S, Oh, Y. Identification of a functional receptor for IGFBP-3. Nature, Medicine, 2001, in preparation.

2. Kim, H-S, Ingermann AR, Tsubaki, J, Twigg, SM, Oh Y. Cellular expression of insulin-like growth factor binding protein-3 arrests the cell cycle and induces apoptosis in MCF-7 human breast cancer cells. J. Biol. Chem., 2001, in preparation.

3. Vorwerk, P, Yamanaka, Y, Spagnoli, A, Oh, Y, Rosenfeld, RG. Insulin and IGF binding by IGFBP-3 fragments derived from proteolysis, baculovirus expression and normal human urine. J. Clin. Endocrinol. Metab., 1998, 83:1392-1395.

4. Yamanaka, Y, Wilson, EM, Rosenfeld, RG, Oh, Y. Inhibition of insulin receptor activation by insulin-like growth factor binding proteins. J. Biol. Chem., 1997, 272:30729-30734.

5. Devi, GR, Yang, D-H, Rosenfeld, RG, Oh Y. Differential effects of insulin-like growth factor (IGF)-binding protein-3 and its proteolytic fragments on ligand binding, cell surface association, and IGF-I receptor signaling. Endocrinology, 2000, 141:4171-4180.

VII. BIBLIOGRAPHY OF PUBLICATIONS AND ABSTRACTS

1. Vorwerk, P, Oh, Y, Lee, PDK, Khare, A, Rosenfeld, RG. Synthesis of IGFBP-3 fragments in a baculovirus system and characterization of monoclonal anti-IGFBP-3 antibodies. J. Clin. Endocrinol. Metab., 1997, 82:2368-2370.

2. Yamanaka, Y, Wilson, EM, Rosenfeld, RG, Oh, Y. Inhibition of insulin receptor activation by insulin-like growth factor binding proteins. J. Biol. Chem., 1997, 272:30729-30734.

3. Oh, Y. IGF-independent regulation of breast cancer growth by IGF binding proteins. Breast Cancer Res Treat 1998, 47:283-293.

4. Vorwerk, P, Yamanaka, Y, Apagnoli, A, Oh, Y, Rosenfeld, RG. Insulin and IGF binding by IGFBP-3 fragments derived from proteolysis, baculovirus expression and normal human urine. J. Clin. Endocrinol. Metab., 1998, 83:1392-1395.

6. Yamanaka, Y, Fowlkes, JL, Rosenfeld, RG, Oh, Y. Characterization of insulin-like growth factor binding protein-3 (IGFBP-3) binding to human breast cancer cells. Endocrinology, 1999, 140:1319-1328.

7. Devi, GR, Yang, D-H, Rosenfeld, RG, Oh, Y. Differential effects of IGFBP-3 and its proteolytic fragments on ligand binding, cell surface association and IGFIR signaling. Endocrinology, 2000, 141:4171-4180.

8. Kim, H-S, Ingermann, AR, Tsubaki, J, Twigg, SM, Oh, Y. Cellular expression of insulin-like growth factor binding protein-3 arrests the cell cycle and induces apoptosis in MCF-7 human breast cancer cells. 4th International Workshop on IGF Binding Proteins, Oct. 2000, Terrigal, Australia.

9. Ingermann, AR, Kim, H-S, Oh, Y. Identification of a functional receptor for IGFBP-3. 4th International Workshop on IGF Binding Proteins, Oct. 2000, Terrigal, Australia.

10. Werner H; **Oh Y**; Roberts CT Jr. Apoptosis in breast cancer. In Programmed Cell Death Volume II: Role in Disease, Pathogenesis and Prevention Mattson MP, Estus S,

Rangnekar V, eds, Advances in Cell Aging and Gerontology Elsevier Science, Netherlands, 2001, vol. 6:1-22.

11. How, HK, Yeoh, A, Quah, TC, Oh, Y, Rosenfeld, RG, Lee, K-O. Absence of IGFBP-3 mRNA and protein in childhood acute lymphoblastic leukemia marrow and reapprearance in remissionmarrow: A new potential marker. Cancer Research, 2001, in submission.

12. Kim, H-S, Ingermann, AR, Tsubaki, J, Twigg, SM, Oh, Y. Cellular expression of insulin-like growth factor binding protein-3 arrests the cell cycle and induces apoptosis in MCF-7 human breast cancer cells. J. Biol. Chem, 2001, in preparation.

13. Ingermann, AR, Kim, H-S, Oh, Y. Identification of a functional receptor for IGFBP-3. Nature, Medicine, 2001, in preparation.

VIII. LIST OF PERSONNEL

Youngman Oh, Ph.D.
Primary Investigator (100% effort)

Classification: Biological Sciences, Cell Biology

Identification of a functional receptor for insulin-like growth factor binding protein 3

Angela R. Ingermann, Ho-Seong Kim and Youngman Oh
Dept. of Pediatrics, Oregon Health Sciences University, 3181 SW Sam Jackson Park Rd.
Portland, OR 97201

Correspondence should be addressed to:
Youngman Oh, Ph.D.
Dept. of Pediatrics, NRC-5
Oregon Health Sciences University
3181 SW Sam Jackson Park Rd
Portland, Oregon 97201-3098, USA
e-mail: ohy@ohsu.edu

Manuscript information:
11 pages of text
6 figures
0 tables

Word and character counts:
243 words in the abstract
38,849 characters in the paper

Abbreviations:
IGF, insulin-like growth factor; IGFBP, IGF binding protein; TGF, transforming growth factor; TNF, tumor necrosis factor; IPTG, isopropyl β-D-thiogalactopyranoside; HRP, horseradish peroxidase; EGFP, enhanced green fluorescent protein; GST, glutathione S-transferase; MTS, 3-(4,5-dimethylthiazol-2-yl)-5-(3-carboxymethoxyphenyl)-2-(4-sulfophenyl)-2H-tetrazolium, inner salt; Rb, retinoblastoma.

Data deposition:
IGFBP-3R accession number, to be obtained

Our laboratory has previously demonstrated that IGFBP-3 acts as a growth inhibitor for human breast cancer cells, and is capable of specific cell surface binding, via sequences in the midregion of the protein, with kinetics consistent with receptor-ligand interactions. In this study, we used this portion of the IGFBP-3 cDNA as bait in the yeast two-hybrid system to identify a putative IGFBP-3 receptor. One of three independent positive clones was a previously unidentified cDNA, encoding a 0.9 kilobase mRNA that is widely distributed in human tissues and cell lines according to northern blot assays. The specific interaction of this clone, later designated IGFBP-3R, with IGFBP-3 was confirmed in a mammalian system by co-immunoprecipitation, western ligand blot, and subcellular colocalization. Monolayer affinity binding assays revealed that IGFBP-3R binds specifically to IGFBP-3 but not other IGFBP species, and that IGFs can displace IGFBP-3 binding to IGFBP-3R. Overexpression of IGFBP-3R led to significantly increased binding of IGFBP-3 to the cell surface, and potentiated IGFBP-3-induced suppression of proliferation. We further demonstrate that this growth inhibition is due to disruption of the cell cycle, as evidenced by significant and specific reductions in the levels of Cyclin D1 and Retinoblastoma proteins, and induction of apoptosis via activation of caspases in human breast cancer cells.

Together, these data demonstrate a physical and functional interaction of the IGFBP-3R with IGFBP-3 in human breast cancer cells, and that this interaction may play a significant role in characterized IGFBP-3 cell growth inhibitory functions.

Insulin-like growth factor binding protein-3 (IGFBP-3), one of six high affinity IGF binding proteins and the most abundant in serum, circulates as a 150 kDa ternary complex with an acid-labile subunit and IGF peptide (1-3). Classically, the principal function of IGFBP-3 has been to transport IGFs, protecting them from rapid clearance and/or degradation, and modulating IGF bioavailability to cell-surface IGF receptors (4-6). The importance of the IGF system in cancer has been addressed in large prospective studies which demonstrated a strong correlation between high IGF-I/low IGFBP-3 levels in circulation and increased risk of breast and prostate cancer, suggesting a potentially protective role for IGFBP-3 in the development of cancer (7, 8).

Recently, more detailed investigations of IGFBP-3 have revealed an important function in regulating the growth of human cancer cells, independent of its role as a modulator of IGF-I bioactivity. A variety of factors that suppress the growth of breast or prostate cancer cells, such as antiestrogens (tamoxifen and ICI 182, 780), TGF-β, retinoic acid, TNF-α and vitamin-D analogs apparently mediate their antiproliferative effects through IGFBP-3, suggesting the existence of a novel endocrine system in human cancer (9-13). In addition, the tumor suppressor p53 induces IGFBP-3 expression, indicating that IGFBP-3 may be a mediator in p53 signaling. More evidently, treatment of breast and prostate cancer cells with IGFBP-3 resulted in inhibition of cell proliferation and induction of apoptosis (14, 15). Together, these data point to IGFBP-3 as a growth-suppressing factor in breast and prostate cancer; however, the specific biochemical/molecular mechanisms involved in IGFBP-3 action are yet to be elucidated.

Furthering this concept, our laboratory has previously demonstrated that IGFBP-3 is capable of specific binding to the cell surface and acting as a growth inhibitor for estrogen-nonresponsive human breast cancer cells (16). The kinetics of specific binding of IGFBP-3 to the cell surface were consistent with receptor-ligand interactions (17). Further, our data indicated that the interaction of IGFBP-3 with the breast cancer cell surface and its subsequent biological effects are mediated through the IGFBP-3 specific cell surface association protein. This suggested the existence of an IGFBP-3-specific receptor participating in the direct inhibitory effect of IGFBP-3 on breast cancer cell growth (10, 18). We, therefore, sought to identify the putative IGFBP-3 receptor using the human breast cancer system. The results presented here describe the cloning and characterization of a novel cDNA encoding a protein, designated IGFBP-3R, that is expressed on the cell surface, interacts specifically with IGFBP-3, and plays an important role in the growth-inhibitory actions of IGFBP-3 on human breast cancer cells.

Materials and Methods

Yeast Two-Hybrid Screen. An Hs578T cDNA library in pGAD10 was generated using the Two-Hybrid cDNA Library Construction Kit (Clontech). The bait plasmid was constructed by amplifying an internal sequence of the IGFBP-3 cDNA (encoding amino acids 88-148) by PCR, then cloning this fragment into the pBTM116 vector, in frame with the LexA DNA binding domain coding sequence. The bait plasmid was then transformed into yeast strain L40, and an isolated transformant colony was then transformatied with the pGAD10:Hs578T cDNA library. 663 transformant colonies were tested for §-galactosidase activity. Plasmid DNA from three strongly positive clones was isolated and transformed into *E. coli* strain TG1. The full length cDNA sequence was confirmed using the 5 RACE system (Life Technologies).

Plasmids, Recomdinant Proteins and Antibodies. pEGFP::IGFBP-3R was generated by subcloning an XhoI-HindIII fragment of the full length IGFBP-3R cDNA into pEGFP-N3 (Clontech) in frame with EGFP. CS/IGFBP-3R^F was generated by first adding the FLAG peptide (DYKDDDK) coding sequence to the 3 end of the full length IGFBP-3R cDNA just 5 to the stop codon using synthetic linkers, then subcloning the product into the EcoRI and XhoI sites of the CS2+ mammalian expression vector. GST::IGFBP-3R protein was generated by subcloning the full length IGFBP-3R cDNA into the SalI site of the pGEX-4T-1 vector (Amersham Pharmacia). This construct was then digested with EcoRI and SfiI to remove a possible signal peptide sequence, the ends were filled and religated, and plasmid was transformed into *E. coli* strain BL21(DE3)pLysS for pr otein purification. FLAG-tagged IGFBP-3R protein (IGFBP-3R^F) was generated by subcloning the full length IGFBP-3R^F cDNA fragment from CS/IGFBP-3R^F into the EcoRI and XhoI sites of pFastBacI. Protein was then overespressed using the Baculovirus expression system (Life Technologies) according to the manufacturer s protocol. Anti-FLAG M2 monoclonal antibody was from Sigma. Anti-cyclin D1 monoclonal antibody was from NeoMarkers/LabVision. Anti-Rb antibody was from BD-PharMingen. HRP-conjugated secondary antibodies were from Amersham Pharmacia. Goat anti-mouse IgG_1 and goat anti-mouse IgG_{2a} fluorescently-conjugated secondary antibodies were from Southern Biotechnology Associates. Goat anti-mouse IgG and goat anti-rabbit IgG fluorescently conjugated secondary antibodies were from Molecular Probes.

Cell Culture and Transfection. All cell lines, except the MCF-7:IGFBP-3 stable lines, were purchased from American Type Culture Collection. All were cultured in Dulbecco s Modified Eagle s Medium/high glucose with 10% fetal bovine serum. MCF-7:IGFBP-3 stable lines were generated and maintained as described in (Kim et al, manuscript attached). Expression of IGFBP-3 was induced with ponasterone A (Invitrogen). Transfection experiments were done using either FuGene 6 (Roche Biochemical) or TransIT-LT1 (Mirus) transfection reagent according to the manufacturer s recommendations. Cell lysates were harvested by washing monolayer cultures in ice-cold PBS, then lysing in Triton lysis buffer (20 mM Tris, pH 7.6, 150 mM NaCl, 1% Triton X-100). Plates were rocked at 4°C for 15 minutes, and lysates collected and centrifuged to clear cellular debris.

Immunoprecipitations and Western Blotting. For immunoprecipitations, cleared cell lysates were diluted in 20 mM Tris, pH 7.6, 150 mM NaCl and adjusted to a final concentration of 0.5% Triton X-100 (IP buffer). Antibodies were added (1-2 µl) followed by the addition of Protein A Fast Flow sepharose (Amersham Pharmacia) or Anti-mouse IgG agarose (Sigma). Reactions were incubated at 4°C for 4 hours — overnight, then beads were washed in 2 X 1 mL IP buffer, suspended in 1X reducing sample buffer, and immunoblotted. Signal was detected using Renaissance Western Blot Chemiluminescence reagents (NEN).

Northern Blotting. The Human Multi-Tissue Northern Blots I & II were purchased from Clontech. Total RNAs from monolayer cultures of human mammary cells were harvested using the RNeasy RNA isolation kit (Qiagen). 5 µg of total RNA from each cell line were run on 1% formaldehyde gels and transferred onto GeneScreen Plus nylon membranes (NEN). ^{32}P-labelled cDNA probes were prepared using the Prime IT II kit (Stratagene). Membranes were hybridized in Rapid-Hyb buffer (Amersham Pharmacia), washed in 0.3X SSC, and exposed.

Cell Monolayer Binding Assay. Cells were seeded into 24-well plates and grown to 60-70% confluency, then transfected according to manufacturer instructions in serum-containing medium for 36 hours. Sf9 cells were seeded into 24-well plates and infected with virus harboring the IGFBP-3R^F cDNA for 48 hours. Cells were washed with cold PBS, then incubated for 3 hours at 12°C in binding buffer (1X Hank s buffered salt solution, 1 mM $CaCl_2$, 1 mM $MgCl_2$, 0.5% BSA) containing ^{125}I-IGFBP-3 (Diagnostic Systems Laboratories) at 50,000 cpm per well in triplicate, with or without unlabelled IGFBP-3 or other competitors as indicated in the text. The binding solution was then aspirated and the cells washed in cold binding buffer (without BSA), lysed in 0.25 N NaOH, and the radiolabelled IGFBP-3 detected in a Wallac gamma counter.

Immunocytochemistry. Cells were seeded in 8-chamber culture slides (Nunc) and transfected at 70-80% confluency. After 48 hours, cells were washed with PBS, and fixed in 4% paraformaldehyde. Slides were then incubated in blocking solution (5% normal goat serum in PBS + 0.1% Triton X-100) for 1 hour at room temperature, then in primary antibody diluted in blocking solution for 1-2 hours at room temperature or 4°C overnight. Cells were washed with PBS and incubated in fluorescently-conjugated secondary antibody + Hoechst stain diluted in blocking solution for 1 hour at room temperature in the dark. Cells were washed in PBS, covered with 50% glycerol and coverslipped. For suspended cell analysis, cells were trypsinized, washed in PBS, blocked and stained as above (without Hoechst stain) in a microfuge tube with gentle agitation. Following the final washes, cells were stained with PI staining solution and dispensed into chamber slides for visualization.

Cell Proliferation Assays. For ^{3}H-thymidine incorporation experiments, cells were seeded in triplicate into 24-well plates, grown to 60-70% confluency, and transfected and treated as indicated in the text. At 48 hours post-transfection, media was replaced with serum-free medium for 24 hours, then 0.1 µCi ^{3}H-thymidine (NEN) was added, and the acid-precipitable radioactivity in each well was assayed 24 hours later. MTS cell proliferation assays were performed in 96-well microtiter plates at 48 hours post-transfection using the CellTiter96 AQueous One Solution Cells Proliferation Assay kit (Promega) according to thr manufacturer s instructions.

Cell Cycle and Apoptosis Assays. All assays analyzed by flow cytometry were done on a Becton-Dickinson FACSCalibur flow cytometer. For cell cycle analysis, cells were seeded into 6-well plates and transfected at 70-80% confluency. At the time of the assay, cells were trypsinized and resuspended in PI staining solution (1X PBS, 100 U/mL RNase, 50 µg/mL propidium iodide) and incubated at RT in the dark for 30 minutes before analysis. For detection of early apoptotic cells, trypsinized cell suspensions were subjected to a FITC-labelled Annexin V binding assay (Santa Cruz Biotechnology, Santa Cruz, CA) according to the manufacturer s directions. For assay of caspase activity, cells were seeded in 96-well plates and transfected at 70-80% confluency. After 48 hours, cells were lysed in 30 µl per well of ice-cold lysis buffer (50 mM HEPES, pH 7.4, 0.1% CHAPS, 0.1% Triton X-100, 1 mM DTT, 0.1 mM EDTA), of which 20 µl were assayed using a combination of two fluorogenic peptide substrates, DEVD-AMC and LEHD-AMC (Biomol), at 40 µM each according to the manufacturer s directions. Serial dilutions of free 7-amino-4-methylcoumarin (AMC, Sigma) were included as a reference standard curve. Reaction kinetics were monitored for up to 16 hours at 37°C in a Bio-Rad Fluoromark microplate fluorometer, with plate readings taken every 10 minutes. Data were analyzed from the linear portion of the reactions using Microplate Manager software (Bio-Rad), and final results were adjusted for protein content.

Results and Discussion

We used the yeast two-hybrid system to identify proteins that interact with IGFBP-3. Since our previous studies identified that a region in the internal portion (amino acids 88-148) of the IGFBP-3 protein is responsible for cell surface binding (17), this region was used as bait in a yeast two-hybrid screen against an Hs578T human breast cancer cell cDNA library. The screen yielded three independent positive clones, two of which matched sequences in the GenBank database: (1) Eps8, epidermal growth factor receptor kinase substrate, and (2) GRP78/BiP, glucose regulated stress protein, or human immunoglobulin heavy chain binding protein. The third cDNA, later designated IGFBP-3R, was not identified in the database and represents a novel gene encoding a predicted protein of 240 amino acids. 5 RACE was used to confirm the 5 end of the cDNA, and showed that the original cDNA isolated from the two-hybrid screen was in fact full length. The protein sequence contains potential N-glycosylation sites, a single leucine-zipper motif which overlaps a putative transmembrane domain near the C-terminus, and a cAMP-dependent phosphorylation site just C-terminal to the putative transmembrane sequence.

To assay for IGFBP-3/IGFBP-3R interaction in a mammalian system, we overexpressed both proteins and performed co-immunoprecipitation and western ligand blot assays. For immunoprecipitations, FLAG-tagged IGFBP-3 (IGFBP-3^{F}) and IGFBP-3R fused to EGFP (EGFP::IGFBP-3R) were overexpressed in COS-7 cells. The EGFP::IGFBP-3R fusion protein displayed a perinuclear and cytoplasmic subcellular localization, as compared to nuclear and cytoplasmic distribution of unfused EGFP. Additionally, when co-transfected cells were immunostained with the M2 antibody against the FLAG sequence, the EGFP::IGFBP-3R and IGFBP-3^{F} appeared to colocalize in the cytoplasm

(data not shown). Figure 1A shows representative results of reciprocal co-immunoprecipitation assays using lysates from these transfected cells. The interaction of IGFBP-3^F and EGFP::IGFBP-3R was evident, and could be demonstrated whether anti-EGFP or anti-FLAG M2 antibody was used for immunoprecipitation. IGFBP-3^F did not interact with unfused EGFP. For the western ligand blot assay, radiolabelled IGFBP-3 was used to detect binding with FLAG-tagged IGFBP-3R (IGFBP-3R^F) that had been immunoprecipitated from cell lysates with anti-FLAG M2 agarose beads, eluted with excess FLAG peptide, and western blotted. An anti-FLAG M2 immunoblot revealed the IGFBP-3R^F as a doublet of roughly 32 and 34 kilodaltons (Figure 1B). The membrane was then stripped and incubated with the ^{125}I-labelled IGFBP-3, which bound to both species. These results demonstrate the interaction of IGFBP-3 and IGFBP-3R in a mammalian system.

Northern analysis of clone IGFBP-3R mRNA expression indicated a wide distribution in human tissues and cell lines. The 0.9 kb mRNA was detected to varying degrees in all cell lines and tissues tested (Figure 2A and data not shown). A second roughly 2 kb transcript was detected in testis, the significance of which, if any, is not known.

To examine the endogenous protein, we generated a rabbit polyclonal antibody against GST-fused IGFBP-3R purified from *E. coli*. The antibody was robust for western immunoblot and immunocytochemistry, as shown in Figure 2, and also for immunoprecipitation (data not shown). The IGFBP-3R antibody recognized the 55 kDa GST::IGFBP-3R fusion protein, and a species of roughly 32 kDa from immunoblotted Hs578T human breast cancer cell lysates (Figure 2B). A species of this size was detected in lysates from all other cell lines tested. No signal was detected from corresponding conditioned media, and cross-reactivity with purified GST was low. In immunocytochemistry experiments, the IGFBP-3R antibody recognized overexpressed FLAG-tagged IGFBP-3R in a pattern identical to that detected with the anti-FLAG M2 antibody (Figure 2C). Surrounding untransfected cells also displayed an identical, though less intense, staining pattern with the IGFBP-3R antibody, the same perinuclear/cytoplasmic subcellular localization pattern as was seen for the EGFP::IGFBP-3R fusion protein.

As IGFBP-3 has been previously demonstrated to specifically bind to the surface of breast cancer cells and subsequently exhibit growth-suppressing activity, we next determined whether IGFBP-3R might participate in this process. We first examined whether IGFBP-3R localizes to the cell surface by immunostaining cells in suspension. Transfected IGFBP-3R^F detected with the anti-FLAG M2 antibody and endogeous IGFBP-3R detected with our polyclonal antibody both displayed a characteristic ring pattern around the surface of the suspended cells (Figure 3A), indicating cell surface localization. To examine the possibility that an IGFBP-3/IGFBP-3R interaction of occurs on the cell surface we used a monolayer affinity binding assay with ^{125}I-labelled IGFBP-3. Overexpression of IGFBP-3R resulted in a 20-60% increase in IGFBP-3 binding to Hs578T and MCF-7 breast cancer cell monolayers relative to cells expressing endogenous levels of IGFBP-3R (Figure 3B, $p<0.1$). The presence of the FLAG-tag at the C-terminus of the IGFBP-3R protein had no effect (data not shown). This results was greatly magnified to a 3.4-fold increase ($p<0.05$) in IGFBP-3 cell surface binding when the same assay was done using Sf9 insect cells infected with Baculovirus harboring the IGFBP-3R^F cDNA, as nearly 100% of these cells overexpress IGFBP-3R^F compared to a 20-30% transfection rate in the breast cancer cells. Binding was competed in a dose-dependent manner with the addition of unlabelled IGFBP-3 or IGF peptides but not by IGF binding proteins -2, -4, -5 or —6 (data not shown), demonstrating IGFBP-3R specificity for binding IGFBP-3 and indicating that binding of IGFBP-3 to IGFs and to IGFBP-3R are mutually exclusive. Furthermore, addition of IGFBP-3 fragments comprising amino acids 88-148, and 98-264 competed for cell surface binding of full-length IGFBP-3 to overexpressed IGFBP-3R, whereas a fragment comprising the N-terminal amino acids 1-97 had no effect (data not shown). This result is consistent with our previous report which identified the region of IGFBP-3 between amino acids 88-148 as being responsible for cell surface binding, and with the fact that the IGFBP-3R cDNA was isolated based on interaction with this region of IGFBP-3.

The classical and well established role for endocrine IGFBP-3 is as a modulator of IGF bioavailability. In general, the binding affinity of IGFBP-3 for IGF peptides is higher than that of IGF receptors, implying that IGFBP-3 can modulate IGF binding to its receptor, thereby regulating IGF biological actions in the cellular environment. Expression of IGFBP-3 in mammary cells is hormonally regulated;

estrogen inhibits expression and secretion of IGFBP-3, whereas antiestrogens, such as tamoxifen and ICI 182,780, stimulate production of IGFBP-3 in estrogen-responsive human breast cancer cells (1, 19-21). Recent studies have revealed that IGFBPs may have specific biological effects in various cell systems, including human breast cancer cells, which are not mediated through interaction with IGF peptides (IGF-independent actions, 10, 22, 23). In further support of this concept, other investigators have recently reported interaction of IGFBP-3 with the retinoid X receptor (24), and translocation of IGFBP-3 to the nucleus via interaction with importin-§ (25). These data suggest the specific role of IGFBP-3 in cell replication with potentially diverse mechanisms.

We and others have reported that the expression and production of IGFBP-3 is specifically stimulated by TGF-β and RA in human breast cancer cells, and postulated a role for IGFBP-3 in TGF-β- and RA-induced growth inhibition in human breast cancer cells (16, 26, 27). Use of IGFBP-3-specific antisense oligodeoxynucleotides has shown that the anti-proliferative effects of TGF-β, RA, TNF-α and vitamin-D analogs in human breast cancer cells are mediated, at least in part, through the IGFBP-3 axis (10-12, 16). Other studies have confirmed that IGFBP-3 functions as a major growth-suppressing factor in various cell systems, each of which may involve the IGFBP-3R: 1) the growth rate is significantly reduced in IGFBP-3-transfected fibroblasts with a targeted disruption of the IGF-I receptor gene (13); 2) purified mouse IGFBP-3 binds to the chick embryo fibroblast cell surface and inhibits cell growth (28); 3) up-regulation of IGFBP-3 expression is correlated with RA-induced cell growth inhibition in cervical epithelial cells (29); 4) the tumor suppressor p53 induces IGFBP-3 expression, indicating that IGFBP-3 may be a mediator in p53 signaling (30); 5) exogenously added IGFBP-3 inhibits estrogen-stimulated breast cancer cell proliferation (14); 6) IGFBP-3 transient transfection results in significant inhibition of colon and lung cancer cell replication (31, 32) and 7) IGFBP-3 induces apoptosis in prostate cancer cells (33). These numerous reports build a solid foundation for IGFBP-3 function in inhibition of cell growth and proliferation in an IGF-independent manner.

We investigated the role of IGFBP-3R in IGFBP-3-mediated growth inhibtion by overexpressing the IGFBP-3R and assaying for cell proliferation in Hs578T and MCF-7 cells. Both of these cell lines produce endogenous levels of the IGFBP-3R, but only Hs578T cells produce IGFBP-3. In these experiments, the proliferation of the Hs578T population was significantly reduced after 48 hours of transfection to 78% of control levels ($p<0.05$), while the MCF-7 cells were unaffected (data not shown). To investigate this further we utilized an inducible stably-transfected subline of MCF-7 cells, MCF-7:IGFBP-3 #3 (Kim et al.) in comparative experiments with wild-type MCF-7 cells. The MCF-7:IGFBP-3 #3 cells express IGFBP-3 when cultured with an inducer compound, ponasterone A. Induction of IGFBP-3 expression in these cells resulted in an inhibition of ^{3}H-thymidine incorporation to 65% of control levels ($p<0.05$). With the additional overexpression of IGFBP-3R, however, ^{3}H-thymidine incorporation was further reduced to 45% of control levels (Figure 4, $p<0.05$). Overexpression of IGFBP-3R had no significant effect on ^{3}H-thymidine incorporation in the absence of IGFBP-3 (either wild type MCF-7 or uninduced MCF-7:IGFBP-3 #3 cells), and ponasterone A had no inhibitory effect in wild type MCF-7 cells. This inhibitory effect on cell proliferation was not seen when IGFBP-3 binding to IGFBP-3R was disrupted by addition of Y60L-IGF-I, an IGF analog which has a 100-fold reduced affinity for IGF receptors but full affinity for IGFBPs, suggesting once again that IGF and IGFBP-3R binding to IGFBP-3 are mutually exclusive (data not shown).

To explore the possible mechanisms involved in IGFBP-3/IGFBP-3R-induced growth inhibition, we first examined effects on specific proteins known to be involved in cell cycle progression. Our recent data concerning IGFBP-3 biological function indicate a significant reduction of cyclin D1 and retinoblastoma (Rb) protein levels in response to induced expression of IGFBP-3 in MCF-7:IGFBP-3 #3 stably-transfected cells, which endogenously express IGFBP-3R (Kim et al.). For this study we used Hs578T and MCF-7 cells, and an IGFBP-3-constitutively expressing MCF-7 cell subline (MCF-7:IGFBP-3 #1, Kim et al.), treated as indicated in Figure 5A. Examination of cell cycle proteins cyclin D1, cyclin E, and p21/Waf1 revealed a specific decrease in the level of cyclin D1 in IGFBP-3R-transfected cells, but only in the presence of IGFBP-3. No effect on cyclin D1 protein was seen in wild-type MCF-7 cells, which do not produce detectable levels of IGFBP-

3, or in control transfected cells, suggesting that both IGFBP-3 and IGFBP-3R are required. Levels of cyclin E and p21/Waf1 were unaffected by these treatments. In addition to Cyclin D1, we further identified a reduction in the levels of retinoblastoma (Rb) protein with overexpression of IGFBP-3R in the presence of IGFBP-3, similarly seen with induced expression of IGFBP-3 in MCF-7:IGFBP-3 #3 cells (Kim et al.). Strikingly, immunocytochemistry experiments revealed that the reduced levels of both of these proteins appeared to be specifically correlated to IGFBP-3R-overexpression (Figure 5B). When cell populations were dually stained for IGFBP-3R transfection and either CyclinD1 or Rb protein, the IGFBP-3R-positive cells showed specific reduction in staining intensity of Cyclin D1 and Rb compared to surrounding untransfected cells. The percentage of IGFBP-3R-positive cells with reduced Cyclin D1 (94%) or Rb (83%) levels was significantly greater than in the untransfected population in both cases (38% and 23%, respectively). These results indicate that disruption of the cell cycle is involved in IGFBP-3/IGFBP-3R-induced growth inhibition, and that this disruption is p21/Waf1 independent.

In addition to disruption of the cell cycle, further investigations into the growth-inhibitory actions of IGFBP-3R and IGFBP-3 were performed using flow cytometry analysis. Transfected MCF-7:IGFBP-3 #3 cells were analyzed for cell cycle profile by propidium iodide DNA staining followed by flow cytometry detection. In the presence of IGFBP-3, the IGFBP-3R-overexpressing cells displayed a 2-fold increase in the sub-G1 population and a concurrent decrease in the S/G2/M population compared to control-transfected or uninduced cells (data not shown). An increase in the sub-G1 population can be indicative of cells undergoing apoptosis, so we investigated this further using an Annexin V binding assay. Transfected Hs578T and MCF-7 cells assayed along a time course showed a significant increase in the population of early apoptotic cells in Hs578T cells transfected with IGFBP-3R compared to control-transfected cells, with an average 2.9-fold increase over 48 hrs (Figure 6A). No significant increase in apoptosis was seen in MCF-7 cells.

We then looked further into mechanisms by which the IGFBP-3/IGFBP-3R interaction might induce apoptosis. Investigations of cells overexpressing IGFBP-3R in the presence of IGFBP-3 revealed that induction of caspase activity may be at least partially responsible for the promotion of apoptosis in these cells (Figure 6B). Using an assay which detects activity from a wide variety of caspases, we analyzed cell lysates from control and IGFBP-3R transiently transfected cells that were incubated with caspase-specific fluorogenic peptide substrates and monitored the kinetics of substrate cleavage for up to 16 hours at 37°C in a microplate fluorometer. A significant increase in caspase activity was detected in the IGFBP-3R-overexpressing cell lysates (37.9 pmol/min/mg) compared to controls (23.0 pmol/min/mg), an increase of 165% ($p<0.05$). This value was less than that obtained with 48 hours of treatment with the positive control apoptosis inducer taxol (81.2 pmol/min/mg), and this may be due to a transfection efficiency of 20-30% with vector alone or IGFBP-3R compared to exogenous treatment of the cells with taxol.

In summary, we have identified a novel gene/protein, designated IGFBP-3R, from human breast cancer cells. This is the first report of an IGFBP-3 cellular receptor that appears to interact and function cooperatively with IGFBP-3 in its previously known and characterized IGF-independent functions. The IGFBP-3R is widely expressed is tissues and cell lines. Subcellular localization is perinuclear and cytoplasmic, with protein also detectable on the cell surface. Data suggest that an IGFBP-3/IGFBP-3R interaction occurs on the cell surface, and that they synergistically suppress DNA synthesis and cell proliferation. Subsequent data indicate that this growth inhibition involves disruption of the cell cycle and promotion of apoptosis, and that to this end the interaction of IGFBP-3 and IGFBP-3R may be involved in regulating components of cell cycle progession and apoptotic pathways, specifically the cellular levels of cyclin D1 and Rb proteins, and activity of caspases, respectively. These data support the hypothesis that IGFBP-3R is a functional receptor for IGFBP-3 in the breast cancer system, and that the interaction of IGFBP-3 and IGFBP-3R may be an important mechanism in the IGF-independent, growth-inhibitory actions of IGFBP-3. Further characterization of the cellular effects of the IGFBP-3/IGFBP-3 receptor axis in breast cancer cells, and the biochemical/molecular mechanisms involved, may yield significant insights into the regulation of cell proliferation in breast cancer. Elucidation of these mechanisms will be informative and important toward the understanding of cancer cell proliferation, potentially leading to avenues of cancer treatment and tumor growth suppression.

This work was supported by Department of Defense grants 17-96-1-6304 and 17-97-1-7204.

1. Rosenfeld, R.G. In Robbins RJ, Melmed S (eds). (1987) *Acromegaly*. Plenum Press, New York, pp 45-53.
2. Neely, E.K., Beuker,s W.M., Oh, Y., Cohen, P., & Rosenfeld, R.G. (1991) *Acta Pediatr. Scand.*. **372**:116-123.
3. Oh, Y., Muller, H.L., Neely, E.K., Lamson, G., & Rosenfeld, R.G., (1993) *Growth Regul.* **3**:113-123.
4. Ruoslahti, E. & Pierschbacher, M.D. (1987) *Science* **238**:491-493.
5. Hintz, R.L., Liu, F. (1977) *J. Clin. Endocrinol. Metab.* 45:988-982.
6. Baxter, R.C, Martin, J.L., Tayler, M.I., et. al. (1986) *Biochem Biophys Res Commun* **139**:1256-1259.
7. Byrne, C., Colditz, G.A., Willett, W.C., Speizer, F.E., Pollak, M., and Hankinson, S.E., (2000) *Cancer Res.* **60**:3744-3748.
8. Chan, J.M., Stampfer, M.J., Giovannucci, E., Ma, J., and Pollak, M. (2000) *Growth Horm IGF Res.* **Suppl A**:S32-3.
9. Huynh, H., Yang, X., and Pollak, M. (1996) *J. Biol. Chem.* **271**, 1016-1021.
10. Oh, Y., Muller, H.L., Ng, L., Rosenfeld, R.G. (1995) *J. Biol. Chem.* **270**, 13589-13592.
11. Gucev, Z.S.; Kelley, K.M.; Rosenfeld, R.G., Oh, Y. (1996) *Cancer Researc*h **56**, 1545-50.
12. Rozen, F., Zhang, J., Pollak, M. (1998) *Int J Oncol.* **13**, 865-869.
13. Colston, K.W., Perks, C.M., Xie, S.P., Holly, J.M. (1998) *J Mol Endocrinol.* **20**, 157-162.
14. Yee, D., Favoni, R.E., Lippman, M.E., & Powell, D.R. (1991) *Breast Cancer Res. Treat* **18**, 3-10.
15. Buckbinder, L., Talbott, R., Velasco-Miguel, S., Takenata, I., Faha, B., Seizinger, B.R., and Kley, N. (1995) Nature **377**, 646-649.
16. Fontana, J.A., Burrows-Meszu, A., Clemmons, D.R., & LeRoith, D. (1991) *Endocrinology* **128**, 1115-1122.
17. Yamanaka, Y., Fowlkes, J.L., Wilson, E.M., Rosenfeld, R.G., & Oh, Y. (1999) *Endocrinology* **140**, 1319-11328.
18. Oh, Y., Muller, H.L., Pham, H.M., & Rosenfeld, R.G. (1993) *J. Biol. Chem.* **268**, 26045-26048.
19. Baxter, R.C., & Martin, J.L. (1989) *Prog Growth Factor Res* **1**, 49-56.
20. Paik, S. (1992) *Breast Cancer Res. Treat.* **22**, 31-38.
21. Clemmons, D.R., Camacho-Hubner, C., & Coronado, E. (1990) *Endocrinology* **127**, 2679-2685.
22. Nickerson, T., Huynh, H., & Pollak, P. (1997) *Biochem. Biophys. Res. Commun.* **237**, 690-693.
23. Maile, L.A., Gill, Z.P., Perks, C.M., & Holly, J.M. (1999) *Endocrinology* **140**, 4040-4045.
24. Liu, B., Lee, H-Y., Weinzimer, S.A., Powell, D.R., Clifford, J.L., Kurie, J.M., & Cohen P. (2000) *J. Biol. Chem.* **275**, 33607-33613.
25. Schedlich, L.J., Le Page, S.L., Firth, S.M., Briggs, L.J., Jans, D.A., & Baxter, R.C. (2000) *J. Biol. Chem.* **275**, 23462-23470.
26. Pratt, S.E., & Pollak, M.N. (1994) *Biochem. Biophys. Res. Commun.* **198**, 292-297.
27. Cohen, P., Peehl, D.M., Lamson, G., & Rosenfeld, R.G. (1991) *J. Clin. Endocrinol. Metab.* **73**, 401-407.\
28. Valentinis, B., Bhala, A., De Angelis, T., Baserga, R., & Cohen, P. (1995) *Mol. Endocrinol.* **9**, 361-367.
29. Delbe, J., Blat, C., Desauty, G., & Harel, L. (1991) *Biochem. Biophys. Res. Commun.* **179**, 495-501.
30. Andreatta-Van Leyen, S., Hembree, J.R., & Eckert R.L. (1994) *J. Cell Physiol.* **160**, 265-274.
31. MacDonald, R.G., Schaffer, B.S., Kang, I.-J., Hong, S.M., Kim, E.J., & Park, J.H. (1999) *J. Gastroenterol. Hepatol.* **14**, 72-78.
32. Hochscheid, R., Jaques, G., & Wegmann, B. (2000) *J. Endocrinol.*. **166**, 553-563.
33. Rajah, R., Valentinis, B., & Cohen, P. (1997) *J. Biol. Chem.* **272**, 12181-12188.

Figure 1. Interaction of IGFBP-3 with IGFBP-3R. A) Coimmunoprecipitation of IGFBP-3^F and EGFP::IGFBP-3R. Cell lysates from transfected cells were incubated with either anti-GFP or anti-FLAG antibody, and immunoprecipitated proteins were detected on western immunoblots with the opposing antibody. B) Western ligand blot of FLAG-tagged IGFBP-3R. Cell lysates from cells overexpressing IGFBP-3R^F (lane 2) were immunoprecipitated with αFLAG M2 agarose beads (lane 3), then eluted with excess FLAG peptide (lane 4). Samples were first immunoblotted with αFLAG M2 antibody (lane 1), then the membrane was stripped and incubated with radiolabelled IGFBP-3 (lanes 2-4).

Figure 2. Expression and distribution of IGFBP-3R mRNA and protein. A) Human multiple tissue northern blots I & II (Clontech), and northern blots containing total RNAs from Hs578T and MCF-7 human breast cancer cell lines and human mammary epithelial cells (HMEC) were probed with ^{32}P-labelled IGFBP-3R cDNA. B) Duplicate western immunoblots of purified unfused GST (lane 1), GST::IGFBP-3R (lane 2), and Hs578T conditioned medium (lane 3) and cell lysate (lane 4) using preimmune serum and αIGFBP-3R polyclonal antibody. Cross-reactivity of the IGFBP-3R antibody with unfused GST was low. IGFBP-3R protein was detected only in cell lysate. C) Detection of transfected IGFBP-3R^F (green) and endogenous IGFBP-3R (red) by immunocytochemistry using αFLAG M2 and αIGFBP-3R antibodies. IGFBP-3R detected with the IGFBP-3R antibody revealed a perinuclear and cytoplasmic localization pattern in all cells, identical to the pattern seen when the overexpressed protein is detected with M2 as shown in the merged image (yellow). Hoechst stain (blue) was used as a nuclear stain.

Figure 3. Cell surface localization of IGFBP-3R and cell surface binding of IGFBP-3. A) Immunostaining of transiently expressed (αFLAG M2 antibody, green) or endogenous (αIGFBP-3R antibody, green) IGFBP-3R in breast cancer cell suspensions displayed a ring pattern indicating cell surface localization. B) Monolayer affinity binding data showed a significant increase in radiolabelled IGFBP-3 cell surface binding on cells overexpressing IGFBP-3R compared to control-transfected cells. The increase in ^{125}I-IGFBP-3 cell surface binding on breast cancer cell monolayers was roughly proportional to the transfection efficiency of 20-30%, whereas in Sf9 insect cells, several-fold higher expression relative to controls yielded even more significant results. * = $p<0.1$, ** = $p<0.05$.

Figure 4. Growth inhibition of breast cancer cells by IGFBP-3/IGFBP-3R. MCF-7:IGFBP-3 #3 and control MCF-7 cells were subjected to a ^{3}H-thymidine incorporation assay with control or IGFBP-3R transfection. No effect was seen in the absence of IGFBP-3 (control MCF-7 and uninduced MCF-7:IGFBP-3 cells). Induction of IGFBP-3 expression in control transfected cells resulted in inhibition of ^{3}H-thymidine incorporation to 65% of control levels. This effect was significantly potentiated in IGFBP-3R-transfected cells where ^{3}H-thymidine incorporation was inhibited further to 45%. * = $p<0.05$.

Figure 5. Specific reduction of cyclin D1 and Rb protein levels in cells overexpressing IGFBP-3R in the presence of IGFBP-3. A) Hs578T, MCF-7, and MCF-7:IGFBP-3 #1 (constitutively expressing IGFBP-3) cells were treated as indicated for 24 hours and equal amounts of harvested cell lysates were assayed by western immunoblot. Overexpression of IGFBP-3R in the presence of IGFBP-3 resulted in a significant reduction in the levels of cyclin D1 and Rb proteins. There was no effect on cyclin E or p21/Waf1. B) Both of these effects were specific to IGFBP-3R-transfected cells as shown by dual immunostaining of transfected Hs578T cells with IGFBP-3R (green) and either cyclin D1 or Rb (red) antibodies.

Figure 6. Induction of apoptosis by IGFBP-3/IGFBP-3R. A) Overexpression of IGFBP-3R in the presence of IGFBP-3 resulted in a significant increase (average of 3.0 fold within 48 hours of transfection) in the percentage of cells in the early stages of apoptosis, as measured by an annexin V binding followed by flow cytometric analysis. B) Overexpression of IGFBP-3R in Hs578T human breast cancer cells caused a significant increase in overall caspase activity compared to control-transfected cells, measured by a fluorogenic caspase activity assay. Activity was increased from a baseline of 23.0 pmol/min/mg in control cell lysates to 37.9 pmol/min/mg in IGFBP-3R-overexpressing cells. * = $p<0.05$.

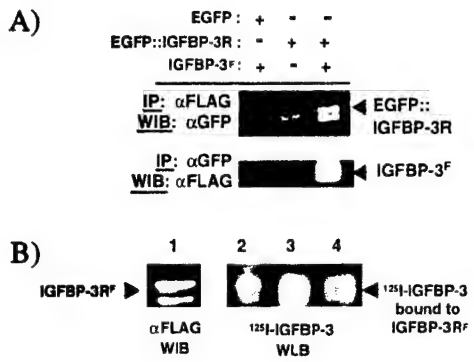
A)
EGFP : + - -
EGFP::IGFBP-3R : - + +
IGFBP-3F : + - +
IP: αFLAG
WIB: αGFP
EGFP::
IGFBP-3R
IP: αGFP
WIB: αFLAG
IGFBP-3F
B)
1
2
3
4
IGFBP-3RF
125I-IGFBP-3
bound to
IGFBP-3RF
αFLAG
WIB
125I-IGFBP-3
WLB

Figure 1.

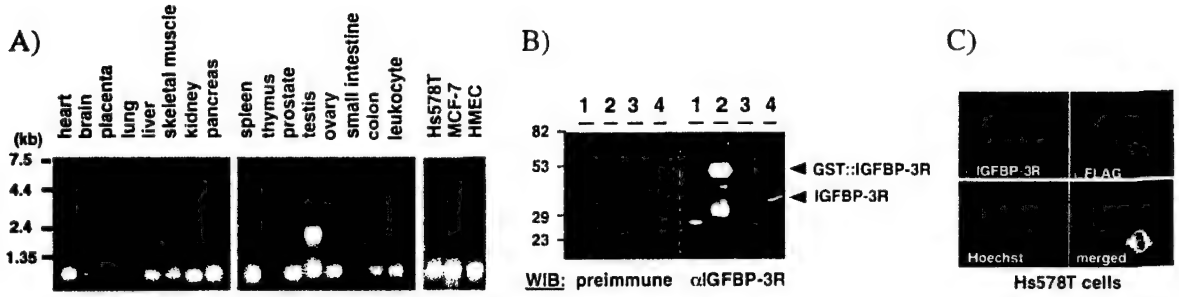
A)
heart
brain
placenta
lung
liver
skeletal muscle
kidney
pancreas
spleen
thymus
prostate
testis
ovary
small intestine
colon
leukocyte
Hs578T
MCF-7
HMEC
(kb)
7.5
4.4
2.4
1.35
B)
1 2 3 4 1 2 3 4
82
53
29
23
GST::IGFBP-3R
IGFBP-3R
WIB: preimmune αIGFBP-3R
C)
IGFBP-3R
FLAG
Hoechst
merged
Hs578T cells

Figure 2.

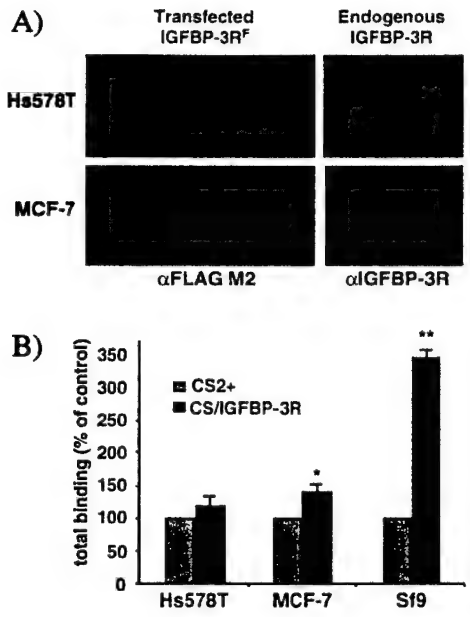
A)
Transfected IGFBP-3R^F
Endogenous IGFBP-3R
Hs578T
MCF-7
αFLAG M2
αIGFBP-3R
B)
total binding (% of control)
350
300
250
200
150
100
50
0
CS2+
CS/IGFBP-3R
*
**
Hs578T
MCF-7
Sf9

Figure 3.

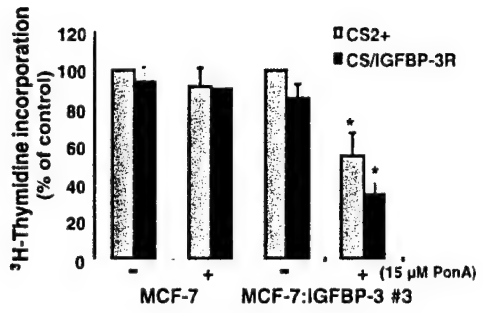
^{3}H-Thymidine incorporation (% of control)
120
100
80
60
40
20
0
CS2+
CS/IGFBP-3R
*
*
-
+
-
+ (15 μM PonA)
MCF-7
MCF-7:IGFBP-3 #3

Figure 4.

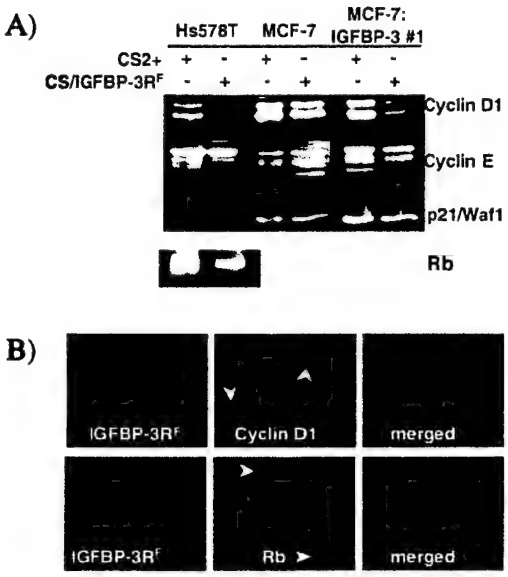
A)
Hs578T
MCF-7
MCF-7: IGFBP-3 #1
CS2+
CS/IGFBP-3R^F
Cyclin D1
Cyclin E
p21/Waf1
Rb
B)
IGFBP-3R^F
Cyclin D1
merged
IGFBP-3R^F
Rb
merged

Figure 5.

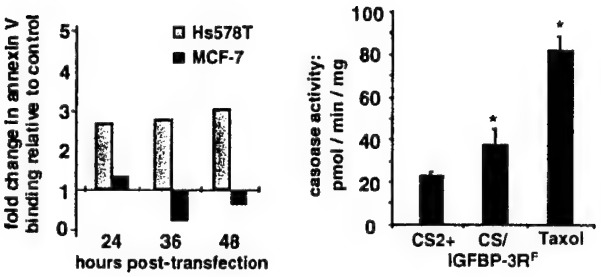
fold change in annexin V binding relative to control
5
4
3
2
1
0
Hs578T
MCF-7
24
36
48
hours post-transfection
casoase activity: pmol / min / mg
100
80
60
40
20
0
*
*
CS2+
CS/ IGFBP-3R^F
Taxol

Figure 6.

Cellular Expression of Insulin-like Growth Factor Binding Protein-3 Arrests the Cell Cycle and Induces Apoptosis Through Ablation of Mitogen-activated Protein Kinase Activity and Activation of Caspases in MCF-7 Human Breast Cancer Cells

Ho-Seong Kim, Angela R Ingermann, Junko Tsubaki, Stephen M Twigg and Youngman Oh

Department of Pediatrics, Oregon Health Sciences University, Portland, Oregon

Running Title: IGFBP-3 arrests cell cycle and induces apoptosis

Address correspondence to : Youngman Oh, Ph.D.,
Associate Professor
Department of Pediatrics
Oregon Health Sciences University
3181 S.W. Sam Jackson Park Road, HRC-5
Portland, OR 97201-3098
Tel: 503-494-1930
Fax: 503-494-0428
Email: ohy@ohsu.edu

This work was supported by the US Army grants DAMD17-96-1-6204 (YO) and DAMD17-97-1-7204 (YO).

[1] The abbreviations used are: IGFBP, insulin-like growth factor binding protein; IGF, insulin-like growth factor; PARP, poly(ADP-ribose) polymerase; cdk, cyclin-dependent kinase; Rb, retinoblastoma protein; MAPK, mitogen-activated protein kinase; ERK, extracellular signal-regulated kinase; AMC, 7-amino-4-methylcoumarin; FITC, fluorescein isothiocyanate; DMEM, Dulbecco's modified Eagle's medium; FBS, fetal bovine serum; SFM, serum-free medium; PBS, phosphate-buffered saline; PAGE, polyacrylamide gel electrophoresis, TBST, tris-buffered saline with 0.1% Tween-20

SUMMARY

The insulin-like growth factor binding protein (IGFBP)-3 has been recently shown to potently inhibit proliferation of various cell types in an insulin-like growth factor (IGF)-independent manner. The goal of the present study was to demonstrate a novel, IGF-independent role for IGFBP-3; cell cycle arrest and induction of apoptosis and to elucidate their possible mechanisms in MCF-7 human breast cancer cells. MCF-7 cells, which do not produce IGF peptides, were stably transfected with an IGFBP-3 cDNA construct using the ecdysone-inducible expression system. Induction of IGFBP-3 in these cells resulted in a dose-dependent inhibition of DNA synthesis as assessed by [^{3}H]-thymidine incorporation assays. This inhibitory effect was abolished by co-treatment with Y60L-IGF-I, an IGF analog which has significantly reduced affinity for the IGF receptor, but which retains high affinity for IGFBP-3, demonstrating specificity and IGF independency. In addition, flow cytometry analysis showed that induced expression of IGFBP-3 led to an arrest of the cell cycle in G1-S phase. Induction of IGFBP-3 resulted in a significant decrease in the mRNA and protein levels of cyclin D1, but not cyclin E, as well as concomitant decreases in the levels of cyclin-dependent kinase (cdk)4, total and phosphorylated-retinoblastoma protein (Rb). Moreover, IGFBP-3 inhibited oncogenic Ras-induced phosphorylation of mitogen-activated protein kinases (MAPKs), suggesting cross-talk between the IGFBP-3 signaling and MAPK signal transduction pathways. IGFBP-3-expressing cells also displayed increased Annexin V binding compared to controls, demonstrating IGFBP-3-induced apoptosis. Additional studies demonstrated that IGFBP-3 caused an increase in caspase activities, suggesting a potential mechanism for the IGFBP-3-induced apoptosis. Taken together, the present study shows that cellular production of IGFBP-3 leads to cell cycle arrest and induction of apoptosis, thereby inhibiting cell proliferation in MCF-7 human breast cancer cells. Our data suggest that IGFBP-3 functions as a negative regulator of breast cancer cell growth, independent of the IGF axis.

Key Words

IGFBP-3, inducible stable cell line, cell cycle arrest, apoptosis, breast cancer, cyclin D1, retinoblastoma protein, mitogen-activated protein kinase, caspase

INTRODUCTION

The insulin-like growth factor binding proteins (IGFBPs[1]) are components of the insulin-like growth factor (IGF) signaling system, and the IGFBP superfamily is comprised of six high-affinity species (IGFBPs 1-6) and several low-affinity binders (IGFBP-related proteins (IGFBP-rPs)) (1-5). The classical role of the IGFBPs involves IGF binding and modulation of IGF signaling; however, recent data suggest that some IGFBPs may play more active, IGF-independent roles in growth regulation in various cell systems (6-19). In particular, IGFBP-3 has been shown to potently inhibit proliferation of various cell types in an IGF-independent manner. This concept of IGF-independent actions of IGFBP-3 is supported by the demonstration that (i) exogenous IGFBP-3 binds to specific proteins on the cell surface, and this interaction is strongly correlated with the ability of IGFBP-3 to inhibit cell growth (8, 9); (ii) overexpression of human IGFBP-3 inhibits cell proliferation (10-12); (iii) IGFBP-3 mediates transforming growth factor-β- (13), retinoic acid- (14), antiestrogen- (15), vitamin D analogs- (16), and tumor necrosis factor-α- (17) induced growth inhibition; (iv) regulation of IGFBP-3 gene expression plays a role in signaling by p53, a potent tumor-suppressor protein (18); and (v) IGFBP-3 fragments inhibit the stimulation of DNA synthesis induced either by IGF-I or insulin (19). Recently, several reports have demonstrated that IGFBP-3 induces apoptosis in PC-3 prostate cancer (20) and MCF-7 breast cancer cells (21), and increases ceramide-induced apoptosis in the Hs578T breast cancer cell line (22). However, the specific mechanism for the IGF-independent action of IGFBP-3 has yet to be elucidated. Moreover, the use of IGFBP-3 purified from biological fluids and recombinant species for biological studies is problematic due to concerns about the purity, bioactivity and post-translational modification of IGFBP-3. In this study, we have used the inducible cellular expression of IGFBP-3 to determine a novel, IGF-independent role for IGFBP-3; cell cycle arrest and induction of apoptosis in MCF-7 human breast cancer cells.

We hypothesized that IGFBP-3 inhibits cell growth in an IGF-independent manner and wished to determine whether its growth-inhibitory effects involve regulation of the cell cycle arrest and/or induction of apoptosis. To address these questions, we generated a subline of MCF-7 cells (which do not produce IGF peptides) stably transfected with an inducible IGFBP-3 cDNA construct using the ecdysone-inducible expression system. This controlled system was used to look carefully at the effects of induced IGFBP-3 expression on the cell cycle and apoptosis. We then investigated possible mechanisms of growth inhibition and the signal transduction pathways involved in the inhibitory actions of IGFBP-3.

EXPERIMENTAL PROCEDURES

Materials

Cells were purchased from the American Type Culture Collection (Rockville, MD). Tissue culture reagents and plastics were purchased from Mediatech (Hemdon, VA), Becton Dickinson (Franklin Lakes, NJ) and Nunc (Naperville, IL). Zeocin, G418, and ponasterone A were purchased from Invitrogen (Carlsbad, CA). Monoclonal antibodies against cyclin D1 were purchased from NeoMarkers (Fremont, CA), cyclin D3 from Calbiochem (Cambridge, MA), cyclins A, E and poly(ADP-ribose) polymerase (PARP) from Santa Cruz Biotechnology (Santa Cruz, CA), cyclin-dependent kinase (cdk)4 from Transduction Laboratories (Lexington, KY). Polyclonal antibodies against retinoblastoma protein (Rb), phospho-Rb, p44/42 mitogen-activated protein kinase (MAPK), and phospho-p44/42 MAPK were purchased from New England Biolabs/Cell Signaling Technology (Beverly, MA). Monoclonal antibody against IGFBP-3 and a radioimmunoassay kit for IGFBP-3 were generously provided by Diagnostic Systems Laboratories (Webster, TX). Recombinant human IGF-I analog, Y60L-IGF-I was the generous gift of Protigen Inc. (Mountain View, CA). Fluorescein isothiocyanate (FITC)-conjugated Annexin V was purchased from Santa Cruz Biotechnology (Santa Cruz, CA). DEVD-7-amino-4-methylcoumarine (AMC) and LEHD-AMC flourogenic caspase substrate peptides were purchased from Biomol (Plymouth Meeting, PA). The ecdysone-inducible expression system was from Invitrogen (Carlsbad, CA). Human cyclin D1 cDNA was purchased from the American Type Culture Collection (Rockville, MD). A constitutively active Ras (RasV12) cDNA expression construct was the kind gift of Dr. Philip Stork, Vollum Institute, OHSU. DNA preparations were made using kits from Qiagen (Chatsworth, CA).

Generation of an MCF-7-derived Inducible IGFBP-3 Cell Line

A cDNA encoding human IGFBP-3 was cloned into the pIND expression vector. This construct was cotransfected with pVgRXR (encoding a hybrid ecdysone / retinoid X receptor) into MCF-7 cells using FuGene 6 transfection reagent (Roche, Indianapolis, IN). Cells were split 48 h later to low density into selective medium containing G418 (800 μg/ml) and zeocin (100 μg/ml). After 14 days, isolated foci of doubly resistant cells were subcultured and expanded. To test for inducible expression of IGFBP-3, each clone was cultured in the presence of the inducer ponasterone A (2-15 μM). Conditioned media were collected to test for ponasterone-inducible expression of IGFBP-3 by western immunoblotting. Hybrid receptor only-transfected cells (MCF-7:EcR) were used as a negative control.

Cell Culture

All cells were maintained in Dulbecco's modified Eagle's medium (DMEM) supplemented with 4.5 g/liter glucose, 110 mg/liter sodium pyruvate, and 10% fetal bovine serum (FBS). Stably transfected MCF-7:EcR cells were maintained in selective medium containing 100 μg/ml zeocin. Stably transfected MCF-7:IGFBP-3 cells were maintained in selective medium containing 800 μg/ml G418 and 100 μg/ml zeocin. For IGFBP-3 induction, cells were seeded and cultured until 60-70% confluent, then switched to serum-free media (SFM) with or without 15 μM ponasterone A for 72 h, unless otherwise indicated in the text. Conditioned media were collected and centrifuged at 1000 X g for 10 min to remove cell debris. For transient transfection assay, IGFBP-3 inducible stable cell line (MCF-7:IGFBP-3 #3) was seeded and cultured until 60-70% confluent, then switched to SFM. Trasient transfection with constituitively active Ras (Ras V12) or mock vector (pcDNA3) was done 2 h later and add ponasterone A on 8 h after transfection.

[^{3}H] Thymidine Incorporation Assay

Cells were seeded and cultured in 24-well dishes. Three days after IGFBP-3 induction, a 4-h pulse of 0.1 mCi of [^{3}H] thymidine (25 Ci/mM; NEN, Boston, MA) in a volume of 25 μl was added to each well. Cells were incubated, and the rate of DNA synthesis was estimated by measuring trichloroacetic acid-precipitable radioactivity as described previously (23).

Flow Cytometry: Cell Cycle and Apoptosis Assays

Cells were seeded and cultured in 6-well dishes, then switched to SFM with or without ponasterone A to induce the expression of IGFBP-3. Cells were harvested, pelleted at 1000 rpm for 5 min and washed three times with phosphate-buffered saline (PBS). For cell cycle analysis, each sample was resuspended in propidium staining solution (50 mg/ml propidium iodide, 100 U/ml RNase A, 0.1% Triton X-100, 0.1% sodium azide in PBS) and incubated for 30 min in the dark. Analysis of apoptotic cells was performed in IGFBP-3 inducible stable cell line using FITC-conjugated Annexin V according to the manufacturer's directions. Data were collected on a FACSCalibur flow cytometer (Becton Dickinson, Franklin Lakes, NJ) equiped with an argon laser. The data were analyzed using Cell Quest software (Becton Dickinson).

Western Immunoblotting

Cell lysates were prepared as described previously with minor modifications (24). In brief, confluent cells were washed with cold PBS, then scraped from plates in the presence of cold RIPA lysis buffer containing 20 mM Tris, pH 8.0, 150 mM NaCl, 1% Nonidet P-40, 0.5% Sodium deoxycholate, 0.1% SDS, containing a protease inhibitor cocktail (Roche, Indianapolis, IN). Cell lysates were rocked for 15 min at 4°C, then centrifuged to remove cell debris. The aliquots were stored at –70°C until use. Conditioned media samples were fractionated by 12% SDS-polyacrylamide gel electrophoresis (SDS-PAGE) under nonreducing conditions, while cell lysate samples were fractionated under reducing conditions. Fractionated proteins were electrotransferred onto Hybond-ECL nitrocellulose (Amersham Pharmacia, Arlington, VA). Membranes were blocked in 5% nonfat dry milk in Tris-buffered saline with 0.1% Tween-20 (TBST), and incubated with primary antibodies diluted in TBST for 2 h at room temperature or overnight at 4°C. Membranes were washed in TBST, then incubated with horseradish peroxidase-conjugated secondary antibodies (Southern Biotechnology Associates, Birmingham, AL), diluted 1:7000, for 1 h at room temperature. Immunoreactive proteins were detected using Renaissance Western Blot Chemiluminescence reagents (NEN, Boston, MA).

Northern Blot Analysis

Total RNAs from monolayer cultures of IGFBP-3 inducible stable cell line cultured with or without ponasterone A were isolated using the RNeasy RNA isolation kit (Qiagen, Chatsworth, CA), and quantitated by absorbance at 260 nm. Five µg of total RNA were electrophoresed on 1% formaldehyde gels and transferred to GeneScreen Plus nylon membranes (NEN, Boston, MA). Membranes were UV crosslinked and stained in 0.02% methylene blue/ 0.3 M NaOAc, pH 5.5, to verify equivalent loading and transfer. ^{32}P-labelled cDNA probes were prepared using the Prime It kit (Stratagene, Cedar Creek, TX). Membranes were hybridized in ULTRAhyb buffer (Ambion, Austin, TX) overnight at 42°C, and washed in 0.1 X SSC as described (3).

Caspase Assay

Cells were seeded in 96-well plates until 90% confluent, then incubated in triplicate with or without ponasterone A for the times indicated. Cells were lysed in 30 µl per well of ice-cold lysis buffer (50 mM HEPES, pH 7.4, 0.1% CHAPS, 0.1% Triton X-100, 1 mM DTT, 0.1 mM EDTA). Twenty µl of each lysate was used in assays for caspase activity using a combination of two fluorogenic peptide substrates, DEVD-AMC

and LEHD-AMC, which together cover a wide range of caspases. Lysates were distributed into a 96-well black plate and diluted in 190 µl of assay buffer (50 mM HEPES, pH 7.4, 100 mM NaCl, 0.1% CHAPS, 10 mM DTT, 1 mM EDTA, 10% glycerol). Serial dilutions of free 7-amino-4-methylcoumarin (Sigma, St. Louis, MO) diluted in assay buffer were included to generate a reference standard curve for determination of the amount of AMC released in each reaction. The plate was pre-incubated for 10 minutes at 37°C, then the reactions were started with the addition of DEVD-AMC and LEHD-AMC to each well to a final concentration of 40 µM each. Reaction kinetics were monitored for up to 16 hours at 37°C in a Bio-Rad Fluoromark fluorometer, with plate readings taken every 10 minutes at excitation/emission of 390 nm/460 nm. Of the remaining cell lysate, 5 µl were assayed for protein content. Data were analyzed from the linear portion of the reactions using Microplate Manager software (Bio-Rad), and final results were adjusted for protein content.

Immunocytochemistry

Cells were seeded in 8-chamber slides and cultured until 70% confluent, then incubated with or without ponasterone A for 48 or 72 hours. Cells were then rinsed twice in PBS, fixed in 4% paraformaldehyde, then rinsed again in PBS. For some antibodies, cells were additionally incubated in ice-cold methanol for 2 minutes on ice. Slides were blocked in 5% normal goat serum/PBS/0.1% Triton for 1-2 hours at room temperature, then incubated with primary antibodies diluted in blocking solution at 4°C overnight. Slides were rinsed 3 times for 5 minutes in PBS and incubated with secondary antibodies diluted in blocking solution for 1 hour at room temperature. Slides were rinsed as before, and cells were covered in 50% glycerol before coverslipping. Data were collected on a Nikon (Melville, NY) Diaphot 300 inverted fluorescent microscope eqipped with a 1.3 megapixel CCD camera (Princeton Instruments, Trenton, NJ) using IPLab software (Scanalytics, Fairfax, VA).

Densitometric and Statistical Analysis

Densitometric measurement of immunoblots were performed using a Bio-Rad GS-670 imaging densitometer (Melville, NY). All experiments were conducted at least three times. The data were analyzed with Student's *t* test, using the Microsoft Excel 98 software package.

RESULTS

Induced Expression of IGFBP-3 in the MCF-7-derived Stable Cell Lines

For these studies, we developed a subline of MCF-7 human breast cancer cells which expresses IGFBP-3 when cultured in medium containing an inducing compound, ponasterone A. The parental MCF-7 cells do not express detectable levels of IGFBP-3, and also do not express IGF peptides (25), making this cell line an ideal choice. A total of 16 selection-resistant clones were generated, and these were tested for inducible expression of IGFBP-3 by western immunoblotting of conditioned media samples. Figure 1 shows the panel of IGFBP-3 protein production from these 16 clones. IGFBP-3 was expressed in clones #2, #3, and #6 in an inducible manner, while constitutively expressed in clones #1 and #16. Expression of IGFBP-3 could be detected within 24 h at the concentrations of ponasterone A ranging from 1 to 15 μM, which did not affect cell viability (data not shown). Clone #3 (MCF-7:IGFBP-3 #3) was used for further experiments. Quantitative analysis of IGFBP-3 protein levels in conditioned media from induced MCF-7:IGFBP-3 #3 cells using a radioimmunoassay indicated that maximal levels of IGFBP-3, ranging from approximately 100-150 ng/ml, occurs on day 3 with 15 μM ponasterone A.

IGF-independent Inhibition of DNA Synthesis by IGFBP-3

Induced expression of IGFBP-3 resulted in an inhibition of DNA synthesis compared to IGFBP-3-uninduced cells (MCF-7:IGFBP-3 #3 without ponasterone A), shown in Fig. 2A. This inhibitory effect of IGFBP-3 was dose-dependent, with 43% inhibition occuring at a concentration of 5 μM ponasterone A ($p<0.001$) and 45% inhibition at 10 μM ponasterone A ($p<0.05$). Meanwhile, an inhibition of DNA synthesis in pVgRXR-transfected control cells (MCF-7:EcR) was not significant. This effect of IGFBP-3 does not result from blocking the mitogenic actions of IGFs by preventing their binding to IGF receptors, because MCF-7 cells, which do not produce IGF peptides (25), were cultured in SFM in our system to exclude the effects of IGFs. Moreover, this IGFBP-3-induced inhibitory effect was abolished by co-treatment with Y60L-IGF-I, an IGF analog with a leucine for tyrosine substitution at amino acid position 60, has a 100-fold reduced affinity for IGF receptors but full affinity for IGFBP-3. Since previous study reported that IGFs abolished the IGFBP-3-induced growth inhibitory effect by forming an IGF-IGFBP-3 complex, thereby blocking IGFBP-3 binding to the cell surface receptor (8), these data demonstrate the specificity of the IGF/IGF receptor-independent action of IGFBP-3 (Fig. 2B).

IGFBP-3 Arrests the Cell Cycle and Regulates Cell Cycle-related Proteins

To identify the mechanism responsible for the growth-inhibitory effect of IGFBP-3, we performed flow cytometry analysis. MCF-7:IGFBP-3 #3 and EcR cells cultured in SFM with or without ponasterone A were used to analyze the cell cycle profile by propidium iodide staining of DNA content followed by flow cytometry detection. The treatment of MCF-7:IGFBP-3 #3 with 15 μM ponasterone A caused a decrease in the percentage of cells in the S phase, from 18.4% in the absence of ponasterone A to 13.8% ($p<0.05$), and an accumulation of cells in the G1 phase from 72.1% to 78.1% ($p<0.05$)(Fig. 3). There was no change in the cell cycle distribution in EcR cells treated with ponasterone A (data not shown). These results suggest that induced expression of IGFBP-3 leads to a cell cycle arrest in the G1/S phase. We further examined whether IGFBP-3 affects the levels of cell cycle-related proteins, such as cyclin D1, cyclin D3, cyclin A, cdk4, Rb, and phospho-Rb, which are key cell cycle regulatory proteins for progression through G1 phase of the cell cycle in breast epithelial cells (27, 28). Firstly, we examined steady-state cyclin D1 mRNA levels by Northern blotting using MCF-7:IGFBP-3 #3 cells cultured in SFM with or without ponasterone A (Fig. 4A). Both cyclin D1 mRNA species, approximately 4.5 and 1.5 kb in size, were observed in MCF-7:IGFBP-3 #3 cells. A significant decline in 4.5-kb cyclin D1 mRNA levels was observed from 24 h after addition of ponasterone A. In contrast, the 1.5-kb mRNA species was not affected by addition of ponasterone A. The expression of IGFBP-3 mRNA was seen at 12 h, before the decrease in expression of cyclin D1 mRNA. Further time course study showed that the expression of IGFBP-3 mRNA was observed as early as 3 h after addition of ponasterone A (data not shown). Hybridization with β-actin verified equal loading of the gel. Further, immunoblot analysis revealed a concomitant decline in the levels of cyclin D1 protein in MCF-7:IGFBP-3 #3 cells in a dose-dependent manner on 72 h after addition of ponasterone A, but not in MCF-7:EcR cells (Fig. 4B). Decreased levels of cyclin D1 in MCF-7:IGFBP-3 #3 cells with ponasterone A was reversed by co-treatment of Y60L-IGF-I (Fig. 4C), suggesting the IGFBP-3 either directly or indirectly is involved in regulating cyclin D1 expression in an IGF/IGF receptor-independent manner.

Further analysis of various cell cycle-related proteins was performed in MCF-7:IGFBP-3 #3 cells cultured in SFM with or without ponasterone A at 0, 24, 48, 72 h. As shown in Fig. 5A, the levels of cyclin D1, cdk4, total Rb, and phosphorylated Rb were decreased from day 1 and levels of cyclin A from day 3, while the levels of cyclins D3 and E were unchanged. These results suggest that IGFBP-3 specifically decreases the levels of cyclin D1, cdk4, and total and phosphorylated Rb in these cells, representing a possible

mechanism for IGFBP-3-induced cell cycle arrest in G1/S phase. Ultimately, the decreased levels of Rb and phosphorylated Rb may serve to directly suppress exit from G1 phase. Additionally, as shown in Fig. 5B, immunocytochemistry experiments revealed a similar pattern of decreased level of these proteins. Immunodetectable levels of Cyclin D1 and phosphorylated Rb proteins were significantly reduced in cells induced to express IGFBP-3 compared to controls.

Effect of IGFBP-3 on the MAPK Signaling Pathway

Previous studies indicated that MAPK cascades modulate the expression of cyclin D1 (29); thus, we examined the effect of IGFBP-3 on MAPK cascade proteins. Fig. 6A shows that the levels of phosphorylated, but not total, p44/42 MAPK was decreased in MCF-7:IGFBP-3 #3 cells after induction of IGFBP-3. Further, immunofluorescent microscopy studies demonstrated that induced expression of IGFBP-3 results in a significant decrease as well as altered subcellular localization of phosphorylated p44/42 MAPK (Fig. 6B). This suggests that the IGFBP-3-mediated decrease in cyclin D1 results, at least in part, through modulation of p44/42 MAPK activity.

To further investigate the cross-talk between IGFBP-3 signaling and the MAPK signaling cascades, we transiently transfected constitutively active Ras (RasV12) into our cell system. As shown in Fig. 7, overexpression of oncogenic Ras resulted in stimulation of DNA synthesis as well as activation of phosphorylated p44/42 MAPK. Induction of IGFBP-3 expression caused a significant inhibition of both oncogenic Ras-induced DNA synthesis and p44/42 MAPK phosphorylation. Taken together, these data suggest that IGFBP-3 antagonizes Ras-MAPK signaling cascades.

IGFBP-3 Induces Apoptosis

At the same time, we determined whether IGFBP-3 could induce apoptosis using the Annexin V binding assay, which is used to identify cells in the early stages of the apoptotic process (26). Fig. 8A shows that induced expression of IGFBP-3 caused increase in the percentage of cells in the apoptosis, from 2.1% in the absence of ponasterone A to 21.8%, suggesting that IGFBP-3 induces apoptosis in this cell system. Additional indication that IGFBP-3 induces apoptosis came from results of assays for caspase activity. The data in Fig. 8B demonstrate that induction of IGFBP-3 expression causes an increase in caspase activity in

these cells as measured by incubating cell lysates with a combination of the purified fluorogenic caspase substrate peptides DEVD-AMC and LEHD-AMC. Caspase activity in uninduced cell lysates was detected at an average of 7.8 pmol AMC released/min/mg to an average of 10 pmol/min/mg with induced IGFBP-3 expression ($p<0.05$) at 48 hrs. In addition, IGFBP-3 increases caspase activity in a dose-dependent manner. Taxol, which reversibly binds to tubulin, used as a control apoptosis inducer resulted in an average of 14.1 pmol AMC released/min/mg. To present further evidence of caspase activation by IGFBP-3, we examined cleavage of one caspase substrate, poly(ADP-ribose) polymerase (PARP) by immunoblotting. This nuclear enzyme is proteolytically cleaved by activated caspases during apoptosis (30). As shown in Fig. 8C, the induced expression of IGFBP-3 resulted in an increase of the 85-kDa carboxy-terminal fragment of PARP (2-fold increase by densitometric measurement), confirming that IGFBP-3 induces apotosis at least, in part, through activation of caspases in the MCF-7 breast cancer cell system.

DISCUSSION

A growing amount of data has demonstrated that some IGFBPs, including IGFBPs -1, -3, -5, and presumably IGFBP-rPs, have their own IGF-independent biological actions (3, 5, 8-11). In particular, the IGF-independent effects of IGFBP-3 have been reported in various cell systems by treatment with recombinant IGFBP-3 exogeneously or use of stable transfection systems. However, its action requires relatively high concentrations of recombinant IGFBP-3, ranging from 300-1500 ng/ml, to achieve biological effects (8, 11, 20, 21). In the present study, we utilized ecdysone-inducible expression system in MCF-7 human breast cancer cells to examine the biological effects of endogenous IGFBP-3 expressed under controlled condition. In our system, human endogenous IGFBP-3 was induced to levels ranging 100-150 ng/ml concentrations comparable to those obtained in conditioned media after treatment with various reagents such as transforming growth factor-β, retinoic acid, tumor necrosis factor-α and antiestrogen, used to investigate the biological functions of IGFBP-3 in various cell systems. Our results demonstrate that relatively low concentration of endogenous IGFBP-3 is sufficient to inhibit DNA synthesis and induces apoptosis, despite relatively high concentrations (300-1000 ng/ml) of recombinant IGFBP-3 which were required to obtain similar biological effects of IGFBP-3 in MCF-7 cells (21). It is tempting to speculate that the difference in the levels of IGFBP-3 required for biological function may result from differences in IGFBP-3 preparations, that is, natural vs. recombinant forms, and endogenous secretory protein from the cell or exogenous form added to the cultures. In addition, post-translational modifications, such as glycosylation and phosphorylation, may affect the activity. On the other hand, sensitivity to IGFBP-3 may determine whether the cell types express the oncogenes or other molecules which influence the signaling pathways in the development of IGFBP-3 insensitivity. Martin and Baxter (31) reported that resistance to IGFBP-3 is induced in normal mammary epithelial cells transfected with oncogenic Ras, therby activating the MAPK/extracellular signal-regulated kinase (ERK) pathway. In contrast, MCF-10A normal human mammary epithelial cells, which require 10-100 ng/ml human plasma-derived IGFBP-3 to achieve a similar level of inhibition to that seen with 500-1500 ng/ml in the transformed cells, are considerably more sensitive to IGFBP-3 than breast cancer cells. Increased activity of oncogenic Ras-dependent signaling pathways is implicated in the development of IGFBP-3 insensitivity (31). It is of note that MCF-7 cells do not express oncogenic Ras, which may explain why such low concentrations of IGFBP-3 are sufficient to elicit biological effects.

The IGF-independent effect of IGFBP-3 has been extensively investigated in variety of cell systems;

however, the mechanisms by which these actions are exerted are not fully elucidated. Recent studies have proposed that IGFBP-3 functions as an apoptosis-inducing agent and that this action is mediated through a p53- and IGF-independent pathway in PC-3 prostate cancer cells (20), whereas IGFBP-3 has no direct inhibitory effect on Hs578T breast cancer cells but could accentuate apoptosis induced by ceramide (22). On the other hand, a vitamin D3 analog (Ro 24-5531) inhibits cell growth and increases IGFBP-3 mRNA and protein levels in human osteosarcoma cell line, and the inhibition in cell growth is accompanied by a decrease in the expression of p34cdc2, a protein critically involved in cell cycle regulation. These studies have provided circumstantial evidence that the action of IGFBP-3 involves cell growth arrest (32). Our present studies focus on identification of the potential mechanism for IGFBP-3-induced growth inhibition, and demonstrate for the first time that IGFBP-3 induces cell cycle arrest in G1 phase by regulating expression of cell cycle-related proteins, in particular cyclin D1, as well as inducing apoptosis by modulating proapoptotic caspase activities.

Since IGFBP-3 prevents cell cycle progression at G1 phase, we determined whether IGFBP-3 affects cell cycle-related proteins in MCF-7:IGFBP-3 #3 cells. Components responsible for the coordinated progression through the cell cycle include the cyclin-dependent kinases (cdks), regulatory cyclin subunits, and cdk inhibitors (33-35). Once extracellular signals activate the synthesis of the regulatory cyclin subunit, appropriate sites on the catalytic subunit must be phosphorylated by the cdk-activating kinase (CAK, also known cdk7) to phosphorylate the product of the Rb gene, resulting in the derepression of E2F/DP-dependent transcription and passage through the S phase of the cell cycle (36, 37). D-type cyclins (cyclins D1, D2, and D3), in conjunction with their catalytic partners, cdk4 and cdk6, execute their critical functions during mid-to-late G1 phase, as cells cross a G1 restriction point (33). Overexpression of cyclin D1 can shorten the G1 cell cycle phase, decrease cell size, and reduce requirements for growth factors (38-40). Microinjection of antisense constructs or antibodies to cyclin D1 into normal fibroblasts can prevent them from entering S phase (38, 41). In contrast, cyclin E is expressed later in G1 phase, and its expression is periodic and maximal at the G1-S transition (42). In our study, we have found that induction of IGFBP-3 leads to inhibition of expression of cyclin D1 mRNA followed by a reduction in protein levels, and concomitant decrease of cdk4, total Rb, and phospho-Rb proteins as an early event and decrease of cyclin A as a late event, indicating a possible mechanism for IGFBP-3-induced cell cycle arrest in the G1/S phase transition. In contrast, cyclin D3 and cyclin E do not show any change, suggesting that cyclin D1 is a major

player in the regulation of G1-S phase progression by IGFBP-3 in MCF-7 cells. Cyclin D1 is important for neoplastic transformation as well as cell cycle pregression. When cyclin D1 is cotransfected with other oncogenes, such as activated Ha-ras or adenovirus E1A into human fibroblast, malignant transformation of cells has been reported (43, 44). Overexpression of cyclin D1 in the mammary gland of transgenic mice induces mammary carcinoma (45). Moreover, dysregulated cyclin D1 expression have been observed in human neoplasia, including breast cancer (46, 47). These results suggest that IGFBP-3, which is able to modulate cyclin D1 expression, has a potential role in a strategy for anti-cancer therapy.

The expression of cyclin D1 is known to be regulated by transcriptional, translational, and post-transcriptional processes (48, 49). Multiple signaling pathways seem to be involved in the regulation of cyclin D1 expression at a transcriptional level. Previous studies have shown that cyclin D1 expression is regulated by the p44/42 MAPK, p38 MAPK, and Jun kinases (JNKs) (29). Moreover, direct induction of cyclin D1 can be achieved by serum, growth factors, cytokines, Rb, oncogenic Ras, and Src kinase (29, 50-53). Ectopic expression of E2F1 inhibits the cyclin D1 protein at the transcriptional level, suggesting a negative feedback for cells already in S phase (54). Decreased expression of cyclin D1 by IGFBP-3 shown in this study may be, at least in part, associated with the decreased level of p44/42 MAPK activity. Our results demonstrated that induced expression of IGFBP-3 results in inhibition of not only basal phosphorylation of p44/42 MAPK, but also oncogenic-Ras-induced phosphorylation of p44/42 MAPK, indicating that IGFBP-3 appears to interact with the Ras-MAPK signaling cascades, presumably on a downstream effector of Ras and thereby regulating cyclin D1 expression and subsequent cell cycle progression. More proximal events of IGFBP-3-induced antagonism of the MAPK signaling pathway will be the subject of future studies in our laboratory.

Beyond arrest of the cell cycle, our data also indicate that cellular expression of IGFBP-3 promotes apoptosis in MCF-7 cells. Apoptosis is a major multi-faceted form of cell death, that has been implicated as playing a role in several human diseases, including cancer. There are series of events involved in the commitment and execution of apoptotic cell death, several of which have been well characterized. Among these are changes in the plasma membrane, with the enzymatically-driven translocation or "flipping" of phosphatidylserine to the extracellular surface. The result of this process can be detected utilizing the binding properties of Annexin V, which binds preferentially to phosphatidylserine and other negatively charged phospholipids. Our results show a clear and significant increase in Annexin V binding in cells induced for

IGFBP-3 expression relative to controls. Another indicator of the apoptotic process is caspase activity. Caspases are a family of evolutionarily related cysteine-dependent proteases, with an universal specificity for Asp in the P_1 position, that play a prominent role during the progression of apoptosis. Activation of caspases and subsequent cleavage of critical cellular substrates are implicated in many of the morphological and biochemical changes associated with apoptotic cell death. Using an assay which detects activity of a broad range of caspases, we demonstrate a measurable and reproducible increase in caspase activity in IGFBP-3-induced cells relative to control uninduced cells, and further the increase in caspase activity was dose-dependent with regard to IGFBP-3. Furthermore, increased cleavage of the caspase substrate poly(ADP-ribose) polymerase (PARP) was observed after induction of IGFBP-3 expression. The nuclear enzyme PARP is proteolytically cleaved by activated caspases, primarily caspases 3 and 7 during apoptosis, but can also be cleaved in vitro by a wide range of caspases (30). It is of note that MCF-7 cells do not express caspase 3 due to a functional deletion of the gene (55), suggesting that the IGFBP-3-induced activation of caspase activity may be mediated primarily through caspase 7 and others. Nevertheless, these three lines of evidence indicate that induction/promotion of apoptosis is a major effect of cellular expression of IGFBP-3 in these cells.

Our previous studies have demonstrated that IGFBP-3 inhibits cell growth in an IGF-independent manner through an IGFBP-3 receptor in Hs578T breast cancer cells (8, 9, 13). In addition, we have sequenced and characterized a novel gene/protein which specifically interacts with IGFBP-3, designated the IGFBP-3 receptor (IGFBP3-R) (unpublished data). When we transfect IGFBP-3R into IGFBP-3-induced cells, DNA synthesis was further inhibited (by an average of 65%) compared to control IGFBP-3-induced cells (an average of 45%), suggesting that IGFBP-3 and IGFBP-3R appear to cooperatively suppress DNA synthesis and cell growth, to an extent greater than that seen with IGFBP-3 alone (unpublished data). Furthermore, the IGFBP-3 R alone results in no significant changes in DNA synthesis and cell growth in the same cell system, suggesting the necessity for an interaction between IGFBP-3 and IGFBP-3R for IGFBP-3-induced biological function.

We conclude that cellular expression of IGFBP-3 inhibits DNA synthesis and cell growth through cell-cycle arrest in G1 phase and induction of apoptosis at physiological concentrations in an IGF-independent manner in MCF-7 breast cancer cells. Regardless of the underlying mechanisms, the present study demonstrates that IGFBP-3 decreases the levels of cyclin D1 protein, followed by cdk4, Rb, and

phospho-Rb, indicating a possible mechanism of cell cycle arrest. Although we cannot exclude additional posttranscriptional and translational regulation of cyclin D1 by IGFBP-3, our results suggest that IGFBP-3 decreases the cyclin D1 expression at the level of transcription, in part, through the decline in p44/42 MAPK expression. This novel cell cycle regulatory and apoptosis-inducing aspect of IGFBP-3 has clinical significance in the prevention and/or treatment of human neoplasia, particularly in conjunction with the IGFBP-3 receptor.

REFERENCES

1. Shimasaki, S., and Ling, N. (1991) *Progress Growth Factor Res.* **3**, 243-266
2. Jones, J. I., and Clemmons, D. R. (1995) *Endocr. Rev.* **16,** 3-34
3. Kim, H. -S., Nagalla, S. R., Oh, Y., Wilson, E., Roberts, C. T. Jr., and Rosenfeld, R. G. (1997) *Proc. Natl. Acad. Sci. U. S. A.* **94,** 12981-12986
4. Baxter, R. C., Binoux, M.A., Clemmons, D. R., Conover, C. A., Drop, S. L. S., Holly, J. M. P., Mohan, S., Oh, Y., and Rosenfeld, R. G. (1998) *Endocrinology* **139,** 4036
5. Hwa, V., Oh, Y., and Rosenfeld, R. G. (1999) *Endocr. Rev.* **20,** 761-787
6. Villaudy, J., Delbe, J., Blat, C., Desauty, G., Golde, A., and Harel, L. (1991) *J. Cell Physiol.* **149,** 492-496
7. Liu, L., Delbe, J., Blat, C., Zapf, J., and Harel, L. (1992) *J. Cell. Biol.* **153,** 15-21
8. Oh, Y., Muller, H.L., Lamson, G., and Rosenfeld, R. G. (1993) *J. Biol. Chem.* **268,** 14964-14971
9. Oh, Y., Muller, H. L., Pham, H. M., and Rosenfeld, R. G. (1993) *J. Biol. Chem.* **268,** 26045-26048
10. Cohen, P., Lamson, G., Okajima, T., and Rosenfeld, R. G. (1993) *Mol. Endocrinol.* **7,** 380-386
11. Valentinis, B., Bhala, A., De Angelis, T., Baserga, R., and Cohen, P. (1995) *Mol. Endocrinol.* **9,** 361-367
12. MacDonald, R. G., Schaffer, B. S., Kang, I.-J., Hong, S. M., Kim, E. J., and Park J. H. Y. (1999) *J. Gastroenterol. Hepatol.* **14,** 72-78
13. Oh, Y., Muller, H. L., Ng, L., and Rosenfeld, R. G. (1995) *J. Biol. Chem.* **270,** 13589-13592
14. Gucev, Z. S., Oh, Y., Kelly, K. M., and Rosenfeld, R. G. (1996) *Cancer Res.* **56,** 1545-1550
15. Huynh, H., Yang, X., and Pollak, M. (1996*) J. Biol. Chem.* **271,** 1016-1021
16. Colston, K. W., Perks, C. M., Xie, S. P., and Holly, J. M. (1998) *J. Mol. Endocrinol.* **20,** 157-162
17. Rozen, F., Zhang, J., and Pollak, M. (1998) *Int. J. Oncol.* **13,** 865-869
18. Buckbinder, L., Talbott, R., Velasco-Miguel, S., Takenata, I., Faha, B., Seizinger, B. R., and Kley, N. (1995) *Nature* **377,** 646-649
19. Lalou, C., Lassarre, C., and Binoux, M. (1996) *Endocrinology* **137,** 3206-3212
20. Rajah, R., Valentinis, B., and Cohen P. (1997) *J. Biol. Chem.* **272,** 12181-12188
21. Nickerson, T., Huynh, H., and Pollak, M. (1997) *Biochem. Biophys. Res. Commun.* **237,** 690-693
22. Gill, Z. P., Perks, C. M., Newcomb, P. V., and Holly, J. M. P. (1997) *J. Biol. Chem.* **272,** 25602-25607
23. Beukers, M. W., Oh, Y., Zhang, H., Ling, N., and Rosenfeld, R. G. (1991) *Endocrinology* **128,** 1201-1203

24. Sakaguchi, K., Yanagishita, M., Takeuchi, Y., and Aurbach, G. D. (1991) *J. Biol. Chem.* **266,** 7270-7278

25. Gebauer, G., Jager, W., and Lang, N. (1998) *Antican. Res.* **18,** 1191-1195

26. Chan, A., Relter, R., Wiese, S., Fertig, G., and Gold, R. (1998) *Histochem. Cell. Biol.* **110,** 553-558

27. Sherr, C. J. (1996) *Science* **274,** 1672-1677

28. Sweeney, K. J., Musgrove, E. A., Watts, C. K., and Surherland, R. L. (1996) *Cancer Treat Res.* **83,** 141-170

29. Lavoie, J. N., L'Allemain, G., Brunet, A., Müller, R., and Pouysségur, J. (1996) *J. Biol. Chem.* **271,** 20608-20616

30. Fernandes-Alnemri, T., Takahashi, A., Armstrong, R., Krebs, J., Fritz, L., Tomaselli, K. J., Wang, L., Yu, Z., Croce, C. M., Salvenson, G., Earnshaw, W. C., Litwack, G., and Alnemri, E. S. (1995) *Cancer Res.* **55,** 6045-6052

31. Martin, J. L., and Baxter, R. C. (1999) *J. Biol. Chem.* **274,** 16407-16411

32. Velez-Yanguas, M. C., Kalebic, T., Maggi, M., Kappel, C. C., Letterio, J., Uskokovic, M., and Helman, L. J. (1996) *J. Clin. Endocrinol. Metab.* **81,** 93-99

33. Sherr, C. J. (1993) *Cell* **73,** 1059-1065

34. Morgan, D. O. (1997) *Annu. Rev. Cell Dev. Biol.* **13,** 261-291

35. Reed, S. I. (1997) *Cancer Surv.* **29,** 7-23

36. Weinberg, R. A. (1995) *Cell* **81,** 323-330

37. Dyson, N. (1998) *Genes Dev.* **12,** 2245-2262

38. Quelle, D. E., Ashmun, R. A., Shurtleff, S.A., Kato, J. Y., Bar-Sagi, D., Roussel, M. F., and Sherr, C. J. (1993) *Genes Dev.* **7,** 1559-1571

39. Resnitzky, D., Gossen, M., Bujard, H., and Reed, S. I. (1994) *Mol. Cell. Biol.* **14,** 1669-1679

40. Imoto, M., Doki, Y., Jian, W., Han, E. K., and Weinstein, I. B. (1997) *Exp. Cell Res.* **236,** 173-180

41. Tam, S. W., Theodoras, A. M., Shay, J. W., Draetta, G. F., and Pagano, M. (1994) *Oncogene* **9,** 2663-2674

42. Dulic, V., Lees, E., and Reed, S. I. (1992) *Science* **257,** 1958-1961

43. Lovec, H., Sewing, A., Lucibello, F. C., Muller, R., and Moray, T. (1994) *Oncogene* **9,** 323-326

44. Hinds, P. W., Dowdy, S. F., Eaton, E. N., Arnold, A., and Weinberg, R. A. (1994) *Proc. Natl. Acad. Sci. U. S. A.* **91,** 709-713

45. Wang, T. C., Cardiff, R. D., Zukerberg, L., Lees, E., Arnold, A., and Schmidt, E. V. (1994) *Nature (Lond.)* **369,** 669-671

46. Buckley, M. F., Sweeney, K. J., Hamilton, J. A., Sini, R. L., Manning, D. L., Nicholson, R. I., deFazio, A., Watts, C. K., Musgrove, E. A., and Sutherland, R. L. (1993) *Oncogene* **8,** 2127-2133

47. Bartkova, J., Lukas, J., Muller, H., Strauss, M., Gusterson, B., and Bartek, J. (1995) *Cancer Res.* **55,** 949-956

48. Choi, Y. H., Lee, S. J., Nguyen, P., Jang, J. S., Lee, J., Wu, M. L., Taqkano, E., Maki, M., Henkart, P. A., and Trepel, J. B. (1997) *J. Biol. Chem.* **272,** 28479-28484

49. Sherr, C. J. (1995) *Trends. Biochem. Sci.* **20,** 187-190

50. Westwick, J. K., Lambert, Q. T., Clark, G. J., Symons, M., Van Aelst, L., Pestell, R. G., and Der, C. J. (1997) *Mol. Cell. Biol.* **17,** 1324-1335

51. Lee, R. J., Albanese, C., Stenger, R., Watanabe, G., Inghirami, G., Haines, G. K., Penar, P., Webster, M., Muller, W. J., Brugge, J., Davis, R., and Pestell, R. G. (1999) *J. Biol. Chem.* **274,** 7341-7350

52. Brown, J. R., Nigh, E., Lee, R. J., Ye, H., Thompson, M. A., Saudou, F., Pestell, R. G., and Greenberg, M. E. (1998) *Mol. Cell. Biol.* **18,** 5609-5619

53. Muller, H., Lukas, J., Schneider, A., Warthoe, P., Bartek, J., Eilers, M., and Strauss, M. (1994) *Proc. Natl. Acad. Sci. U. S. A.* **91,** 2945-2949

54. Watanabe, G., Albanese, C., Lee, R. J., Reutens, A., Vairo, G., Henglein, B., and Pestell, R. G. (1998) *Mol. Cell. Biol.* **18,** 3212-3222

55. Kirsch, D., Doseff, A., Chau, B. N., Lim, D. S., de Souza-Pinto, N. C., Hansford, R., Kastan, M. B., Lazebnik, Y. A., and Hardwick, J. M. (1999) *J. Biol. Chem.* **274,** 21155-21161

Fig.1. Panel of IGFBP-3 expression in 16 clones tested for induction with ponasterone A. MCF-7 cells were stably transfected using the ecdysone-inducible system. Transfected cells were selected in G418- and Zeocin-containing medium. Incubation of the cells with Ponasterone A induces the expression of IGFBP-3. Clones 1 and 16 constitutively expressed IGFBP-3; clones 2, 3, and 6 expressed IGFBP-3 in an inducible manner.

Fig. 2. Inhibitory effect of IGFBP-3 on DNA synthesis in inducible stably transfected MCF-7 cells. A) Cells were treated with ponasterone A at concentrations of 0-10 μM for 72 h in SFM prior to assessing DNA synthesis by [^{3}H]-thymidine incorporation. Significant decreases in DNA synthesis compared with noninducible MCF-7:IGFBP-3 #3 cells were seen. * , $p<0.05$; ** , $p<0.001$ compared with cells without ponasterone A. B) Cells were treated with Y60L-IGF-I (100 ng/ml), an IGF-I analog with significantly reduced affinity for the IGF receptor but high affinity for IGFBPs, in the presence or absence of ponasterone A (10 μM) as indicated for 72 h prior to assay for [^{3}H]-thymidine incorporation. The inhibitory effect of IGFBP-3 was abolished by Y60L-IGF-I, demonstrating IGFBP-3 specificity and IGF independency. * , $p<0.05$ compared with cells treated with 10 μM ponasterone A.

Fig. 3. Cell cycle arrest in the IGFBP-3-induced cells. Asynchronous MCF-7:IGFBP-3 #3 cells were seeded with or without ponasterone A in SFM for 72 h. The percentages of cells in the various phases of the cell cycle were determined by propidium iodide staining for DNA content and subsequent flow cytometry. These data show that induced expression of IGFBP-3 resulted in an arrest of the cell cycle in the G1 phase. *, $p<0.05$ compared with cells without ponasterone A.

Fig. 4. Induced IGFBP-3 expression causes a reduction in cyclin D1 at mRNA and protein levels. A) Northern blot analysis of a time course of cyclin D1 and IGFBP-3 expression in induced and uninduced cells. With the induction of IGFBP-3, expression of the 4.5-kb cyclin D1 mRNA species is decreased. Expression of the 1.5-kb species is not affected. β-actin was used as a control. B) Western immunoblot analysis of cyclin D1 protein in the MCF-7:IGFBP-3 #3 and MCF-7:EcR cells after treatment with increasing concentrations of ponasterone A for 72 h. Induction of IGFBP-3 results in a significant decrease in the level of cyclin D1 protein. C) Co-treatment with Y60L-IGF-I reverses the decreased level of cyclin D1 protein showed in IGFBP-3-induced cells, demonstrating specificity of IGFBP-3.

Fig. 5. Cell cycle-related proteins affected by induction of IGFBP-3 expression. A) Western immonoblot analysis of various cell cycle-related proteins in the MCF-7:IGFBP-3 #3 cells cultured in SFM in the presence or absence of ponasterone A at indicated time. The expression of cyclin D1, cdk4, total Rb, and phospho-Rb starts to decline from day 1 in the IGFBP-3-induced cells, presenting a possible direct mechanism for IGFBP-3-induced cell cycle arrest. A decrease of cyclin A expression is evident after day 3. B) Immunofluorescent staining of cells showing the decrease in cyclin D1 and phosphorylated Rb detectable levels with the induction of IGFBP-3.

Fig. 6. IGFBP-3 induction causes a decrease in active MAPK. A) Western immunoblot analysis of p44/42 MAPK and phosphorylated p44/42 MAPK in the MCF-7:IGFBP-3 #3 cells cultured in SFM in the presence or absence of ponasterone A at indicated time. The phosphorylation of MAPKs declines with induction of IGFBP-3. B) Immunofluorescent staining of phospho-p44/42 MAPK in control uninduced and IGFBP-3-induced cells. A decrease in detectable levels of phospho-MAPK is evident, as well as altered subcellular localization.

Fig. 7. IGFBP-3 antagonizes Ras-induced MAPK signaling. MCF-7:IGFBP-3 #3 cells were transfected with a constitutively active Ras (RasV12) construct, which increased A) DNA synthesis and B) phosphorylation of p44/42 MAPK. Induction of IGFBP-3 expression by addition of ponasterone A at 8 h after transfection abrogated both of these RasV12-induced effects. Thymidine incorporation assay was done at 48 h after addition of ponasterone A, while preparation of cell lysates for immunoblotting was done at 12 h. * , $p<0.05$ compared with cells without ponasterone A.

Fig. 8. Induction of apoptosis in the MCF-7:IGFBP-3 #3 cells. A) Annexin V binding assay. Asynchronous MCF-7:IGFBP-3 #3 cells were seeded in 10% FBS with or without ponasterone A for 72 h. Cells were incubated with Annexin V, then binding of Annexin V was determined by flow cytometry. IGFBP-3-induced cells showed significantly increased binding of Annexin V, an indicator of cells undergoing apoptosis. B) Caspase assay. Asynchronous MCF-7:IGFBP-3 #3 cells were cultured in SFM with or without ponasterone A, and taxol as a control apoptosis inducer for 48 h, and cell lysates were assayed for caspase activity using DEVD-AMC and LEHD-AMC. Induction of IGFBP-3 caused a dose-dependent increase in caspase activity compared to control uninduced levels. * , $p<0.05$ compared with cells without ponasterone A. C) Detection of PARP cleavage to the p85 protein species as detected by western immunoblotting. An increase in the p85 species was seen in lysates from IGFBP-3-induced cells compared to uninduced controls.

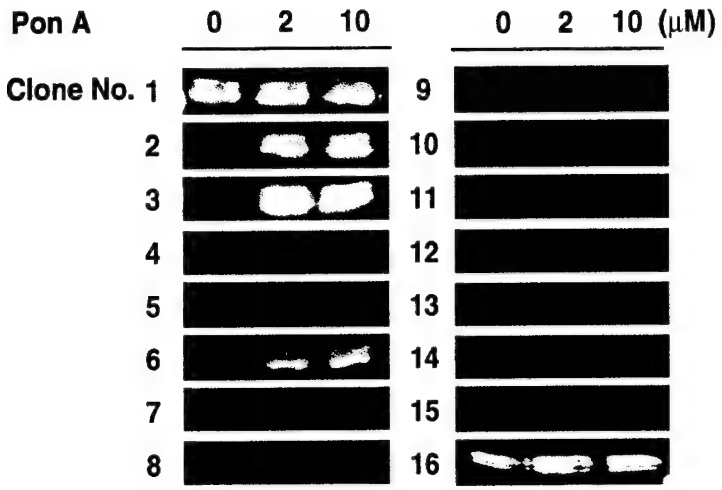
Pon A
0 2 10
0 2 10 (μM)
Clone No. 1
2
3
4
5
6
7
8
9
10
11
12
13
14
15
16

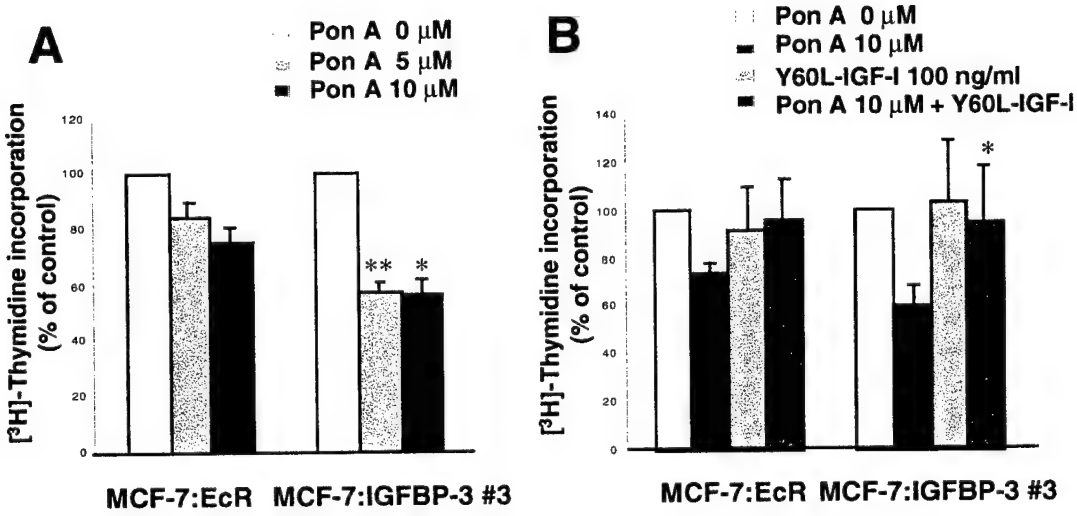
A
Pon A 0 μM
Pon A 5 μM
Pon A 10 μM
[³H]-Thymidine incorporation (% of control)
120
100
80
60
40
20
0
**
*
MCF-7:EcR
MCF-7:IGFBP-3 #3
B
Pon A 0 μM
Pon A 10 μM
Y60L-IGF-I 100 ng/ml
Pon A 10 μM + Y60L-IGF-I
[³H]-Thymidine incorporation (% of control)
140
120
100
80
60
40
20
0
*
MCF-7:EcR
MCF-7:IGFBP-3 #3

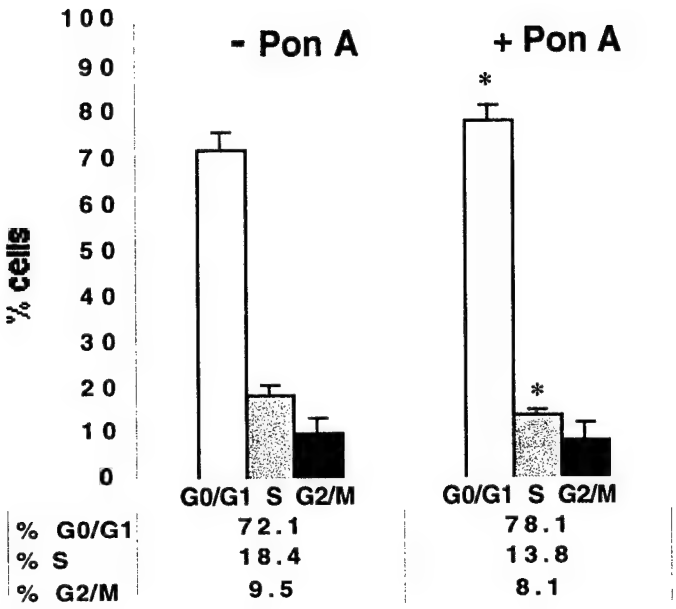

MCF-7:IGFBP-3 #3

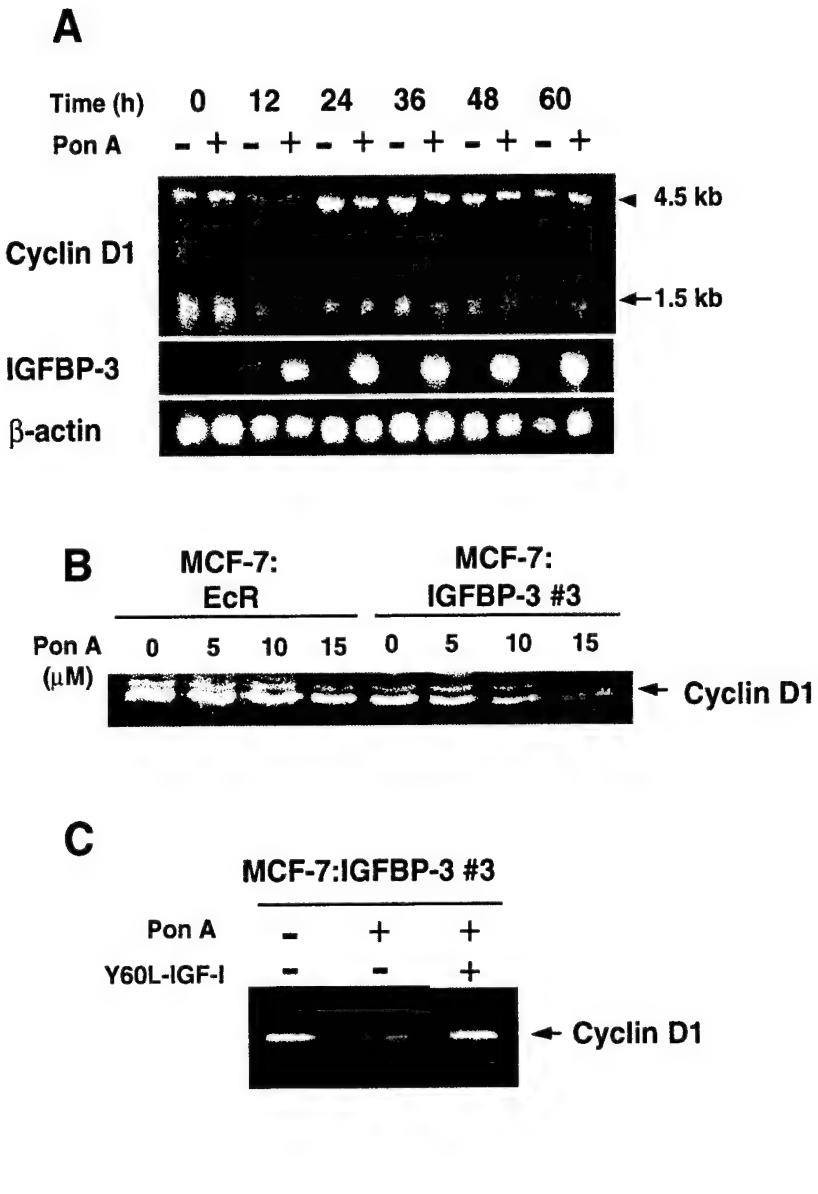
A
Time (h) 0 12 24 36 48 60
Pon A - + - + - + - + - + - +
Cyclin D1
4.5 kb
1.5 kb
IGFBP-3
β-actin
B
MCF-7: EcR
MCF-7: IGFBP-3 #3
Pon A (μM) 0 5 10 15 0 5 10 15
Cyclin D1
C
MCF-7:IGFBP-3 #3
Pon A - + +
Y60L-IGF-I - - +
Cyclin D1

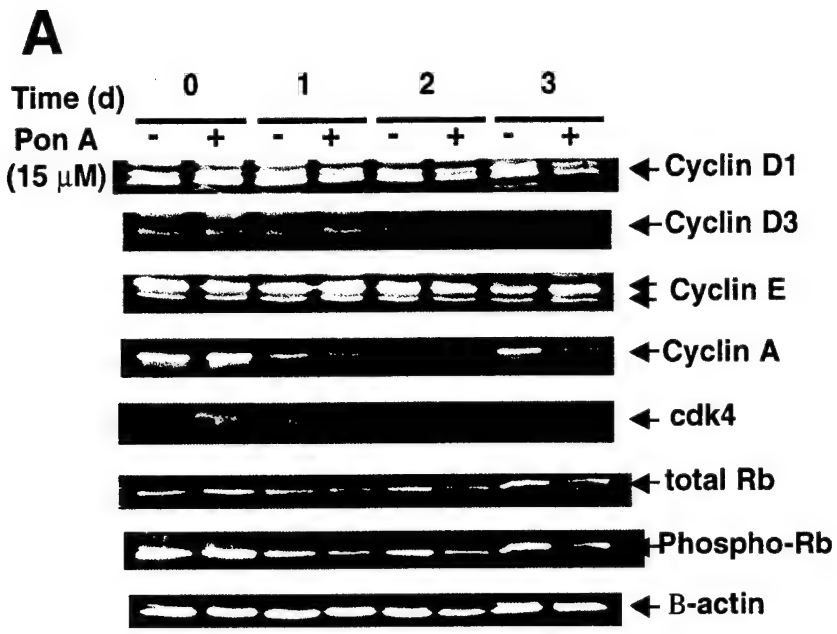
A
Time (d)
0
1
2
3
Pon A
(15 μM)
- + - + - + - +
Cyclin D1
Cyclin D3
Cyclin E
Cyclin A
cdk4
total Rb
Phospho-Rb
B-actin

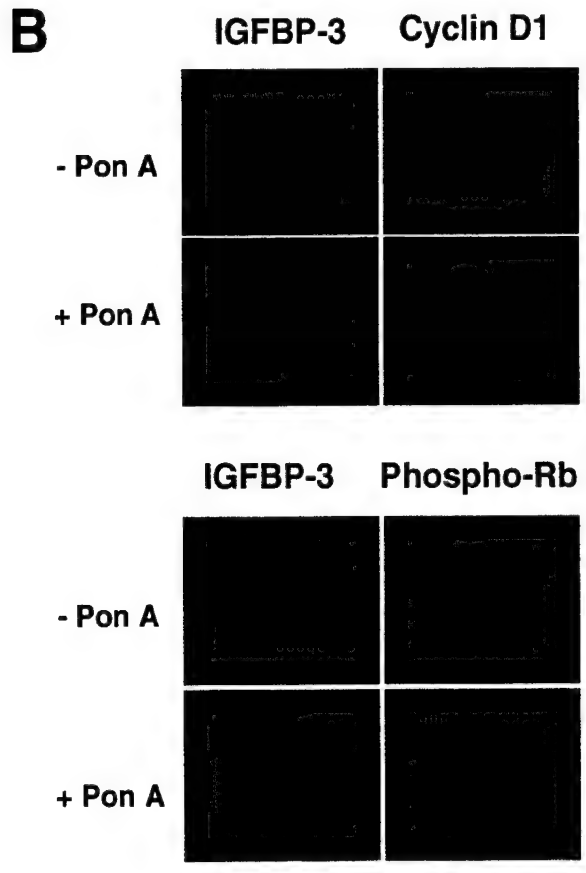
B
IGFBP-3
Cyclin D1
- Pon A
+ Pon A
IGFBP-3
Phospho-Rb
- Pon A
+ Pon A

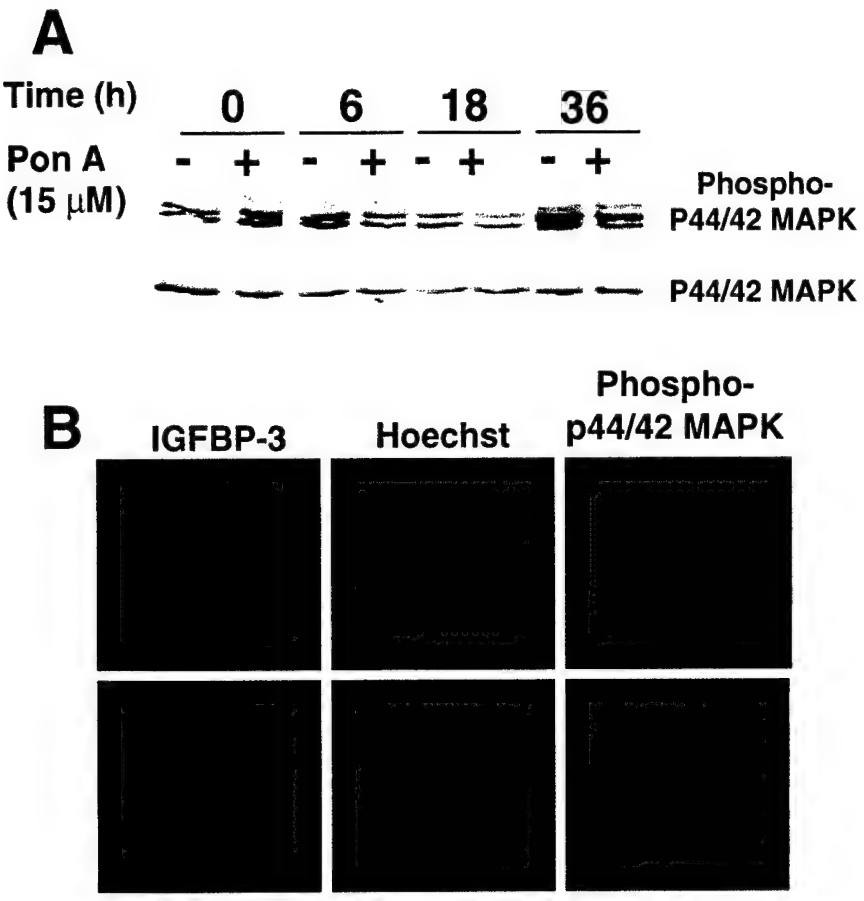
A
Time (h)
0
6
18
36
Pon A
(15 μM)
- + - + - + - +
Phospho-
P44/42 MAPK
P44/42 MAPK
B
IGFBP-3
Hoechst
Phospho-
p44/42 MAPK

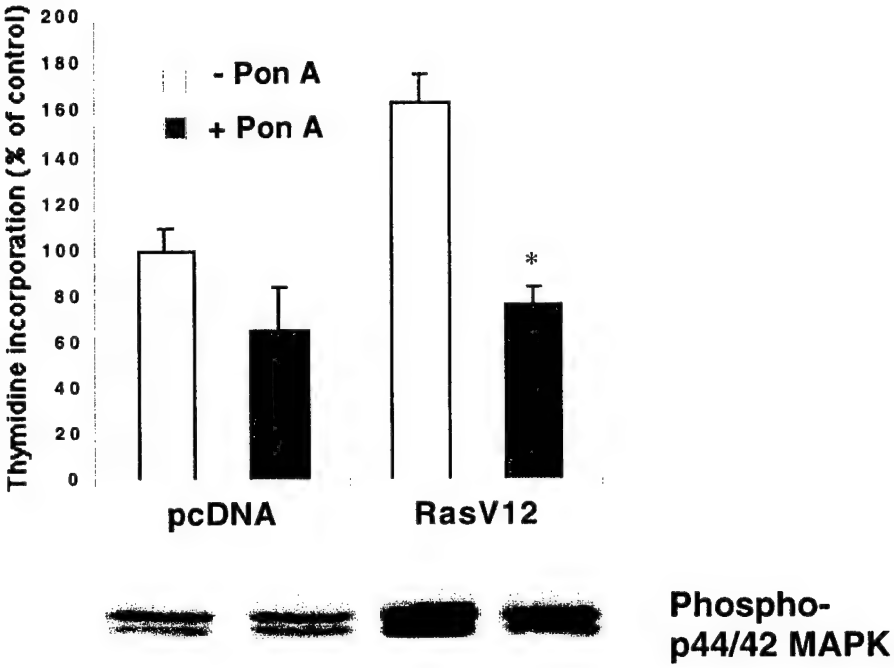
Thymidine incorporation (% of control)
200
180
160
140
120
100
80
60
40
20
0
- Pon A
+ Pon A
*
pcDNA
RasV12
Phospho-
p44/42 MAPK

A

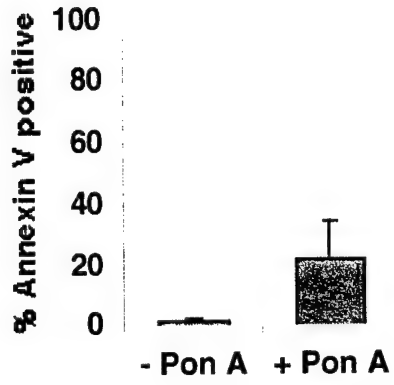
% Annexin V positive
100
80
60
40
20
0
- Pon A
+ Pon A

B

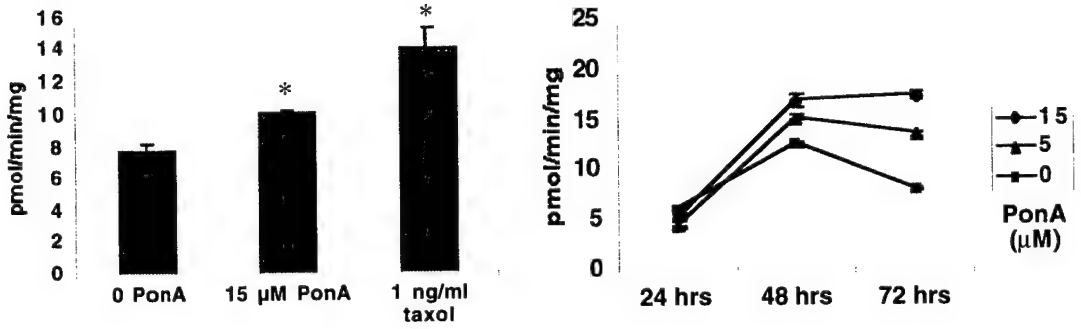
pmol/min/mg
16
14
12
10
8
6
4
2
0
*
*
0 PonA
15 µM PonA
1 ng/ml taxol
pmol/min/mg
25
20
15
10
5
0
24 hrs
48 hrs
72 hrs
15
5
0
PonA (µM)

C


Pon A - +
full length PARP
p85

0021-972X/98/$03.00/0
Journal of Clinical Endocrinology and Metabolism

Vol. 83, No. 4
Printed in U.S.A.

INSULIN AND IGF BINDING BY IGFBP-3 FRAGMENTS DERIVED FROM PROTEOLYSIS, BACULOVIRUS EXPRESSION AND NORMAL HUMAN URINE.

PETER VORWERK, YOSHITAKA YAMANAKA, ANNA SPAGNOLI, YOUNGMAN OH, RON G. ROSENFELD.#

Dept. Pediatrics NRC5, Oregon Health Sciences University, 3181 Sam Jackson Park Road, Portland, OR, 97201-3042

ABSTRACT

Recombinant human IGFBP-3 was proteolysed with different concentrations of plasmin for various periods of time. The major IGFBP-3 fragment resulting from this digestion migrated at ca. 15 kDa in nonreducing SDS-PAGE. Following the identification of this fragment as an N-terminal IGFBP-3 fragment, by use of N-terminus-specific monoclonal antibody and amino acid sequence analysis, we constructed and expressed a similar fragment in a baculovirus expression system. The fragments resulting from plasmin digestion, as well as the baculovirus-expressed recombinant human IGFBP-3^{1-97}, retain weak IGF binding and show specific insulin binding on cross-linking and western ligand blot. RhIGFBP-3^{1-97} can inhibit insulin receptor autophosphorylation in insulin receptor-overexpressing NIH 3T3 cells. Insulin and IGF binding to IGFBP-3 fragments could be further demonstrated in normal urine. These data indicate the physiological significance of IGFBP-3 fragments derived from proteolysis in vivo.

INTRODUCTION

IGFBPs are important regulators of IGF action, by modulating IGF binding to its receptors. IGFBP-3 is the major serum IGFBP and transports 70-90% of the circulating IGFs. In target cell systems, it sequesters IGFs and inhibits their hormonal action, but may, under specific conditions, also potentiate IGF action or exert IGF-independent effects (1,2). IGFBP-3 can be modified by proteolysis under various conditions. Initially described in human pregnancy serum, limited IGFBP-3 proteolysis and its significance *in vivo* have become intensive research subjects (3-6). Prostate specific antigen, matrix metalloproteinases, plasmin and thrombin have all been identified as IGFBP-3 proteases (7-12). Reports about limited proteolysis of IGFBP-3 by plasmin and the physiological relevance of the resulting fragments have provided different results with respect to size, sequence and IGF binding ability (11,12). Our laboratory has reported recently the ability of IGFBPs to specifically bind insulin (18). The N-terminal part of IGFBP-3 was shown to bind insulin and inhibit its interaction with the insulin receptor. In the present study, we have employed purified plasmin from human serum to proteolyse recombinant IGFBP-$3^{E.coli}$ *in vitro*, and have characterized the major resulting fragment and expressed it in a baculovirus expression system. Using baculovirus-expressed rhIGFBP-3^{1-97}, we describe the ability of this fragment to specifically bind IGFs and insulin and inhibit insulin receptor autophosphorylation.

MATERIAL AND METHODS

RhIGF-I, purchased from Bachem (Torrance, CA), was iodinated as described previously (13); IGFBP-$3^{E.coli}$ was a gift from Celtrix (Santa Clara, CA); plasmin was from Fluka (Ronkonkoma, NY), and ^{125}insulin was a gift from DSL (Webster, TX).

Proteolysis of IGFBP-$3^{E.coli}$ - 0.5 µg of IGFBP-$3^{E.coli.}$ were digested with different concentrations of plasmin (0.1 to 100 µg plasmin per 0.5 µg IGFBP-3) for 30 min at 37°C in Tris buffer (0,02 M tris, ph 7,4; 0,15 M NaCl). After digestion, the reaction was stopped with SDS sample buffer and loaded immediately on a 15% SDS-PAGE.

Expression and purification of human IGFBP-3^{1-97} fragment- The cDNA for IGFBP-3^{1-97} was generated by PCR amplification from the human IGFBP-3 cDNA and subcloned into pFASTBAC1 baculovirus expression vector (Gibco) using the unique EcoRI site at nt. position 917 in the IGFBP-3 cDNA (19). At the 3' end, a FLAG epitope (DYKDDDDK) followed by a stop codon and an unique XbaI site were introduced after aa position 97 of IGFBP-3. Primers (A) 5'-GTGAATTCTCGAGCTCGTCGA (915-935) and (B) 5'-GCTCTAGACTACTTGTCATCGTCGTCCTTGTAGTCG CGCAGGCGGCTGACGGCACTAG (1396-1418) were used, and the resulting PCR product was subcloned into the expression vector. After sequencing, the construct was introduced into viral DNA and transfected into SF-9 insect cells, according to the vendor's protocol. Western immunoblots (WIB) were performed with FLAG specific anti-M2 antibody (Kodak) and our polyclonal α-IGFBP-3 antibody (14). Large scale protein purification was done as described previously (13). Purity and concentration of IGFBP-3^{1-97} was determined by staining with Coomassie Blue and comparison with known amounts of IGFBP-$3^{E.coli}$

Western ligand blot (WLB)- Samples of plasmin-digested IGFBP-$3^{E.coli}$ or IGFBP-3^{1-97} were subjected to reducing SDS-PAGE (15% gel), electroblotted onto nitrocellulose filters, incubated overnight with $1.5x10^6$ cpm of ^{125}IGF-I or ^{125}insulin, washed, dried, and exposed to Biomax MS film (Eastman Kodak) for 4 to 14 days .

Affinity cross-linking - Plasmin-digested IGFBP-$3^{E.coli}$ or IGFBP-3^{1-97} was incubated with ^{125}IGF-I or ^{125}insulin (50,000 cpm) in the presence or absence of unlabeled ligand. After cross-linking with DSS, samples were subjected to SDS-PAGE (15% gel) and autoradiography on Biomax MS film.

Insulin receptor (IR) autophosphorylation assay - was performed as described previously (18). Briefly, confluent IR-overexpressing NIH3T3 cells were incubated in serum-free medium overnight and treated for 3 min with DMEM containing 75 ng/ml bovine insulin and different concentrations of IGFBP-3^{1-97}, which had been preincubated for 2h at 4°C. Cells were washed, solubilized and the lysate subjected to 8% SDS-PAGE. The β-subunit of the IR was detected by 4G10 anti-phosphotyrosine antibody.

Preparation of urine: Overnight urine from a healthy 4 year-old girl was filtered and concentrated with centriprep 10 (Amicon, Beverly, MA).

RESULTS

Proteolysis of IGFBP-3 by plasmin - Fig. 1A shows the immunoblot of IGFBP-$3^{E.coli}$ digested by different concentrations of plasmin, on a nonreducing 15% SDS-PAGE. At the lowest plasmin concentration, five different-sized IGFBP-3 fragments were detected (27-, 21-, 20-, 18-, and 15-kDa). On increasing the plasmin concentration 500-1000 fold, only the 15 kDa fragment remained stable. Similar results have been detected by digesting

0.5 μg IGFBP-3 with 15 μg plasmin for up to 4 hours (data not shown). Fig. 1B shows a WLB of plasmin-digested IGFBP-3 with ^{125}IGF-I (left panel) and ^{125}insulin (right panel). The predominant 15 kDa fragment is able to bind radiolabeld IGF-1, as well as insulin. Affinity cross-linking of IGFBP-3 proteolysed by plasmin with radiolabeled IGF-I or insulin, was also performed (Fig. 1C) The 15 kDa fragment could be crosslinked to radiolabeled IGF-I (left panel) and insulin (right panel).

Figure 1A: WIB of plasmin-digested IGFBP-3. In each lane 0.5 μg nonglycosylated IGFBP-3 were digested with different amounts of plasmin as indicated above and separated on a 15% SDS-PAGE under nonreducing conditions.

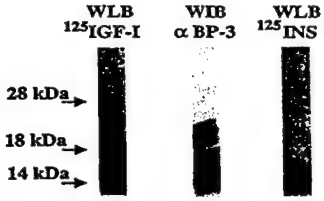

Figure1B: WLB of plasmin digested IGFBP-3. 5μg IGFBP-3$^{E.coli}$ were digested with 500μg plasmin and separated on a 15% SDS-PAGE under reducing conditions. WLB was done with radiolabled IGF-I (left lane) or insulin (right lane), and the control WIB is shown in the middle.

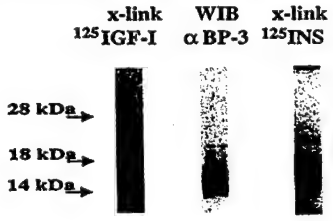

Figure1C: Cross-linking of plasmin digested IGFBP-3 (200 ng) to ^{125}IGF-I (left lane) or ^{125}insulin (right lane) and subsequent separation on a 15% nonreducing SDS-PAGE. WIB of the digestion is shown in the middle.

The NH_2-terminal sequence analysis of the 15 kDa IGFBP-3 fragment revealed that this fragment represents the NH_2 -terminal portion of IGFBP-3. Based on published cleavage sites for plasmin and other proteases, the size of the fragment, and the amino acid sequence of the 15 kDa fragment, we determined this fragment to be IGFBP-3$^{1-97}$.

Construction and expression of FLAG-tagged IGFBP-3$^{1-97}$ Fig. 2A is a WIB of the fractions collected during purification of FLAG-tagged IGFBP-3$^{1-97}$. Analysis of the purified protein and subsequent Coomassie staining (data not shown) showed a protein of approximately 16,000 molecular weight and 99% purity. Deglycosylation studies demonstrated a 15,000 Mw core protein with one N-linked glycosylation site. WLB of IGFBP-3$^{1-97}$ (Fig. 2 B) shows the ability of the synthetic fragment to bind ^{125}IGF-1 (left) or ^{125}insulin (right).

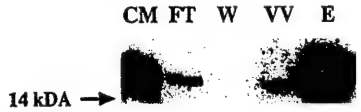

Figure 2A: WIB of baculovirus-expressed IGFBP-3$^{1-97}$ using anti-M2 antibody. CM-conditioned medium (30ml); FT-flow-through (30ml); W-wash (30ml); VV-void volume (1ml); E-elution (4ml). 25μl of each fraction were separated on a 15% SDS-PAGE under reduced conditions.

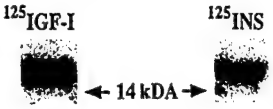

Figure 2B: WLB of baculovirus expressed IGFBP-3$^{1-97}$. 12μg of IGFBP-3$^{1-97}$ were separated on a 15% gel under reduced conditions and incubated with ligand, as indicated above.

Cross-linking of IGFBP-3$^{1-97}$ to ^{125}IGF-I and ^{125}insulin was performed. For both ^{125}IGF-I and ^{125}insulin, a dose-dependent linear increase in binding of the ligand to the fragment, starting at < 30 nmol fragment concentration, could be detected (data not shown). Competitive affinity cross-linking was performed with 100 pmol IGFBP-3$^{1-97}$. Both ^{125}IGF-I and ^{125}insulin bound specifically to the fragment, as shown by competition with unlabeled IGF-I or insulin, respectively (fig. 2C). Subsequent competition of labeled insulin with cold IGF-I or labeled IGF-I with cold insulin showed similar competition in both experiments (data not shown), indicating a similar, if not identical, binding site for IGF-I and insulin.

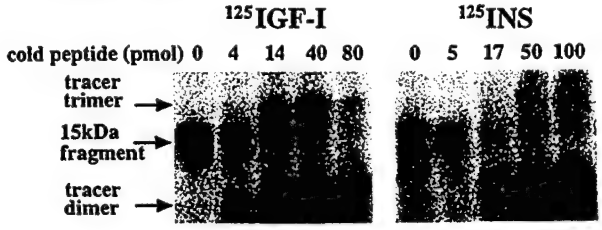

Figure 2C: Competitive affinity cross-linking of IGFBP-3$^{1-97}$ to ^{125}IGF-I (left) or ^{125}insulin (right). 100 pmol IGFBP-3$^{1-97}$ were crosslinked to ^{125}IGF-I or ^{125}insulin. Competition was done with the same unlabeled ligand at the concentrations indicated above.

Inhibition of Insulin receptor autophosphorylation by IGFBP-3$^{1-97}$
Figure 3A shows the anti-phosphotyrosine WIB of total cell lysate from insulin receptor-overexpressing NIH 3T3 cells, after insulin stimulation in the absence or presence of different amounts of rhIGFBP-3$^{1-97}$. The β-subunit of the insulin receptor was detected by anti-phosphotyrosine antibody. In contrast to full length IGFBP-3, the IGFBP-3$^{1-97}$ fragment was able to inhibit the autophosphorylation of the insulin receptor β-subunit in a dose-dependent manner. IGFBP-3$^{1-97}$ readily inhibited IR autophosphorylation more than 50% at a concentration of 10pmol and 90% at 100pmol (fig. 3B). It is of note that after preincubation of insulin and IGFBP-3$^{1-97}$, additional treatment with excess

insulin (100ng/ml) overcomes the inhibitory effect of IGFBP-3^{1-97}, suggesting that inhibition by IGFBP-3^{1-97} is through insulin binding (data not shown).

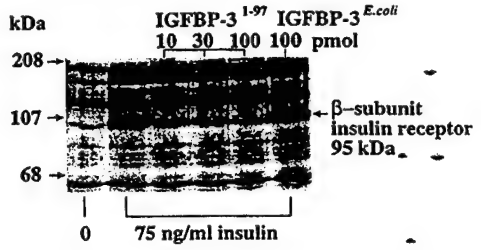

Figure 3A: Inhibition of IR autophosphorylation by IGFBP-3^{1-97}. Left lane: no insulin; lanes 2-6 (left to right): 75 ng/ml insulin; lanes 3-5: coincubation with 10, 30 or 100 pmol IGFBP-3^{1-97}; lane 6: coincubation with 100pmol IGFBP-$3^{E.coli}$.

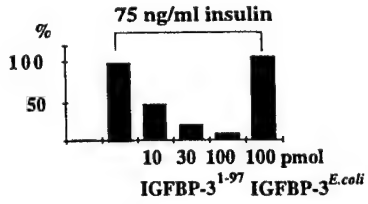

Figure 3B: Inhibition of IR autophosphorylation by IGFBP-3^{1-97}. Densitometric readings of 3 representative gels. Stimulation with 75 ng/ml insulin = 100%.

IGF-I and insulin binding of urinary IGFBP-3 fragments:
In concentrated urine, we detected IGFBP-3-related bands at 42/44 kDa, 29 kDa and 17.7 kDa by WIB with polyclonal αIGFBP-3 antibody under nonreducing conditions (data not shown). Under reducing conditions, the 17.7 kDa IGFBP-3 fragment migrates in 15% SDS-PAGE at approx. 14 kDa. Figure 4 shows a WLB of urine with radiolabeled IGF-I or insulin. The corresponding WIB identified two major IGFBP-3 fragments, at 29 and 14 kDa, both of which are detected by the radiolabeled ligands. The other bands (such as 18 kDa) could not be detected by IGFBP-3-immunoblot, and could result from other IGFBPs in urine which retain the ability to bind IGF-I and insulin.

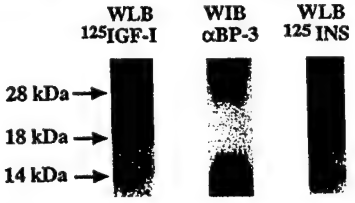

Figure 4: WLB of 30µl 500x concentrated urine under reducing conditions. The 29 kDa and the 14 kDa fragments are detected by IGFBP-3 antibody (middle). Both ^{125}IGF-I and ^{125}insulin can recognize these fragments in WLB . The 18 kDa band is not detected by WIB and presumably is a fragment of another IGFBP.

DISCUSSION

In vitro proteolysis of IGFBP-3 by plasmin is a convinient model for the study of the structure and action of IGFBP-3 fragments, since several laboratories have shown that plasmin is part of the *in vivo* proteolytic activity for IGFBP-3 under various conditions (6,10,12). In the present study, we describe an IGFBP-3 fragment derived from *in vitro* plasmin digestion. Previous studies identified this fragment as part of the N-terminal domain of IGFBP-3 (16). Because the N-terminus of IGFBP-3 is one of the highly conserved regions among the binding proteins and considered as a major IGF binding site, we expected the IGFBP$^{1-97}$ fragment to bind IGFs, although with reduced affinity. This assumption was supported by our previous report off a 17.7 kDa urinary IGFBP-3 fragment which binds IGF, although with reduced affinity compared to intact IGFBP-3. Similar to the IGFBP-3^{1-97} peptide, this fragment is glycosylated at one site and the deglycosylated core protein migrates at ca. 15 kDa in a nonreducing SDS-PAGE (20). Western immunoblots performed with previously described monoclonal IGFBP-3 antibodies (16) confirmed this 17.7 kDa urinary fragment as an N-terminal fragment (data not shown).

Our laboratory has reported recently on the ability of IGFBPs, especially IGFBP-7, to bind insulin (18). It could be shown additionally, that under reduced conditions, IGFBP-3 and a synthetic fragment similar to the highly conserved N-terminal region of IGFBP-3 (aa 1-87) bind insulin in WLB. This N-terminal fragment was able to inhibit insulin-induced autophosphorylation of the insulin receptor and subsequent IRS-1 phosphorylation in insulin receptor-overexpressing NIH-3T3 cells. In the present study, we demonstrate the ability of a physiological IGFBP-3 fragment to bind IGF and insulin in WLB and solution cross-linking. We were able to express this fragment in a baculovirus system and to purify it. Due to oligomerisation of synthetic IGFBP-3^{1-97} and possible conformational changes during immobilization of the fragment on the nitrocellulose membrane, binding to IGF-I and insulin in WLB could only be demonstrated under reducing conditions. Solution binding with subsequent cross-linking of the ligand to the fragment under more physiological conditions, however, could clearly demonstrate binding of both ligands to the fragment. The observation that this 15kDa IGFBP-3 fragment can bind IGF, albeit with decreased affinity, is consistent with our previous studies of IGFBP-3 fragments in urine (20), but in contrast with the report by Lalou et. al. (11); the failure of the latter group to detect specific IGF binding probably reflects technical aspects of the methods employed, although we cannot rule out the possibility that their plasmin-generated IGFBP-3 fragment differs from ours.

Insulin and IGF-I binding to a N-terminal urinary IGFBP-3 fragment described above was demonstrated by WLB with concentrated urine. Immunoprecipitation with a monoclonal antibody specific against the N-terminal part of IGFBP-3 and subsequent affinity cross-linking or WLB with ^{125}insulin or ^{125}IGF-I confirmed these findings (data not shown). For studying IGFBP-3 fragments from biological fluids, urine seems to be suitable, since the number and concentration of proteins, especially albumin and other IGFBPs, is limited and the concentration of the IGFBP-3 fragments is relatively high. Recent binding studies with biotinylated IGF-I in WLB demonstrated the IGF-I binding capacity of smaller IGFBP-3 fragments (17); this method was several times more sensitive than the usual WLB with radiolabeled ligand. By use of an extremely sensitive X-ray film, such as Biomax MS, however, we were able to detect binding with radioligands. The affinity of the described IGFBP-3 fragment for IGF-I, IGF-II (data not shown) and insulin is almost the same, in contrast to intact IGFBP-3, which has a much greater affinity for IGF than for insulin. IGFBP-3 proteolysis results,

therefore, in a dramatic decrease in IGF affinity, with a simultaneously increasing affinity for insulin. Insulin binding to proteolytic IGFBP-3 fragments and subsequent inhibition of insulin receptor action could play an important role in the microenvironment of the cell, where, in addition to IGFBP-3, a variety of other IGFBPs and IGF receptors compete for IGF. In contrast to IGFs, which are almost all trapped in complexes with IGFBPs, insulin is much more accessible for binding to the IGFBP-3 fragments. Whether the binding of insulin and subsequent inhibition of insulin action explain the IGF-independent actions of IGFBP-3 and its fragments remains to be seen (2, 11). This is unlikely to be the full explanation of IGFBP-3 action, however, in light of the ability of IGFBP-3 fragments to inhibit FGF (21).

Bereket and coworkers (15) reported the active involvement of insulin in the regulation of the IGFBP-3 protease activity in children with IDDM. They demonstrated that insulin administration during the first weeks of IDDM dramatically reduced serum proteolysis of IGFBP-3. It is also known that under conditions in which serum proteolysis of IGFBP-3 is increased (pregnancy, NIDDM, postsurgical catabolism or severe illness), insulin resistance is a common feature. How insulin itself is involved in the regulation of IGFBP-3 proteolysis, however, has to be further investigated.

ACKNOWLEDGMENTS

We thank B.J.Drucker for the 4G10 anti-phosphotyrosine monoclonal antibody, W.I.Wood for the IGFBP-3 cDNA and E. Wilson for her excellent technical help. This work was supported by a research grant from DFG, Bonn Germany (to PV), NIH grants # CA 58110 and DK51513 (to RGR) and US Army grant # DAMD 17-96-1-6204 (to YO).

REFERENCES:

1 Jones JI, Clemmons DR: Insulin-like growth factos and their binding proteins: Biological actions. Endocr Rev. 1995; 16 3-34

2 Oh Y, Mueller HL, Lamson G, Rosenfeld RG: Insulin-like growth factor (IGF)-independent action of IGF-binding protein-3 in Hs578T human breast cancer cells. J Biol Chem. 1993; 268: 14964-14971

3 Giudice LC, Farrell EM, Pham H, Lamson G, Rosenfeld RG: Insulin-like growth factor binding proteins in maternal serum throughout gestation and in the puerperium: effects of a pregnancy-associated serum protease activity. J Clin Endocrinol Metab. 1990; 71: 806-816.

4 Hossenlopp P, Segovia B, Lassarre C, Roghani M, Bredon M, Binoux M: Evidence of enzymatic degradation of insulin-like growth factor-binding proteins in the 150K complex during pregnancy. J Clin Endocrinol Metab. 1990; 71: 797-805.

5 Gargosky SE, Pham HM, Wilson KF, Liu F, Guidice LC, Rosenfeld RG: Measurement and characterization of insulin-like growth factor binding protein-3 in human biological fluids: discrepancies between radioimmunoassay and ligand blotting. Endocrinology. 1992; 131: 3051-3060.

6 Bang P, Fielder PJ: Human pregnancy serum contains at least two distinct proteolytic activities with the ability to degrade insulin-like growth factor binding protein-3. Endocrinology. 1997; 138: 3912-3917

7 Cohen P, Graves HCB, Peehl DM, Kamarei M, Guidice LC, Rosenfeld RG: Prostate-specific antigen is an insulin-like growth factor binding protein-3 protease found in seminal plasma. J Clin Endocrinol Metab. 1992; 75: 1046-1053

8 Campbell PG, Novak JF, Yanosick TB, McMaster JH: Involvement of the plasmin system in dissociation of the insulin-like growth factor-binding protein complex. Endocrinology. 1992;1401-1412

9 Fielder PJ, Rosenfeld RG, Gaves HCB, Grandbois K, Maack CA, Sawamura S, Sommer A, Cohen P: Biochemical analysis of prostate specific antigen-proteolyzed insulin-like growth factor binding protein-3. Growth Regulation. 1994; 1: 164-172

10 Fowlkes JL, Enghild JJ, Suzuki K, Nagase H: Matrix metalloproteinases degrade insulin-like growth factor binding protein-3 in dermal fibroblast cultures. J Biol Chem. 1994; 269: 25742-25746.

11 Lalou C, Lassarre C, Binoux M: A proteolytic fragment of insulin-like growth factor (IGF) binding protein-3 that fails to bind IGFs inhibits the mitogenic effects of IGF-I and insulin. Endocrinology. 1996; 137: 3206-3212.

12 Booth BA, Boes M, Bar RS: IGFBP-3 proteolysis by plasmin, thrombin, serum: heparin binding, IGF binding, and structure of fragments. Am J Physiol. (Endocrinol Metab.) 1996; 34: E 465-E470

13 Oh, Y, Nagalla SR, Yamanaka Y, Kim HS, Wilson E, Rosenfeld RG: Synthesis and characterization of insulin-like growth factor biding protein (IGFBP)-7. 1996 J Biol Chem. 271, 30322-30325

14 Wilson E, Oh Y, Rosenfeld R: Generation and characterization of an IGFBP-7 antibody. J Clin Endocrinol Metab. 1997; 82: 1301-1303

15 Bereket A, Lang CH, Belethen SL, Fan J, Frost RA, Wilson TA: Insulin-like growth factor binding protein-3 proteolysis in children with insulin-dependent diabetes mellitus: a possible role for insulin in the regulation of IGFBP-3 protease activity. J Clin Endocrinol Metab. 1995; 80: 2282-2288

16 Vorwerk P, Oh Y, Lee PDK, Khare A, Rosenfeld RG: Synthesis of IGFBP-3 fragments in a baculovirus system and characterization of monoclonal anti-IGFBP-3 antibodies. J Clin Endocrinol Metab. 1997; 82: 1301-1303

17 Op de Beeck L, Verlooy JEA, Van Buul-Offers SC, Du Caju MVL: Detection of serum insulin-like growth factor binding proteins on western ligand blots by biotinylated IGF and enhanced chemiluminescence. J Endocrinol. 1997; 154: R1-R5.

18 Yamanaka Y, Rosenfeld RG Wilson E, Oh Y: Inhibition of insulin receptor activation by insulin-like growth factor binding proteins. J Biol Chem. 1997: 272: 30729-30734

19 Wood WI, Cachianes G, Henzel WJ, Winslow GA, Spencer SA, Hellmiss R, Martin JL, Baxter RC: Cloning and expression of the growth hormone-dependent insulin-like growth factor-binding protein. Mol Endocrinol 1988; 2: 1176-1185.

20 Spagnoli A, Gargosky SE, Spadoni GL, Macgillivray, Oh Y, Boscherini B, Rosenfeld RG: Characterization of a low molecular mass form of insulin-like growth factor binding protein-3 (17.7 kilodaltons) in urine and serum from healthy children and growth hormone (GH)-deficient patients. J Clin Endocrinol Metab. 1995; 80: 3668-3675

21 Zadeh SM, Binoux M: The 16 kDa proteolytic fragment of insulin-like growth factor (IGF) binding protein-3 inhibits the mitogenic action of fibroblast growth factor on mouse fibroblasts with a target disruption of the type 1 IGF receptor gene. Endocrinology. 1997; 138: 3069-3072

THE JOURNAL OF BIOLOGICAL CHEMISTRY
Vol. 272, No. 49, Issue of December 5, pp. 30729–30734, 1997
Printed in U.S.A.

Inhibition of Insulin Receptor Activation by Insulin-like Growth Factor Binding Proteins*

(Received for publication, July 30, 1997, and in revised form, September 19, 1997)

Yoshitaka Yamanaka‡, Elizabeth M. Wilson, Ron G. Rosenfeld, and Youngman Oh§

From the Department of Pediatrics, School of Medicine, Oregon Health Sciences University, Portland, Oregon 97201

The insulin-like growth factors (IGFs) are transported by a family of high-affinity binding proteins (IGFBPs) that protect IGFs from degradation, limit their binding to IGF receptors, and modulate IGF actions. The six classical IGFBPs have been believed to have no affinity for insulin. We now demonstrate that IGFBP-7/mac25, a newly identified member of the IGFBP superfamily that binds IGFs specifically with low affinity is a high-affinity insulin binding protein. IGFBP-7 blocks insulin binding to the insulin receptor and thereby inhibiting the earliest steps in insulin action, such as autophosphorylation of the insulin receptor β subunit and phosphorylation of IRS-1, indicating that IGFBP-7 is a functional insulin-binding protein. The affinity of other IGFBPs for insulin can be enhanced by modifications that disrupt disulfide bonds or remove the conserved COOH terminus. Like IGFBP-7, an NH_2-terminal fragment of IGFBP-3 (IGFBP-$3^{(1-87)}$), also binds insulin with high affinity and blocks insulin action. IGFBPs with enhanced affinity for insulin might contribute to the insulin resistance of pregnancy, type II diabetes mellitus, and other pathological conditions.

Insulin-like growth factors (IGFs)-I[1] and -II are structurally related to insulin, sharing approximately 50% amino acid homology with insulin in the A- and B-chain regions but retaining a connecting peptide, as well as a carboxyl-terminal extension (1). The anabolic and mitogenic actions of IGFs are mediated largely through the type 1 IGF receptor, which, like the insulin receptor, is a heterotetrameric, membrane-spanning tyrosine kinase (2).

It has been accepted dogma that, unlike insulin, the IGFs bind to a family of binding proteins (IGFBPs) with high affinity and specificity (3–5). The six well characterized IGFBPs have significant sequence homology, including a GCGCCXXC motif as part of 10–12 conserved cysteines at the amino terminus and six conserved cysteines at the carboxyl terminus. We have recently characterized two additional secreted proteins with lower affinity for IGFs (IGFBP-7/mac25 and IGFBP-8/CTGF) and two additional potential members of the IGFBP superfamily (6–9). The structure of IGFBP-7 revealed the presence of amino-terminal conserved sequences, including 11 cysteines, but lower sequence homology in the normally well-conserved COOH terminus. IGFBPs 1–6 are believed to function as carrier proteins for IGFs, delaying degradation of IGF peptides and increasing their half-lives and inhibiting IGF access to receptors (10–14).

Proteolysis of IGFBPs, as observed during pregnancy, results in IGFBP fragments with decreased affinity for IGFs and, thereby, promotes enhanced access of IGFs to their receptors (15, 16). Recent studies have demonstrated that several of these IGFBPs, especially IGFBP-3, may also be capable of directly inhibiting cell growth in an IGF-independent manner (17–23). Both intact IGFBP-3 and IGFBP-3 proteolytic fragments have been shown to be capable of blocking the mitogenic effect of insulin (24, 25). Whether these effects reflect inhibition of insulin signaling pathways or a direct effect of IGFBP-3 and its fragments on cell growth remains unclear.

We have, therefore, reevaluated the ability of IGFBPs 1–6, IGFBP-7, and IGFBP-3 proteolytic fragments to bind insulin and have demonstrated that IGFBP-7 and NH_2-terminal fragment of IGFBP-3 (IGFBP-$3^{(1-87)}$) not only bind insulin specifically but also modulate insulin binding to its receptor and subsequently inhibiting insulin-stimulated autophosphorylation of the insulin receptor β subunit and phosphorylation of IRS-1.

EXPERIMENTAL PROCEDURES

Materials—High performance liquid chromatography-purified hIGFBP-1 from human amniotic fluid was kindly provided by Dr. D. R. Powell (Baylor College of Medicine, Houston, TX) (26). Recombinant human IGFBP-3 (rhIGFBP-3), a nonglycosylated 29 kDa core protein expressed in *Escherichia coli* cells, was the generous gift of Celtrix, Inc. (Santa Clara, CA) (27). Recombinant human IGFBP-2, -4, -5, and -6 were purchased from Austral Biologicals (San Ramon, CA). The cDNA for IGFBP-7 (mac25) was cloned, and baculovirus recombinants were made as described in (7). IGF-I was purchased from Bachem California (Torrance, CA). IGF-II was kindly provided by Lilly. Bovine insulin was purchased from Sigma. [(Gln^6, Ala^7, Thr^{18}, Leu^{19}, Leu^{27}] IGF-II ([QAYLL]IGF-II), a synthetic IGF-II analog, was synthesized as described previously (28). Human placentas were stripped of their membranes, washed in 0.25 M sucrose, and homogenized with a polytron (29). Crude microsomal membrane preparations were obtained via differential centrifugation (30). Anti-phosphotyrosine monoclonal antibody (4G10) was a generous gift from Dr. B. J. Druker (Dept. of Hematology and Medical Oncology, Oregon Health Sciences University). ^{125}I-(A14)-monoiodinated insulin was purchased from Amersham Corp. ^{125}I-labeled growth hormone and ^{125}I-prolactin were kindly provided by DSL (Webster, TX). $Na^{125}I$ was obtained from Amersham Corp. Iodination was performed by a modification of the chloramine-T technique to specific activities of 350–500 μCi/μg for IGF-I and -II. Reagents used for SDS-polyacrylamide gel electrophoresis (PAGE) were purchased from Bio-Rad Laboratories (Richmond, CA).

Cell Culture—NIH-3T3 cells overexpressing the human insulin receptor were kindly gifted from Dr. C. T. Roberts, Jr. (Dept. of Pediatrics, Oregon Health Sciences University) and grown in Dulbecco's modified Eagle's medium + 10% fetal calf serum + 500 μg/ml geneticin at 37 °C

* This work was supported by National Institutes of Health Grant CA58110 (to R. G. R.); U. S. Army Grant DAMD 17-96-1-6204 (to Y. O.). The costs of publication of this article were defrayed in part by the payment of page charges. This article must therefore be hereby marked "*advertisement*" in accordance with 18 U.S.C. Section 1734 solely to indicate this fact.

‡ Present address: Dept. of Pediatrics, Okayama University Medical School, 2-5-1 shikata-cho, Okayama 700, Japan.

§ To whom correspondence should be addressed: Dept. of Pediatrics, School of Medicine, Oregon Health Sciences University, 3181 S. W. Sam Jackson Park Rd., NRC5, Portland, OR 97201. Tel.: 503-494-1930; Fax: 503-494-1933; E-mail: ohy@ohsu.edu.

[1] The abbreviations used are: IGF, insulin-like growth factor; IGFBP, IGF binding protein; IRS-1, insulin receptor substrate-1; PAGE, polyacrylamide gel electrophoresis; m.o.i., multiplicity of infection; WLB, Western ligand blot; DTT, dithiothreitol.

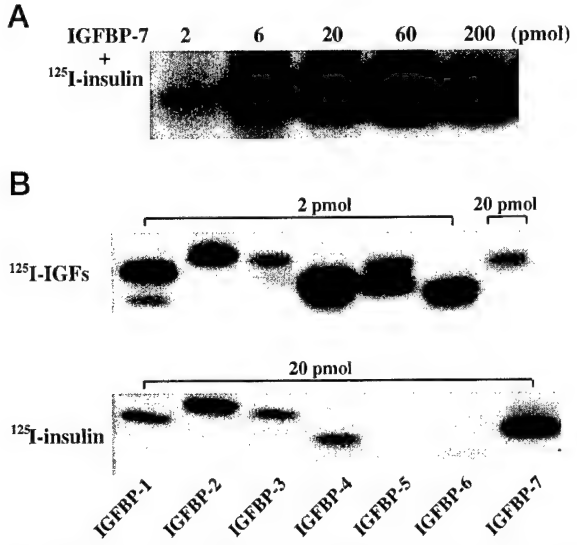

FIG. 1. **Affinity cross-linking of IGFBP with ^{125}I-insulin or ^{125}I-IGFs.** *A*, 2–200 pmol of IGFBP-7 were incubated with ^{125}I-insulin (20,000 cpm) for 16 h at 4 °C. At the end of incubation, disuccinimidyl suberate was added to a final concentration of 0.5 mM. After cross-linking for 15 min at 4 °C, the samples were subjected to 12% SDS-PAGE and autoradiography. *B*, IGFBPs 1–7, at the concentrations indicated in the figure, were incubated with a mixture ^{125}I-IGF-I (10,000 cpm) and ^{125}I-IGF-II (10,000 cpm) (*top*), or ^{125}I-insulin (20,000 cpm) (*bottom*) and cross-linked as in Fig. 1*A*.

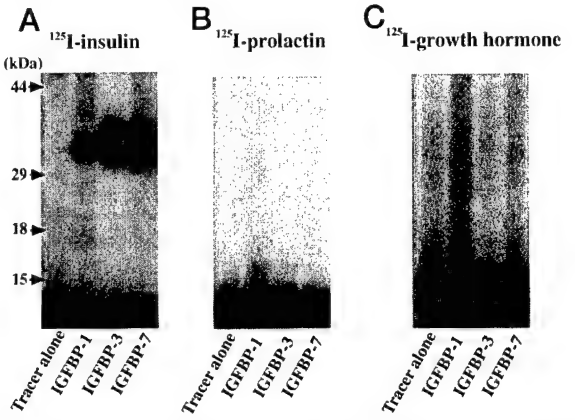

FIG. 2. **Specificity of IGFBP binding to ^{125}I-insulin.** Autoradiogram of ^{125}I-insulin (*A*), ^{125}I-prolactin (*B*), and ^{125}I-labeled growth hormone (*C*) cross-linked to 20 pmol of IGFBP-1, -3, or -7, as in Fig. 1.

with 5% CO_2. High Five cells were maintained in ExCell 405 Media (JRH Biosciences, Lenexa, KS) at 27 °C. The wild-type baculovirus (AcNPv) was obtained from Invitrogen Inc. (Carlsbad, CA). All tissue culture media and components were purchased from Life Technologies, Inc.

Affinity Cross-linking—Aliquots of reagents plus binding buffer (50 mM Tris-HCl, pH 7.4) were incubated with ^{125}I-insulin (20,000 cpm), ^{125}I-IGF-I (20,000 cpm), or ^{125}I-IGF-II (20,000 cpm) with or without indicated reagents, at the concentrations indicated under "Results" and in Figs. 1–3 for 16 h at 4 °C. At the end of incubation, the cross-linking reagent disuccinimidyl suberate (Pierce) was added to a final concentration of 0.5 mM. After cross-linking for 15 min, the samples were subjected to 12% SDS-PAGE and autoradiography. Bands were quantified by densitometry, as calculated by a densitometer (Bio-Rad).

Generation and Purification of Recombinant IGFBP-3$^{(1-87)}$—Polymerase chain reaction was used to add a FLAG epitope sequence (DYKDDDDK) and a new stop codon immediately following amino acid 87 of the mature IGFBP-3. After sequencing, this fragment was subcloned into the baculovirus expression vector pFASTBAC1 (Life Technologies, Inc.) and transfected into Sf9 insect cells, and viral recombinants were identified by immunoblotting with the anti-FLAG M2 antibody (Eastman Kodak, New Haven, CT). Recombinant protein was purified from the media of High Five cells after infecting at an m.o.i. = 3 for 3 days at 27 °C. The media was collected, and the protein was purified over anti-FLAG M2 affinity beads according to the manufacturer protocol by elution with the FLAG peptide. The purified protein was subjected to SDS-PAGE in a 15% gel and stained with Coomassie Blue or transferred to nitrocellulose for immunodetection. Protein fractions were pooled, concentrated, and quantitated by comparison with known amounts of BSA by silver staining (Bio-Rad). Immunoblotting using the enhanced chemiluminescence (ECL) detection technique was performed as described in Wilson *et al.* (31) using a 1:3000 dilution of anti-FLAG M2 antibody and incubating for 16 h at 4 °C and then in a 1:3000 dilution of anti-mouse IgG horseradish peroxidase (Amersham Corp.) for 1 h at room temperature.

Western Ligand Blot Analysis—Ligand blotting was performed as described in Hossenlopp *et al.* (32) with minor modifications. Briefly, IGFBP-1, IGFBP-3, IGFBP-3$^{(1-87)}$, and IGFBP-7 at the concentrations indicated in the text and figures in SDS sample buffer (62.5 mM Tris-HCl, pH 6.8, 40% glycerol, and 2.3% SDS) with or without 100 mM dithiothreitol (DTT) were analyzed by SDS-PAGE (12 or 15%). Separated proteins were electroblotted onto nitrocellulose filters, which were incubated overnight with 1.5×10^6 cpm of ^{125}I-insulin or a mixture of ^{125}I-IGF-I and ^{125}I-IGF-II, washed, dried, and exposed to film (Biomax; Eastman Kodak).

Insulin Receptor Binding Assay—20,000 cpm of ^{125}I-insulin were preincubated for 2 h at 4 °C with unlabeled IGFBP-3, IGFBP-7, and insulin at concentrations indicated in the figure and then incubated with 50 μg of microsomal placental crude membranes in 500 μl of binding buffer (50 mM Tris-HCl, 0.5% BSA, pH 7.4) for 16 h at 4 °C. Samples were centrifuged at 10,000 × *g* for 10 min at 4 °C. After samples were centrifuged, pellets were counted in a γ-counter.

Tyrosine Phosphorylation Assay—Confluent NIH-3T3 cells stably transfected with the human insulin receptor cDNA were exposed for 3 min to 100 ng/ml insulin, which had been preincubated with IGFBP-3, IGFBP-3$^{(1-87)}$, or IGFBP-7 for 2 h at 4 °C. The reaction was quenched by solubilization buffer (1% Nonidet P-40, 20 mM Tris-HCl, pH 8.0, 1 mM EDTA, 150 mM NaCl, 10% glycerol, 12 units/ml aprotinin, 1 mM phenylmethylsulfonyl fluoride, and 1 mM Na_3VO_4). Solubilized proteins were separated by SDS-PAGE (8%) and visualized by immunoblot analysis. For immunoblot analysis, the filters were blocked in TBS-T containing 5% non-fat dry milk for 1 h at room temperature and then incubated with anti-phosphotyrosine monoclonal antibody (1.5 μg/ml) diluted by Tris-buffered saline + 0.1% Triton X-100 overnight at 4 °C. The filters were then rinsed and incubated in a 1:3000 dilution of goat anti-mouse IgG-conjugated horseradish peroxidase (Amersham Corp.) for 1 h at room temperature. Immunoreactive proteins were visualized using the ECL detection system. Alternatively, solubilized proteins were immunoprecipitated with anti-IRS-1 antibody (Upstate Biotechnology, Lake Placid, NY) and were subjected to immunoblot using anti-phosphotyrosine antibody as above. In parallel, solubilized proteins were subjected to immunoblot using anti-IRS-1 antibody.

Statistical Analysis—Data were analyzed with a two-tailed Student's *t*-test, using the software program Instat 2.01 (Graphpad, San Diego, CA). Values are expressed as means ± S.D.

RESULTS

Affinity Cross-linking of IGFBPs 1–7—To evaluate the affinity of IGFBPs 1–7 for IGFs and insulin, the affinity cross-linking was performed with ^{125}I-IGF-I + ^{125}I-IGF-II or ^{125}I-insulin. Affinity cross-linking of IGFBP-7 with ^{125}I-insulin shows that IGFBP-7 binds insulin in a dose-dependent manner (Fig. 1*A*). As shown in Fig. 1*B*, *top panel*, the expected sizes of individual IGFBPs coupled to 7 kDa ^{125}I-IGF-I or ^{125}I-IGF-II were detected on the SDS-PAGE gel. In a similar way, Fig. 1*B*, *bottom panel*, showed ^{125}I-insulin bound to IGFBPs 1–7 with proper size of bands. This data demonstrates that IGFBPs 1–6 also bind insulin but with significantly reduced affinity compared with their affinities for IGFs. In contrast, the ratio of insulin:IGF binding for IGFBP-7 was approximately 500-fold higher than for IGFBPs 1–6 by densitometric analysis.

To establish the specificity of IGFBP binding to insulin, we attempted to cross-link IGFBP-1, -3, and -7 with ^{125}I-prolactin (Fig. 2*B*) and ^{125}I-growth hormone (Fig. 2*C*), as well as with ^{125}I-insulin (Fig. 2*A*). Although these IGFBPs failed to bind the other proteins, binding of ^{125}I-insulin was confirmed. Furthermore, analysis of competitive affinity cross-linking revealed

that the relative affinities of IGFBP-7 are: insulin ≥ IGFs ≥ [QAYLL] IGF-II (an IGF-II analog whose affinity for IGFBPs 1–6 is normally 100-fold less than that of native IGF-II). In contrast, affinities for IGFBP-3 are: IGFs ≫ insulin > [QAYLL] IGF-II (Fig. 3, *A* and *B*). The binding of IGFBP-3 or -7 to ^{125}I-IGFs or ^{125}I-insulin was competitively displaced by both IGFs and insulin, suggesting that the insulin binding site may be at, or near, the IGF binding site. IGFBP-7 was found to have similar affinity for IGFs and insulin (IC_{50} = 20–34 nM). Previous studies have suggested that IGF binding sites reside on both the NH_2- and COOH-terminal regions of the IGFBP-3 molecule; each binding site is individually capable of low-affinity binding, whereas high-affinity binding of IGFs requires the presence of both binding domains. Taken together, our data suggest that the low affinity of IGFBP-7 for IGFs and the relatively high affinity for insulin, compared with those of IGFBPs 1–6, can be attributed to the lack of conserved amino acid sequence and cysteines at the COOH terminus of IGFBP-7 (only 1 of the 6 cysteines is conserved) although IGFBP-7 retains 11 of the 12 cysteines found in the IGFBPs at the NH_2 terminus. High-affinity binding of IGFBPs to IGFs thus appears to require proper structural configuration involving both NH_2- and COOH-terminal ligand-binding domains.

Reduction or Fragmentation of IGFBPs Enhances the Affinity for Insulin—Insulin binding to IGFBPs can be further demonstrated by use of WLB. It appears that insulin binding to IGFBPs is much less effective in WLBs, especially in the absence of DTT compared with that seen in solution binding, as assessed by affinity cross-linking (Fig. 1). This presumably reflects changes in the tertiary structure of IGFBPs during SDS-PAGE. However, WLB demonstrated that reduction of

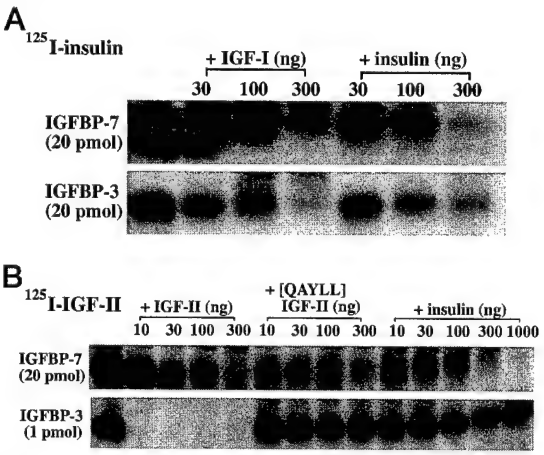

FIG. 3. **Competitive affinity cross-linking of IGFBP-7 and -3.** *A*, ^{125}I-insulin was cross-linked to 20 pmol of IGFBP-7 (*top*) or IGFBP-3 (*bottom*) alone or in the presence of unlabeled IGF-I or insulin. *B*, ^{125}I-IGF-II was cross-linked to 20 pmol of IGFBP-7 (*top*) or 1 pmol of IGFBP-3 (*bottom*) alone or in the presence of unlabeled IGF-II, [QAYLL] IGF-II, or insulin. Cross-linking was performed as in Fig. 1.

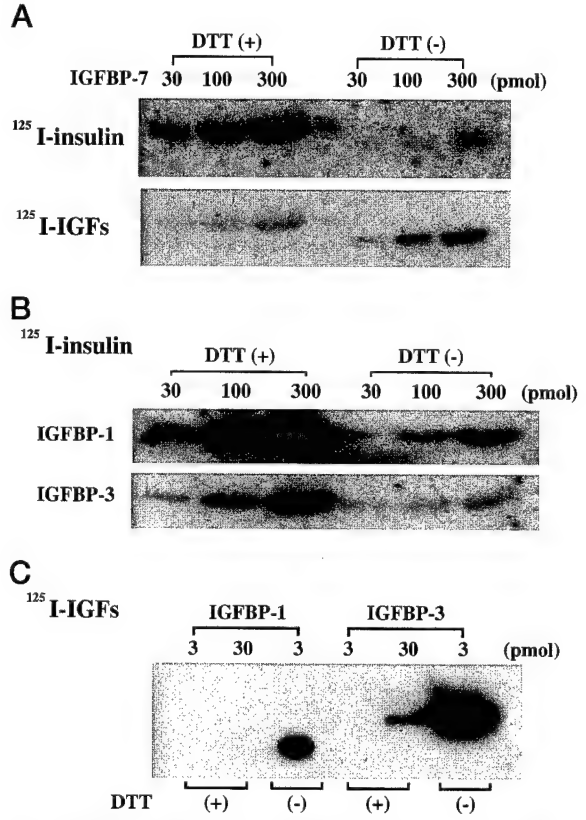

FIG. 4. **Western ligand blot of IGFBP-1, -3, and -7.** IGFBP-1, -3, and -7 at the concentrations indicated in the figures with or without 100 mM DTT were processed by SDS-PAGE. *A*, 12%; *B* and *C*, 15%.

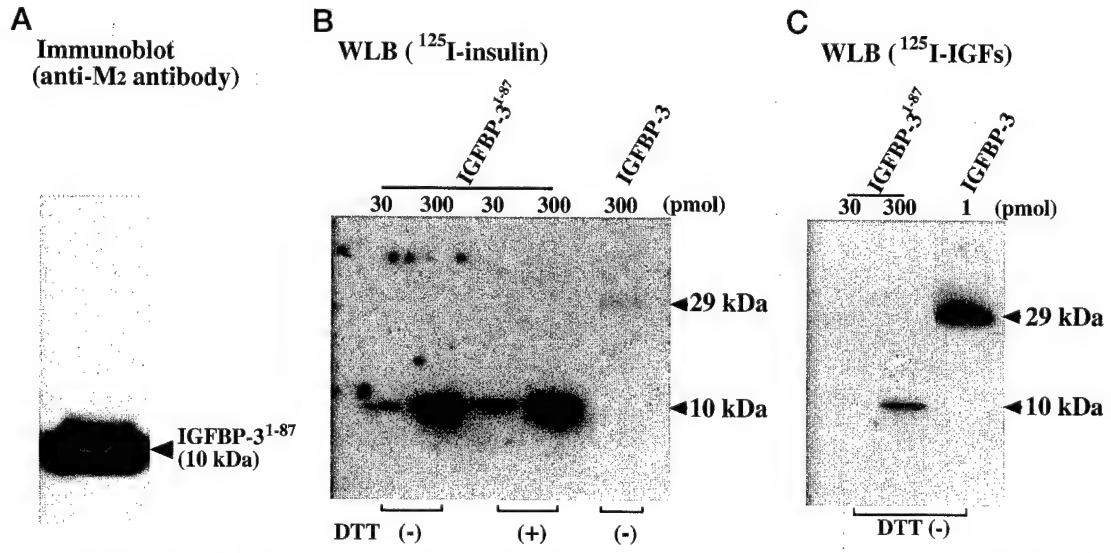

FIG. 5. **Characterization of IGFBP-3$^{(1-87)}$.** *A*, the purified FLAG-tagged IGFBP-3$^{(1-87)}$ was subjected to SDS-PAGE (15%) and then to immunoblot with anti-M2 antibody. IGFBP-3 and IGFBP-3$^{(1-87)}$ were subjected to SDS-PAGE with or without DTT, and electroblotted onto filters, which were incubated with ^{125}I-insulin (*B*) or ^{125}I-IGFs (*C*).

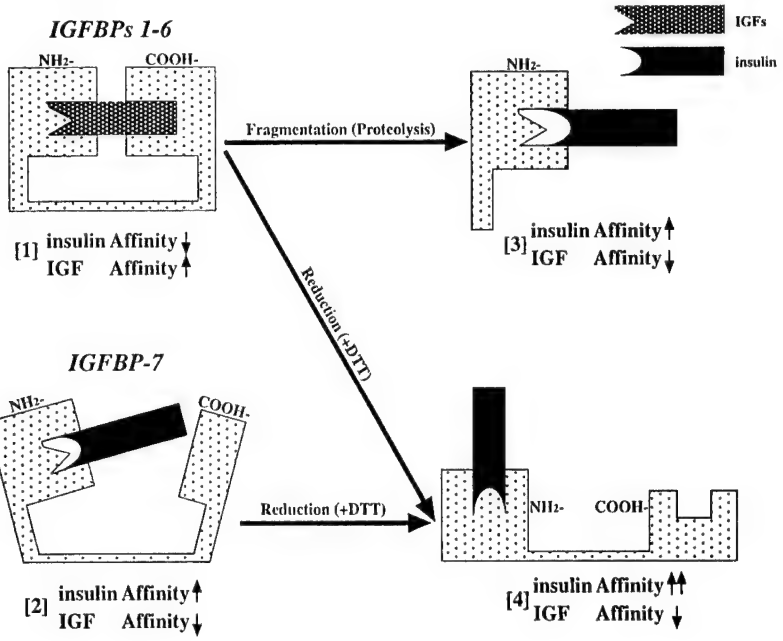

FIG. 6. **Schematic representation of IGFBP binding to insulin and IGFs.** [*1*], the conserved NH_2-terminal and COOH-terminal sequences and the appropriate ternary structures formed by disulfide bonds result in high affinity for IGFs but low affinity for insulin in IGFBPs 1–6. [*2*], IGFBP-7 lacks the ternary structure necessary for high affinity IGF binding but can still bind insulin; reduction of disulfide bridges produces a structure that is further conducive to insulin binding. [*3*, *4*], when IGFBPs 1–6 are either reduced or fragmented, the insulin binding site at the NH_2 terminus of the IGFBP molecule is exposed, resulting in increased affinity for insulin and diminished affinity for IGFs.

IGFBPs -1, -3, and -7 with DTT resulted in a marked decrease in affinity for IGF but increased affinity for insulin (Fig. 4). These data indicate that disulfide bonds and the tertiary structure of IGFBP molecules are, at least in part, responsible for the relatively low affinity for insulin and high affinity for IGF. To further test this hypothesis, we expressed human IGFBP-$3^{(1-87)}$ in a baculovirus system, which was epitope-tagged with the FLAG sequence at the COOH end (Fig. 5*A*). While the affinity for IGF was greatly diminished in IGFBP-$3^{(1-87)}$, the affinity for insulin was significantly increased in IGFBP-$3^{(1-87)}$, compared with that of intact IGFBP-3 (Fig. 5, *B* and *C*). Reduction of IGFBP-$3^{(1-87)}$ with DTT resulted in a modest increase in affinity for insulin, suggesting that disulfide bonds within the IGFBP-$3^{(1-87)}$ fragment still limit, at least in part, the binding affinity for insulin. These results suggest that disulfide bonds between the NH_2 and COOH termini result in a ternary structure for the IGFBPs that confers high affinity for IGFs. To enhance the affinity for insulin, the IGFBP-3 molecule must be modified by either disrupting the ternary structure (under reducing conditions) or by eliminating or modifying the COOH-terminal domain (IGFBP-$3^{(1-87)}$ or IGFBP-7). A schematic model is depicted in Fig. 6.

IGFBP-7 and IGFBP-3^{1-87} Modulate Insulin Binding to Its Receptor and Inhibit Insulin Action—We next investigated the biological relevance of IGFBP-7 binding to insulin. Insulin receptor binding assays were performed using ^{125}I-insulin and crude human placental microsomal membranes in the presence or absence of unlabeled insulin, IGFBP-3, or IGFBP-7. IGFBP-3, at concentrations as high as 300 pmol, did not block insulin binding. The specific binding of ^{125}I-insulin to human placental insulin receptors was inhibited, however, by IGFBP-7 (60% by 100 pmol, and 90% by 300 pmol) (Fig. 7), indicating that IGFBP-7 can compete with insulin receptors for binding of insulin. Inhibition of insulin binding to placental membranes by IGFBP-7 was further confirmed by affinity cross-linking studies (data not shown). Thus, 100–300 pmol of IGFBP-7, but not IGFBP-3, inhibit insulin binding to placental membranes. This discrepancy between IGFBP-3 and IGFBP-7 action presumably reflects the higher affinity of the latter protein for insulin, as suggested in Fig. 1. Although care must be exercised in estimating affinities from cross-linking experiments, it appears likely that IGFBP-7 binds insulin more effectively than does IGFBP-3 although with lower affinity than that exhibited by the insulin receptor.

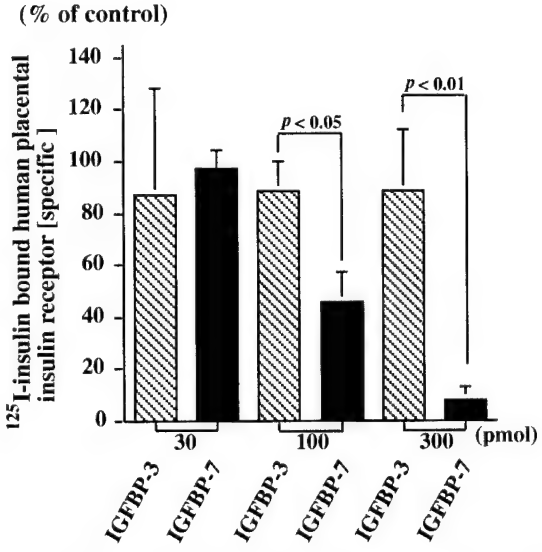

FIG. 7. **Insulin receptor binding.** 20,000 cpm of ^{125}I-insulin were preincubated for 2 h at 4 °C with unlabeled IGFBP-3, IGFBP-7, and insulin at concentrations indicated in the figure and then incubated with 50 μg of microsomal placental crude membranes for 16 h at 4 °C. After samples were centrifuged, pellets were counted in a γ-counter. Data corresponding to means ± S.D. for three independent experiments are shown.

The effect of IGFBPs on insulin receptor signaling pathways, such as receptor autophosphorylation and IRS-1 phosphorylation, was tested. IGFBP-$3^{(1-87)}$ and IGFBP-7 blunted insulin-stimulated autophosphorylation of the insulin receptor β subunit in a dose-dependent manner, with 55 and 80% inhibition at concentrations of 100 pmol of IGFBP-$3^{(1-87)}$ or IGFBP-7, respectively (Fig. 8*A*). IGFBP-3 was ineffective at these concentrations, as predicted by the inability of IGFBP-3 to inhibit insulin binding to placental membranes. Similarly, the insulin-stimulated phosphorylation of IRS-1 was inhibited 65 and 85% by 100 pmol of IGFBP-$3^{(1-87)}$ or IGFBP-7, respectively (Fig. 8*B*). These differences did not reflect reduced concentrations of IRS-1 among samples tested, as demonstrated by IRS-1 immunoblots. Taken together, our data demonstrate that IGFBP-7

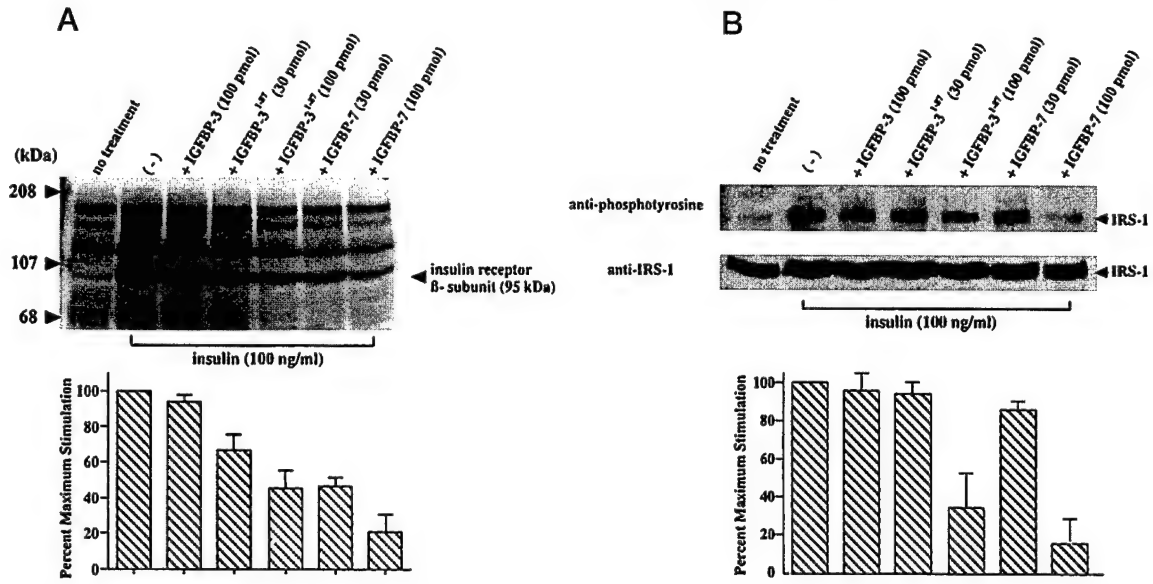

FIG. 8. **Tyrosine phosphorylation assay.** *A*, confluent NIH-3T3 cells stably transfected with the human insulin receptor cDNA were exposed for 3 min to 100 ng/ml insulin, which had been preincubated with IGFBP-3, IGFBP-3$^{(1-87)}$, or IGFBP-7 for 2 h at 4 °C. After quenching, solubilized proteins were separated by SDS-PAGE (8%) and visualized by immunoblot analysis using an anti-phosphotyrosine monoclonal antibody. *B*, alternatively, solubilized proteins were immunoprecipitated with anti-IRS-1 antibody and were subjected to immunoblot using anti-phosphotyrosine antibody. In parallel, solubilized proteins were subjected to immunoblot using anti-IRS-1 antibody. Data corresponding to means ± S.D. for three independent experiments are shown and are depicted relative to maximum stimulation (100 ng/ml insulin), which was assigned a value of 100%.

and IGFBP-3$^{(1-87)}$ have the ability to bind insulin and subsequently inhibit insulin binding to the insulin receptor, resulting in the inhibition of insulin-stimulated autophosphorylation of the insulin receptor β subunit and phosphorylation of IRS-1.

DISCUSSION

Current dogma proposes that a major difference between insulin and IGFs is that only IGFs have the ability to bind IGFBPs 1–6 with high affinity. In addition, we recently have shown that IGFBP-7 also binds both IGF-I and IGF-II but with at least 5–25-fold lower affinity than do the other IGFBPs. However, it has been shown that several IGFBPs may play roles in regulating insulin action. IGFBP-1 production is suppressed by insulin and carbohydrate and stimulated by hypoglycemia, suggesting that IGFBP-1 might play a counterregulatory role in glucose homeostasis. Proteolyzed IGFBP-3 fragments, but not intact IGFBP-3, inhibited the mitogenic effect of insulin, suggesting that proteolyzed IGFBP-3 fragments may have the ability to regulate insulin signaling pathways, despite having significantly reduced affinity for IGFs. In the present studies, we have tested the ability of IGFBPs to bind insulin and regulate insulin action. We demonstrate that IGFBPs have the ability to bind insulin, and that fragmented IGFBP-3 has increased affinity for insulin, resulting in the inhibition of insulin action. Our further studies have revealed that IGFBP-3 fragments, either generated by plasmin digestion or present in normal human urine, bind insulin with relatively high affinity, supporting the physiological relevance of IGFBP-3 fragments on insulin action.[2]

Thus, recent studies have demonstrated that the current view of IGFBPs must be modified by the following observations: 1) IGFBP proteolysis results in peptide fragments with decreased affinity for IGFs (15, 16); 2) additional related proteins with low affinity for IGFs indicate the existence of an IGFBP superfamily (7, 9); 3) IGFBPs can bind insulin, as well as IGFs, and the affinity for insulin can be increased by modification of the protein by reduction of disulfide bonds or proteolysis of the protein; and 4) IGFBPs can, under certain conditions, inhibit insulin binding to its receptor and reduce the resulting stimulation of receptor and IRS-1 phosphorylation.

Immunoblot studies with antibodies specific for IGFBP-7 have demonstrated the presence of the mature protein in the conditioned media of a number of cell lines, as well as in cerebrospinal fluid, urine, amniotic fluid, and serum (31). Quantitative studies await the development of radioimmunoassays. Proteolytic fragments of IGFBP-3, as well as other IGFBPs, were originally identified in pregnancy serum but subsequently have been found in a wide variety of clinical conditions, including critically ill patients, patients with catabolic disease, diabetes mellitus, or noninsulin-dependent diabetes mellitus (15, 16, 33–38). Many of these diseases are characterized by insulin resistance of varying degrees, as measured by decreased insulin receptor tyrosine kinase activity and defective insulin receptor signaling (39–42). It is tempting to speculate that this insulin resistance might reflect increased concentrations of IGFBP-3 fragments or IGFBPs with enhanced affinity for insulin, such as IGFBP-7. These proteins may compete with insulin receptors for peptide binding, much as IGFBPs sequester IGF peptides from IGF receptors. These observations thus support a novel model for the interactions of the IGF and insulin pathways and suggest a potential new approach to our understanding of the pathophysiology of insulin resistance.

Acknowledgments—We thank P. Rotwein, C. T. Roberts, Jr., and B. J. Druker for critical comments, and T. Oda for technical advice.

[2] P. Vorwerk, Y. Yamanaka, G. Spagnoli, Y. Oh, and R. G. Rosenfeld, submitted for publication.

REFERENCES

1. Daughaday, W., and Rotwein, P. (1989) *Endocr. Rev.* **10,** 68–91
2. Yardin, Y., and Ullrich, A. (1988) *Annu. Rev. Biochem.* **57,** 443–478
3. Jones, J. I., and Clemmons, D. R. (1995) *Endocr. Rev.* **16,** 3–34
4. Rosenfeld, R. G., Lamson, G., Pham, H., Oh, Y., Conover, C., De, L. D., Donovan, S. M., Ocrant, I., and Giudice, L. (1990) *Recent Prog. Horm. Res.* **46,** 99–159
5. Shimasaki, S., and Ling, N. (1991) *Prog. Growth Factor Res.* **3,** 243–266
6. Murphy, M., Pykett, M. J., Harnish, P., Zang, K. D., and George, D. L. (1993) *Cell Growth Differ.* **4,** 715–722
7. Oh, Y., Nagalla, S. R., Yamanaka, Y., Kim, H.-S., Wilson, E., and Rosenfeld, R. G. (1996) *J. Biol. Chem.* **271,** 30322–30325

8. Swisshelm, K., Ryan, K., Tsuchiya, K., and Sager, R. (1995) *Proc. Natl. Acad. Sci. U. S. A.* **92,** 4472–4476
9. Kim, H.-S., Nagalla, S. R., Oh, Y., Wilson, E., Roberts Jr., C. T., and Rosenfeld, R. G. (1997) *Proc. Natl. Acad. Sci. U. S. A.*, in press
10. Cohen, P., Peehl, D. M., and Rosenfeld, R. (1991) *J. Clin. Endocrinol. Metab.* **73,** 401–407
11. McCusker, R. H., Busby, W. H., Dehoff, M. H., Camacho, H. C., and Clemmons, D. R. (1991) *Endocrinology* **129,** 939–949
12. Shimasaki, S., Shimonaka, M., Zhang, H. P., and Ling, N. (1991) *J. Biol. Chem.* **266,** 10646–10653
13. Baxter, R. C., and Martin, J. L. (1989) *Proc. Natl. Acad. Sci. U. S. A.* **86,** 6898–6902
14. Conover, C. A., Clarkson, J. T., and Bale, L. K. (1996) *Endocrinology* **137,** 2286–2292
15. Giudice, L. C., Farrell, E. M., Pham, H., Lamson, G., and Rosenfeld, R. G. (1990) *J. Clin. Endocrinol. Metab.* **71,** 806–816
16. Lassarre, C., and Binoux, M. (1994) *Endocrinology* **134,** 1254–1262
17. Gucev, Z. S., Oh, Y., Kelley, K. M., and Rosenfeld, R. G. (1996) *Cancer Res.* **56,** 1545–1550
18. Huynh, H., Yang, X., and Pollak, M. (1996) *J. Biol. Chem.* **271,** 1016–1021
19. Oh, Y., Muller, H. L., Lamson, G., and Rosenfeld, R. G. (1993) *J. Biol. Chem.* **268,** 14964–14971
20. Oh, Y., Muller, H. L., Ng, L., and Rosenfeld, R. G. (1995) *J. Biol. Chem.* **270,** 13589–13592
21. Oh, Y., Muller, H. L., Pham, H., and Rosenfeld, R. G. (1993) *J. Biol. Chem.* **268,** 26045–26048
22. Valentinis, B., Bhala, A., DeAngelis, T., Baserga, R., and Cohen, P. (1995) *Mol. Endocrinol.* **9,** 361–367
23. Rajah, R., Valentinis, B., and Cohen, P. (1997) *J. Biol. Chem.* **272,** 12181–12188
24. Cohen, P., Lamson, G., Okajima, T., and Rosenfeld, R. G. (1993) *Mol. Endocrinol.* **7,** 380–386
25. Lalou, C., Lassarre, C., and Binoux, M. (1996) *Endocrinology* **137,** 3206–3212
26. Liu, F., Powell, D. R., and Hintz, R. L. (1990) *J. Clin. Endocrinol. Metab.* **70,** 620–628
27. Spratt, S. K., Tatsuno, G. P., Yamanaka, M. K., Ark, B. C., Detmer, J., Mascarenhas, D., Flynn, J., Talkington-Verser, C., and Spencer, E. M. (1990) *Growth Factors* **3,** 63–72
28. Beukers, M. W., Oh, Y., Zhang, H., Ling, N., and Rosenfeld, R. G. (1991) *Endocrinology* **128,** 1201–1203
29. Casella, S. J., Han, V. K., D'Ercole, A. J., Svoboda, M. E., and Van Wyk, J. J. (1986) *J. Biol. Chem.* **261,** 9268–9273
30. Marshall, R. N., Underwood, L. E., Voina, S. J., Foushee, D. B., and Van Wyk, J. J. (1974) *J. Clin. Endocrinol. Metab.* **39,** 283–292
31. Wilson, E. M., Oh, Y., and Rosenfeld, R. G. (1997) *J. Clin. Endocrinol. Metab.* **82,** 1301–1303
32. Hossenlopp, P., Seurin, D., Segovia-Quinson, B., Hardouin, S., and Binoux M. (1986) *Anal. Biochem.* **154,** 138–143
33. Bang, P., Brismar, K., and Rosenfeld, R. G. (1994) *J. Clin. Endocrinol. Metab.* **78,** 1119–1127
34. Bereket, A., Lang, C. H., Blethen, S. L., Gelato, M. C., Fan, J., Frost, R. A., and Wilson, T. A. (1995) *J. Clin. Endocrinol. Metab.* **80,** 1312–1317
35. Fielder, P. J., Thordarson, G., Talamantes, F., and Rosenfeld, R. G. (1990) *Endocrinology* **127,** 2270–2280
36. Hossenlopp, P., Segovia, B., Lassarre, C., Roghani, M., Bredon, M., and Binoux, M. (1990) *J. Clin. Endocrinol. Metab.* **71,** 797–805
37. Liu, F., Baxter, R. C., and Hintz, R. L. (1992) *J. Clin. Endocrinol. Metab.* **75,** 1261–1267
38. Rutishauser, J., Schmid, C., Hauri, C., Froesch, E. R., and Zapf, J. (1993) *FEBS Lett.* **334,** 23–26
39. Freidenberg, G. R., Reichart, D., Olefsky, J. M., and Henry, R. R. (1988) *J. Clin. Invest.* **82,** 1398–1406
40. Caro, J. F., Ittoop, O., Pories, W. J., Meelheim, D., Flickinger, E. G., Thomas, F., Jenquin, M., Silverman, J. F., Khazanie, P. G., and Sinha, M. K. (1986) *J. Clin. Invest.* **78,** 249–258
41. Arner, P., Pollare, T., Lithell, H., and Livingston, J. N. (1987) *Diabetologia* **30,** 437–440
42. Haring, H., and Obermaier-Kusser, B. (1989) *Diabetes Metab. Rev.* **5,** 431–441

0013-7227/00/$03.00/0
Endocrinology

Vol. 141, No. 11
Printed in U.S.A.

Differential Effects of Insulin-Like Growth Factor (IGF)-Binding Protein-3 and Its Proteolytic Fragments on Ligand Binding, Cell Surface Association, and IGF-I Receptor Signaling*

GAYATHRI R. DEVI†, DOO-HYUN YANG‡, RON G. ROSENFELD, AND YOUNGMAN OH

Department of Pediatrics, School of Medicine, Oregon Health Sciences University, Portland, Oregon 97201-3042

ABSTRACT

Insulin-like growth factor (IGF)-binding protein-3 (IGFBP-3), the predominant IGF carrier protein in circulation, is posttranslationally modified *in vivo* by IGFBP-3 protease(s) into a number of fragments. Based on the ascertained and predicted recognition sites for known IGFBP-3 proteases, FLAG-epitope tagged intact IGFBP-3, NH_2-terminal $^{(1-97)}$, intermediate fragment $^{(88-148)}$, and COOH-terminal fragments $^{(98-264}$ and $^{(184-264)}$ were generated in a baculovirus and/or *Escherichia coli* expression system and examined, by Western ligand blot and affinity cross-linking assays, for their ability to bind IGF and insulin. The NH_2- and COOH-terminal fragments bound both IGF and insulin specifically (albeit with significantly reduced affinity) for IGF but higher affinity for insulin, when compared with intact IGFBP-3. The effect of IGFBP-3 and the fragments on IGF-I receptor (IGFIR) signaling pathways was studied by testing IGF-I-induced receptor autophosphorylation in IGFIR-overexpressing NIH-3T3 cells. IGFBP-3 showed a dose-dependent inhibition of autophosphorylation of the β-subunit of IGFIR. The $^{(1-97)}$ NH_2-terminal fragment inhibited IGFIR autophosphorylation at high concentrations, and this effect seems largely attributable to sequestration of IGF-I. In contrast, no inhibition of IGF-I-induced IGFIR autophosphorylation was detectable with the $^{(98-264)}$ and $^{(184-264)}$ COOH-terminal fragments, despite their ability to bind IGF. However, unlike the $^{(1-97)}NH_2$-terminal fragment, the COOH-terminal fragments of IGFBP-3 retained their ability to associate with the cell surface, and this binding was competed by heparin, similar to intact IGFBP-3. (*Endocrinology* **141:** 4171–4179, 2000)

THE INSULIN-LIKE GROWTH factors (IGF)-I and -II play an active role in cell proliferation and exist in association with distinct and specific IGF-binding proteins designated as IGFBPs 1–6 (1) and possibly IGFBP-related proteins (IGFBP-rPs) (2). IGFBP-3, the major IGFBP in adult serum, binds both IGFs with high affinity and specificity, and it serves as a carrier of IGFs, prolonging their half lives, as well as modulating their proliferative and anabolic effects on target cells by regulating IGF bioavailability. Exogenous IGFBP-3 has also been demonstrated to significantly inhibit the growth of various cells, including Hs578T estrogen receptor-negative human breast cancer cells (3). Decreased cell growth was observed when human IGFBP-3 complementary DNA (cDNA) was transfected into mouse Balb/c fibroblast cells (4) and into fibroblast cells derived from mouse embryos homozygous for a targeted disruption of the type I IGF receptor gene (5). The mechanism of this inhibition seems to be both IGF-independent and IGF receptor-independent and is mediated, presumably, through binding to specific IGFBP-3 receptors (6–8).

IGFBP-3 may be posttranslationally modified by IGFBP-3 protease(s) present in biological fluids or culture media (plasmin, prostate-specific antigen (PSA), matrix metalloproteases) (9) and those whose activity has been demonstrated only *in vitro* like that of stromelysin 3, thrombin (10). Serum IGFBP proteases(s) have been detected in diabetes (11, 12), renal (13), pregnancy (14), malignancy (15, 16), and following traumatic conditions or invasive procedures, such as surgery. Cleavage sites in IGFBP-3 have been located at the beginning of the variable domain (residues 95–98), particularly residue 97, which is the cleavage site for PSA, plasmin, human serum, and thrombin and yields a fragment of approximately 16 kDa or 20 kDa (glycosylated IGFBP-3) (10). However, the COOH-terminal fragments, containing a highly basic heparin-binding domain, have only been detected *in vitro* by plasmin digestion of intact IGFBP-3 and these fragments seem to inhibit degradation of other binding proteins (17). It is recognized that IGFBP proteolysis also occurs in the normal state outside of the bloodstream (18, 19) and that, in the cell environment, it is an essential mechanism in regulating the bioavailability of IGF. Both intact IGFBP-3 and IGFBP-3 proteolytic fragments have been shown to be capable of blocking the mitogenic effect of IGFs (20). Whether these actions primarily represent IGF-dependent or IGF-independent remains to be determined.

Received March 28, 2000.

Address all correspondence and requests for reprints to: Gayathri R. Devi, Ph.D., AVI BioPharma, Inc., 4575 SW Research Way, Suite 200, Corvallis, Oregon 97333. E-mail: grdevi@avibio.com.

* This research was supported by US Army Grants DAMD17-99-1-9522 (to G.R.D.) and DAMD17-96-1-6204 and DAMD17-96-1-7204 (to Y.O.H.) and by NIH Grants R01-DK-51513 (to R.G.R.) and CA-58110 (to R.G.R.).

† Present address: AVI BioPharma Inc., 4575 SW Research Way, Suite 200, Corvallis Oregon 97333.

‡ Present address: Department of Surgery, Chonbuk National University Medical School, Chonju, Korea.

Our laboratories have demonstrated that the NH_2-terminal recombinant fragments of IGFBP-3 $^{(1-87)}$ and $^{(1-97)}$ retain the ability to bind IGF, albeit with substantially reduced affinity. Additionally, these fragments specifically bind insulin and modulate insulin binding to its receptor (21, 22). Based on these studies, it has been hypothesized that the conserved NH_2- and COOH-terminal sequences, as well as the appropriate ternary structure formed by disulfide bonds in the six classical IGFBPs, are all required for high-affinity binding of IGFs. A recent study had indicated that a natural COOH-terminal fragment of human IGFBP-2 retained partial IGF-binding activity (23), and a COOH-terminal, 13-kDa IGFBP-5 fragment (isolated from hemofiltrate) showed similar results (24). However, there is limited information on the binding characteristics of the IGFBP-3 COOH-terminal domain and the resultant biological effects of proteolytic fragments containing either the NH_2- or COOH-terminal residues.

In this study, we demonstrate the ability of COOH-terminal fragments of IGFBP-3 to bind IGFs. The $^{(98-264)}$ IGFBP-3 fragment and the $^{(1-97)}NH_2$-terminal fragment are both characterized, furthermore, by the ability to bind insulin with low affinity, but with higher affinity than is the case for intact IGFBP-3. Additionally, we have examined the effect of intact IGFBP-3 and the IGFBP-3 fragments on IGF-I-stimulated autophosphorylation of the IGF-I receptor (IGFIR) β-subunit and their ability to associate with the cell surface.

Materials and Methods

Antibodies and reagents

IGF-I and IGF-II were purchased from Austral Biologicals (Santa Clara, CA). ^{125}I-IGF-I (specific activities between 50–70 μCi/μg by a modification of chloramine-T technique) and IGFBP-3 monoclonal antibody were kindly provided by Diagnostic Systems Laboratories, Inc., Webster, TX. IGFBP-3$^{Escherichia\ coli}$ was obtained from Celtrix Pharmaceuticals, Inc. (Santa Clara, CA). ^{125}I-(A14)-monoiodinated insulin was purchased from Amersham Pharmacia Biotech (Piscataway, NJ). Bovine insulin was purchased from Sigma (St. Louis, MO). Antiphosphotyrosine monoclonal antibody (4G10) was a generous gift from Dr. B. J. Druker (Department of Hematology and Medical Oncology, Oregon Health Sciences University). Reagents used for SDS-PAGE were purchased from Bio-Rad Laboratories, Inc. (Richmond, CA).

Cell culture

NIH-3T3 cells overexpressing the human IGFIR were kindly gifted from Dr. C. T. Roberts, Jr. (Department of Pediatrics, Oregon Health Sciences University) and grown in DMEM with 10% FCS plus 500 μg/ml geneticin at 37 C with 5% CO2.

Generation and purification of recombinant IGFBP-3 proteolytic fragments

$^{(1-97)}$IGFBP-3 and $^{(88-148)}$IGFBP-3 FLAG-epitope tagged fragments were generated and purified in baculovirus and tested to be 99% pure, as described earlier (25, 26). The cDNAs for the COOH-terminal fragments $^{(98-264)}$ and $^{(184-264)}$ were generated by PCR amplification from the human IGFBP-3 cDNA and a FLAG epitope sequence (DYKDDDDK), and a stop codon was added immediately following amino acid 264. The signal peptide sequences of IGFBP-3 cDNA were ligated to NH_2-termini of IGFBP-3 fragments. After sequencing, the 98–264 amplicon was then subcloned into the baculovirus expression vector pFASTBAC1 (Life Technologies, Inc., Grand Island, NY) and transformed into DH10Bac *Escherichia coli* cells. The amplified DNA was transfected into Sf9 insect cells (ATCC, Manassas, VA), and large-scale protein purification was begun by infecting the P2 virus into 10^8 HI-5 insect cells (Invitrogen, Carlsbad, CA), at a multiplicity of infection of 3, at 27 C for 3 days. The media from the infected cells were collected and concentrated, and the resultants were bound to an anti-M2 antibody column overnight at 4 C, and the FLAG tagged $^{(98-264)}$ protein was then eluted by using FLAG peptide (0.5 μg/ml), as described earlier (27). The purified protein was subjected to SDS-PAGE in a 15% gel and stained with Coomasie blue. Further, the fragment was also identified by immunoblotting with the M2 anti-FLAG antibody (Eastman Kodak Co., New Haven, CT) and anti-IGFBP-3 monoclonal antibody (Diagnostic Systems Laboratories, Inc.). Eluted fractions from an anti-M2 antibody column were pooled, concentrated, and quantitated by comparison with known amounts of BSA and IGFBP-3$^{Escherichia\ coli}$ after silver staining.

The $^{(184-264)}$IGFBP-3 amplicon, after sequencing, was subcloned in the C-terminal end of glutathione S-transferase (GST) in the plasmid pGEX4T and transformed into *Escherichia coli* cells. The culture was grown overnight in LB-ampicillin and induced with 2 mM IPTG, and the cell lysates of the $^{(184-264)}$ GST fusion protein were prepared. The lysates were incubated with GST Sepharose beads for 1 h at RT and then washed. Purity and concentration of the fragments were determined by comparison with known amounts of BSA standards after silver staining. Further, the purified protein was subjected to SDS-PAGE in a 15% gel and stained with Coomasie Blue and also transferred to nitrocellulose and identified by immunoblotting with M2 anti-FLAG antibody (1:3000 dilution).

Affinity cross-linking

Intact IGFBP-3 or the NH_2- and COOH-terminal fragments were incubated with ^{125}I-IGF-I or ^{125}I-insulin (50,000 cpm), in the presence or absence of unlabeled ligand, in a 100-μl vol for 16 h at 4 C and then cross-linked with 0.5 mM disuccinimidyl suberate (DSS) for 15 min at 4 C. The samples were then subjected to SDS-PAGE (12% or 15% gels) under reducing conditions, and autoradiography on Biomax MS film (Eastman Kodak Co.). Bands were quantified by densitometry (Bio-Rad Laboratories, Inc.).

Western ligand blot analysis

Ligand blotting was performed as described by Hossenlopp at al (28), with minor modifications. Briefly, samples of intact IGFBP-3 $^{(1-97)}$, IGFBP-3, and $^{(98-264)}$IGFBP-3 fragments, at the concentrations indicated in the figure legends, were subjected to SDS-PAGE (12% or 15% gel) under reducing or nonreducing conditions, electroblotted onto nitrocellulose filters, incubated with 1.5×10^6 cpm of ^{125}I-insulin or a mixture of ^{125}I-IGF-I and ^{125}I-IGF-II, washed, dried, and exposed to film (Biomax).

Monolayer ^{125}I-IGF-I affinity cross-linking

^{125}I-IGF-I (100,000 cpm) was preincubated in a microfuge tube for 2 h at 4 C, in the presence or absence of cold IGF-I, intact IGFBP-3 (30 nM) $^{(98-264)}$, IGFBP-3 (250 nM) $^{(184-264)}$, IGFBP-3 (250 nM), or $^{(1-97)}$IGFBP-3 (250 nM), in binding buffer (50 mM HEPES, 150 mM NaCl, 0.5% BSA). Confluent NIH-3T3 cells stably transfected with the human IGFIR cDNA (NIH-3T3-IGFIR cells) were incubated in serum free medium overnight. The cells were washed once with PBS. The cells were incubated with the ^{125}I-IGF-I/IGFBP-3 combinations in triplicate wells for 3 h at 15 C. The cells were then washed with PBS and cross-linked with DSS for 15 min at 4 C, and the reaction was quenched with 100 mM Tris/HCl. The cells were solubilized with sample buffer. The covalent ligand-receptor (^{125}I-IGF-I-IGFIR) complex in the lysates was resolved on a nonreducing 6% SDS-PAGE, followed by autoradiography. Another set of the same samples of cell lysates was run on a 15% SDS-PAGE under reducing conditions and immunoblotted with M2 anti-FLAG antibody or anti-IGFBP-3 monoclonal antibody, and the cell-associated bands were detected with enhanced chemiluminescence (Amersham Pharmacia Biotech).

Determination of cell-surface association of intact IGFBP-3 and the fragments

Confluent monolayers of NIH-3T3-IGFIR cells were incubated in serum free medium overnight. Intact IGFBP-3 (30 nM); fragments 98–264 (250 nM), 184–264 (250 nM), or 1–97 (250 nM) in the presence or absence of 100 μg/ml heparin (Sigma), in binding buffer, was added to the cells.

In a similar experiment, cells were treated with heparin (100 μg/ml) for 1 h, before addition of the peptides as listed above. The treatments were carried out at 15 C for 3 h. The cells were washed with PBS and cross-linked with DSS, as described above. The solubilized cell lysates were then run on a 15% SDS-PAGE and immunoblotted with anti-IGFBP-3 monoclonal antibody and detected with enhanced chemiluminescence.

IGF-I-induced IGFIR autophosphorylation assay

Confluent monolayers of serum-starved NIH-3T3-IGFIR cells were exposed for 5 min to 7 nM IGF-I, which had been preincubated with/without intact IGFBP-3 $^{(1-97)}$, IGFBP-3 ,or $^{(98-264)}$IGFBP-3 for 2 h at 4 C. The reaction was quenched by solubilization buffer [1% Nonidet P-40, 20 mM Tris-HCl (pH 8.0), 1 mM EDTA, 150 mM NaCl, 10% glycerol, 12 U/ml aprotinin, phenylmethylsulfonyl fluoride, and 1 mM Na_3VO_4]. Solubilized proteins (25 μl of the cell lysates) were separated by SDS-PAGE (7.5%) under reducing conditions and visualized by immunoblot analysis. For immunoblot analysis, the filters were blocked in Tris-buffered saline (TBS) with 2% gelatin for 1 h at room temperature and then incubated with antiphosphotyrosine monoclonal antibody (1.5 μg/ml) diluted by TBS + 0.1% Triton X-100 (TBST) for 1 h at room temperature. The filters were then rinsed in 1 × TBST and incubated in a 1:5000 dilution of goat antimouse IgG-conjugated horseradish peroxidase (Amersham Pharmacia Biotech) for 1 h at room temperature. Immunoreactive proteins were visualized using an enhanced chemiluminescence detection system.

Results

Expression of the IGFBP-3 recombinant fragments

Based on the ascertained and predicted PSA recognition sites in IGFBP-3 and the recognition sites for other known IGFBP-3 proteases, such as metalloproteases and plasmin, both intact IGFBP-3 and four different recombinant fragments were generated in a baculovirus and/or *Escherichia coli* expression system. Each peptide was coupled with a FLAG-epitope tag at the carboxyterminus, as shown in Fig. 1A. The purified proteins were immunoblotted with anti-FLAG M2 or anti-IGFBP-3 monoclonal antibody for estimation of their molecular weights. Intact IGFBP-3 and all the fragments were detectable by anti-FLAG M2 antibody under reducing (Fig. 1B) and nonreducing conditions. Dimerized forms of the proteins were identified in anti-FLAG M2 immunoblots run under nonreducing conditions (data not shown). Small discrepancies between the M_r for intact IGFBP-3 $^{(1-97)}$, IGFBP-3 $^{(98-264)}$, IGFBP-3, and $^{(88-148)}$IGFBP-3 proteins seen on the immunoblots relative to the predicted Mr, which is purely based on amino acid composition of the proteins, may have arisen because of N-linked glycosylation. There are three potential N-glycosylation sites (Fig. 1A): Asn^{89}, Asn^{109}, and Asn^{172}, in IGFBP-3 (29). The anti-IGFBP-3 monoclonal antibody detected intact IGFBP-3 and $^{(98-264)}$IGFBP-3 under both nonreducing (Fig. 1B) and reducing conditions (data not shown). The fragment 1–97 was detectable only under nonreducing conditions. The 184–264 and 88–148 fragments were not detected effectively with this antibody.

Analysis of IGF binding to the IGFBP-3 proteolytic fragments

To determine whether the regions encompassed by the IGFBP-3 fragments contained a functional IGF-I-binding/cross-linking site, the proteins were incubated with ^{125}I-IGF-I and then affinity cross-linked with DSS and analyzed by SDS-PAGE. The data in Fig. 2A demonstrate that ^{125}I-IGF-I

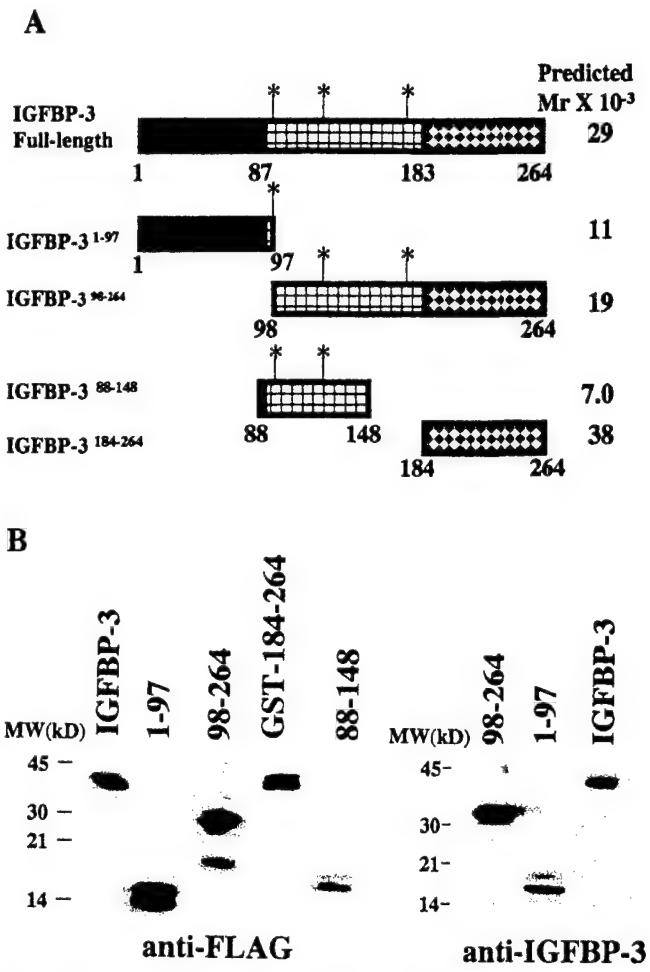

FIG. 1. Expression of FLAG-epitope tagged human IGFBP-3 and its fragments. A, The cDNA for preparation of the IGFBP-3 fragments was synthesized by a series of PCR reactions using the human IGFBP-3 cDNA as template and incorporating sequence encoding a COOH-terminal FLAG epitope tag. The *dark boxes*$^{(1-87)}$ represent the conserved NH_2-terminal region; the *diamond striped boxes*$^{(183-264)}$, the conserved COOH-terminal region; and the *square striped boxes*$^{(88-182)}$, the variable intermediate region of IGFBP-3. The predicted molecular weights (MW) are based on the amino acid composition of the proteins. B, Protein expression was analyzed by immunoblotting using the M2 monoclonal antibody under reducing conditions or the IGFBP-3 monoclonal antibody under nonreducing conditions, coupled to ECL.

can be cross-linked to the $^{(1-97)}$IGFBP-3 and $^{(98-264)}$IGFBP-3 fragments in a dose-dependent manner. Significant IGF cross-linking was observed at 50 nM concentrations of $^{(1-97)}$IGFBP-3, which was completely saturated by 100 nM concentrations. In the case of $^{(98-264)}$IGFBP-3, a dose-dependent increase in IGF binding with increasing protein concentrations with saturation of binding occurred by 500-nM concentration range. The expected sizes of the individual proteolytic fragment coupled to 7-kDa ^{125}I-IGF-I were detected, shown as 25- and 41-kDa bands, respectively. A faint band at 39 kDa is potentially a dimerized form of $^{1-97}$ fragment cross-linked to IGF-I.

For estimation of the affinity of IGF-I binding, the proteolytic fragments were affinity cross-linked with ^{125}I-IGF-I in the presence of increasing amounts of unlabeled IGF-I or insulin ranging between 0.15–4.5 μM. A dose-dependent dis-

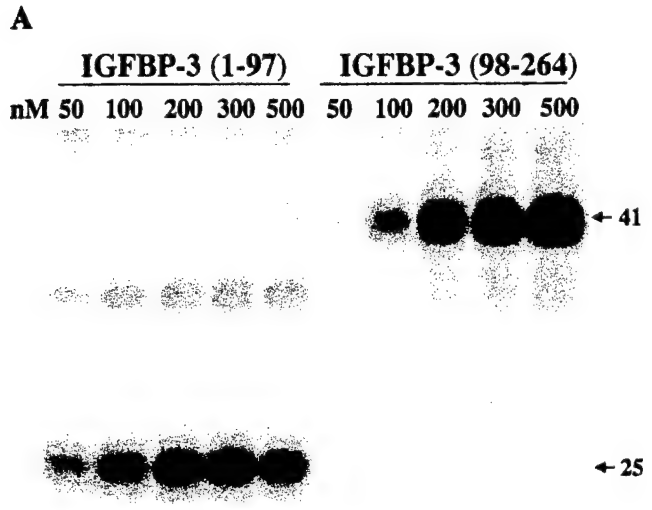

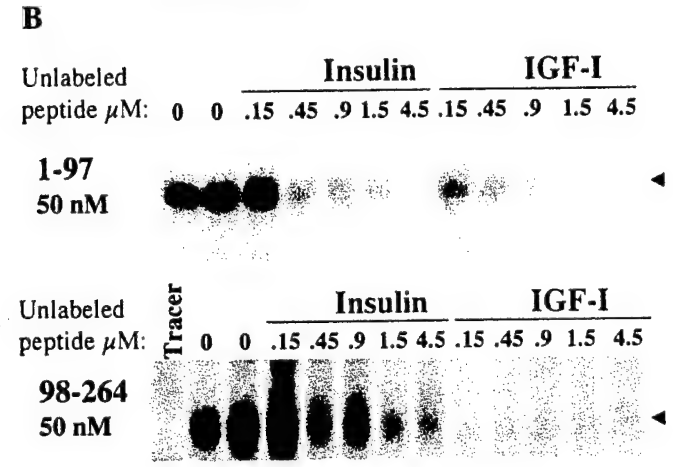

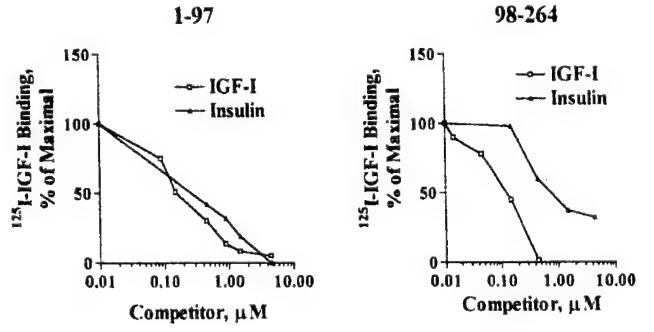

FIG. 2. IGF binding analysis. A, ^{125}I-IGF-I affinity cross-linking: IGFBP-3 proteolytic fragments were incubated with ^{125}I-IGF-I (1×10^5 cpm) in a 100 μl vol for 16 h at 4 C and then cross-linked with 0.5 mM DSS for 15 min at 4 C. The affinity-labeled fragments were separated on a 15% SDS polyacrylamide gel under reducing conditions. An autoradiogram of the gel is shown. Values associated with the *arrows* indicate the calculated molecular weights of the major radioactive species. B, Competitive ^{125}I-IGF-I affinity cross-linking: IGFBP-3 fragments (50 nM) equivalent to 5 pmol, were incubated with radiolabeled IGF-I in the presence or absence of the indicated concentrations of unlabeled IGF-I or insulin. Cross-linking was then done with DSS, followed by SDS-PAGE under reducing conditions. The autoradiogram shown is representative of three replicates. The arrows indicate the major radioactive species. C, Quantitative analysis of radiolabeled ^{125}I-IGF-II displacement from IGFBP-3 fragments: the gels shown in B were densitometrically analyzed for quantitative estimation of the radioactivity associated with the individual bands, except in the case of 98–264 displacement with cold IGF-I, in which affinity cross-linking was done with lower concentrations of cold IGF-I, to construct the displacement curve. The data have been expressed as a percentage of maximal band intensity.

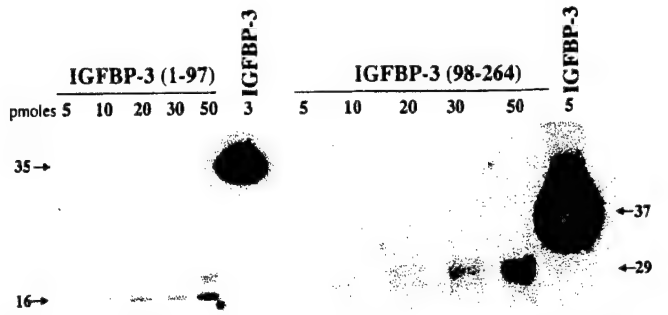

FIG. 3. IGF-I Western ligand blot. IGFBP-3 and the proteolytic fragments (indicated concentrations) were electrophoresed on 12% SDS-PAGE under nonreducing conditions. After electroblotting to nitrocellulose, the blots were incubated with a mixture of ^{125}I-IGF-I and ^{125}I-IGF-II. Values associated with the arrows indicate the calculated molecular weights of the major radioactive species.

placement of ^{125}I-IGF-I labeling of the IGFBP-3 fragments 1–97 and 98–264 was observed with increasing concentrations of unlabeled IGF-I (Fig. 2B). Quantitative analysis of the radioactive bands in these gels was done by densitometric analysis, and the data were plotted, as a function of IGF-I or insulin concentration, to construct ^{125}I-IGF-I displacement curves (Fig. 2C). Calculation of the unlabeled IGF-I concentrations required to achieve 50% displacement of binding (IC_{50}) indicated that $^{(1-97)}$IGFBP-3 fragment had an IC_{50} value of 0.2–0.3 μM. The $^{(98-264)}$IGFBP-3 fragment binding to ^{125}I-IGF-I was completely displaced by 0.15 μM unlabeled IGF-I (Fig. 2B) and, using lower concentrations of unlabeled IGF-I in similar experiments, revealed the IC_{50} to be in the range of 0.1–0.15 μM (Fig. 2C). In addition, insulin was also able to compete for ^{125}I-IGF-I binding to the fragments, especially to $^{(1-97)}$IGFBP-3. The IC_{50} values calculated for unlabeled insulin to compete for ^{125}I-IGF-I binding revealed that the 1–97 fragment had an IC_{50} value of about 0.3 μM insulin, which was at least 3-fold lower than that of the 98–264 fragment (IC_{50} = 0.8–1 μM), as shown in Fig. 2C. In summary, the $^{(1-97)}$IGFBP-3 showed slightly lower binding affinity for IGF-I, relative to $^{(98-264)}$IGFBP-3, and ^{125}I-IGF-I binding to the fragments was equipotently displaced by insulin.

Further, the ability of the fragments to bind IGF-I and IGF-II was assessed by Western ligand blotting. The data in Fig. 3 demonstrate that both the 1–97 and 98–264 fragments were able to bind to a mixture of IGF-I and IGF-II at concentrations as low as 5–10 pmol. It is to be noted, however, that the intensity of the major radiolabeled bands was much lower than that observed with intact IGFBP-3 at similar concentrations. The 20-kDa faint band observed in the case of $^{(1-97)}$IGFBP-3 is probably a different glycosylation product of the 16-kDa fragment.

Analysis of insulin binding to IGFBP-3 fragments

The observations that insulin could compete for ^{125}I-IGF-I binding to the fragments led us to assess their insulin binding activity. Both $^{(1-97)}$IGFBP-3 and $^{(98-264)}$IGFBP-3 showed a strong ^{125}I-insulin cross-linking band, in comparison with that observed with IGFBP-3 at similar concentrations (Fig. 4a). Unlabeled insulin was able to dose-dependently inhibit ^{125}I-insulin binding to both the NH_2 and COOH-terminal fragments (Fig. 4B), although even higher concentrations of unlabeled insulin could not completely displace ^{125}I-insulin binding to the $^{(98-264)}$IGFBP-3, suggesting a slow dissociation rate. Calculation of the unlabeled insulin concentrations required to achieve IC_{50} indicated that the $^{(1-97)}$IGFBP-3 had an IC_{50} value ranging between 0.3–0.4 μM, whereas nearly 1 μM unlabeled insulin was required to cause 50% displacement of ^{125}I-insulin binding to the $^{(98-264)}$ fragment (Fig. 4c). IGF-I was also able to compete for the ^{125}I-insulin binding to the fragments, although higher concentrations of IGF-I were required in the case of $^{(98-264)}$IGFBP-3. In summary, the $^{(1-97)}$IGFBP-3 showed significantly high affinity for insulin, relative to the $^{(98-264)}$IGFBP-3 fragment.

Further, Western blot analysis with iodinated insulin showed that both the 1–97 and the 98–264 fragments bound insulin. The IGFBP-3 intermediate fragment $^{(88-148)}$, which lacks both the NH_2- and COOH-terminal domains, showed no binding to IGF-I, IGF-II,or insulin, in Western ligand blot (data not shown).

IGFBP-3 and 1–97 fragment inhibit IGF-I interaction with the IGFIR

To determine, whether the ability of intact IGFBP-3 and the amino- and carboxyterminal fragments to bind IGFs *in vitro* lead to sequestration of IGFs *in vivo*, a ^{125}I-IGF-I monolayer affinity cross-linking assay was done in the NIH-3T cells overexpressing the IGFIR (NIH-3T3-IGFIR). The data in Fig. 5A shows that ^{125}I-IGF-I specifically cross-links with the IGFIR shown as a 230-kDa band under nonreducing conditions. ^{125}I-IGF-I binding to IGFIR was completely displaced by 100 nM unlabeled IGF-I. Further, the IGF-I-IGFIR complex formation was completely inhibited by preincubation of the iodinated IGF-I with unlabeled IGFBP-3 (30 nM) and about 90% inhibited by preincubating with 250 nM concentration of $^{(1-97)}$ NH_2-terminal fragment. The cross-linked band was not inhibited, however, by preincubation of the ^{125}I-IGF-I with 250 nM of $^{(98-264)}$IGFBP-3 or the $^{(184-264)}$IGFBP-3 fragment.

The same set of samples were resolved on an immunoblot and probed with M2 anti-FLAG antibody. Results in Fig. 5B show that the carboxyterminal fragments $^{(98-264)}$, $^{(184-264)}$, and intact IGFBP-3 molecules associated with the cell surface in the presence of IGF-I. $^{(1-97)}$IGFBP-3, however, showed no cell-associated band.

The carboxyterminal fragments have the ability to associate to the cell surface

Since, compared with the NH_2-terminal fragment, the $^{(98-264)}$ COOH-terminal IGFBP-3 fragment failed to inhibit binding of IGF-I to the IGFIR, we wanted to study the ability of the fragments to associate with the cell surface in the absence of IGF-I. Monolayer cross-linking was carried out with the FLAG-epitope tagged intact IGFBP-3 $^{(1-97)}$ or $^{(98-264)}$ fragments in NIH-3T3-IGFIR cells, and the cell-associated proteins were detected by immunoblotting the cell lysates with anti-IGFBP-3 monoclonal antibody. The $^{(98-264)}$ carboxyterminal fragment and intact IGFBP-3 molecules associated with the cell surface. $^{(1-97)}$IGFBP-3, however, showed no cell-associated band (Fig. 6, lanes 2 and 5). Further, there was no detectable shift in molecular weights of the cross-linked proteins when compared with control (Fig. 1B) noncross-linked protein preparations.

To test whether the ability of intact IGFBP-3 and the carboxylterminal fragment to bind to the cell surface was via the heparin-binding domains, cells were preincubated with heparin (100 μg/ml) and then treated with the peptides; alternatively, the peptides were preincubated with heparin and then added to the cells, followed by monolayer cross-linking in both cases (Fig. 6). Similar results were observed in both types of experiments, *i.e.* heparin blocked the cell surface association of intact IGFBP-3 (Fig. 6, lanes 3 and 4) and the $^{(98-264)}$IGFBP-3 fragment (Fig. 6, lanes 6 and 7).

Inhibition of IGFIR signaling

Since intact IGFBP-3 and its fragments have the ability to bind IGFs and thereby impede its interaction with the IGFIR, we analyzed the potential biological manifestation of this interaction on IGFIR signaling. This was carried out by testing the effect of IGFBP-3 and its fragments on IGF-I-induced IGFIR autophosphorylation in NIH-3T3-IGFIR cells. Control experiments with IGF-I revealed that 5-min treatments with 7–14 nM of the peptide showed maximal intensity autophosphorylation of the 95-kDa band of the β-subunit of IGFIR in antiphosphotyrosine immunoblots (Fig. 7A).

IGFBP-3 inhibited IGF-I-stimulated autophosphorylation of the IGFIR β-subunit in a dose-dependent manner (Fig. 7B). Quantification of the inhibition of the phosphorylated subunit of IGFIR was carried out by densitometrically analyzing the specific 95-kDa band and the 116-kDa nonspecific band in each gel. The ratio of the two band intensities was used to normalize and calculate the percentage of maximal IGF-I-stimulated IGFIR autophosphorylation detected in the presence of IGFBP-3 and the IGFBP-3 fragments (Fig. 7C). IGFBP-3 caused 50% inhibition of the IGF-I-induced autophosphorylation at 5–7 nM concentration range, and by 15–20 nM IGFBP-3 concentrations, complete inhibition of IGFIR autophosphorylation was observed. In contrast, the $^{(1-97)}$IGFBP-3 fragment inhibited receptor autophosphorylation only at higher concentrations (50–70% inhibition at 100–250 nM concentrations). The $^{(98-264)}$IGFBP-3 and $^{(184-264)}$IGFBP-3 fragments, however, did not show any significant inhibition of IGF-I-induced IGFIR autophosphorylation, even at 250 nM concentrations (Fig. 7, B and C), although these fragments were able to bind IGF-I in binding assays.

Discussion

We report herein that IGFBP-3 fragments are capable of binding IGF-I and IGF-II, although with lower affinity than that seen with intact IGFBP-3. Further, the fragments have the ability to bind insulin with higher affinity than observed

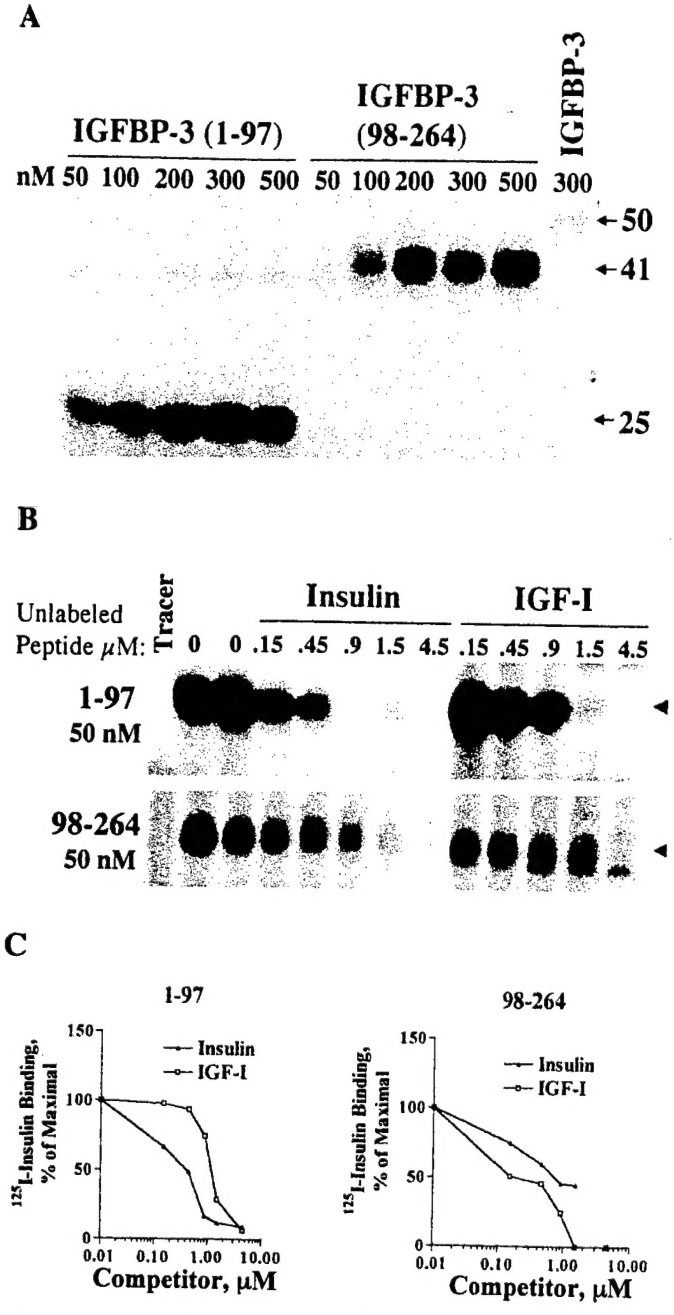

FIG. 4. Insulin binding analysis. A, ^{125}I-insulin affinity cross-linking: IGFBP-3 proteolytic fragments were incubated with ^{125}I-insulin (1×10^5 cpm) in a 100 μl vol for 16 h at 4 C and then cross-linked with 0.5 mM DSS for 15 min at 4 C. The affinity labeled fragments were separated on a 15% SDS polyacrylamide gel. An autoradiogram of the gel is shown, which is representative of three replicates. Values associated with the *arrows* indicate the calculated molecular weights of the major radioactive species. B, Competitive ^{125}I-insulin affinity cross-linking: IGFBP-3 and the proteolytic fragments (50 nM) equivalent to 5 pmol, were incubated with radiolabeled insulin in the presence or absence of the indicated concentrations of unlabeled insulin or IGF-I. Cross-linking was then done with DSS, followed by SDS-PAGE. The autoradiogram of the dried gel is shown. The *arrows* indicate the major radioactive species. C, Quantitative analysis of radiolabeled ^{125}I-insulin displacement from IGFBP-3 fragments: the gels shown in B were densitometrically analyzed for quantitative estimation of the radioactivity associated with the individual bands. The data have been expressed as a percentage of maximal band intensity.

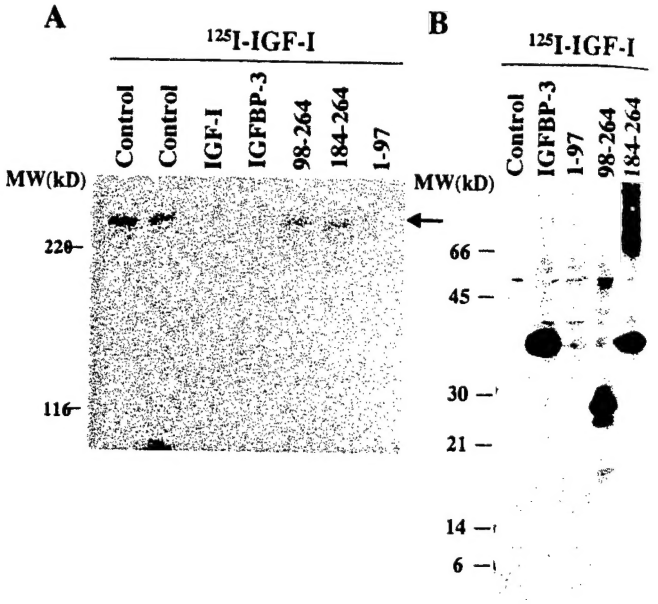

FIG. 5. Monolayer affinity cross-linking with ^{125}I-IGF-I. A, ^{125}I-IGF-I was preincubated at 4 C in the presence or absence of unlabeled IGF-I (100 nM), IGFBP-3 (30 nM), or fragments (250 nM); and then these treatments were added to confluent monolayers of NIH-3T3-IGFIR cells for 3 h at 15 C. After washing, the cells were cross-linked, and cell lysates were run on a 6% SDS-PAGE gel. The *arrow* indicates the IGFIR species cross-linked to radiolabeled IGF-I. B, A set of the same cell lysates were run on a 15% SDS-PAGE, under reduced conditions, and immunoblotted with M2 anti-FLAG monoclonal antibody.

with intact IGFBP-3. The principal conclusion is that the high-affinity binding of IGFs by IGFBP-3 requires proper tertiary configuration of the NH_2- and COOH-terminal domains. This observation is further supported by the recent concept of an IGFBP superfamily (30, 31). Over the course of evolution, the classical IGFBPs, which have well-conserved NH_2- and COOH-terminal domains, evolved into high-affinity IGF-binders (1). In contrast, the IGFBP-rPs (low-affinity IGFBPs) only share the conserved NH_2-terminal domain (32). This structural difference, combined with the present data, strongly implicate the importance of the IGFBP COOH-terminal domain in conferring high-affinity IGF binding.

The concept that interaction between NH_2- and COOH-terminal domains is essential for high-affinity IGF binding was initially conceived based on observations that proteolysis of IGFBPs in biological fluids results in fragments that have diminished or no binding affinities for IGFs (33). The *in vitro* generation of recombinant fragments or fragments isolated by limited proteolysis supports the *in vivo* data. A 16-kDa fragment corresponding to the NH_2-terminus and a small portion of intermediate region, generated by proteolytically modifying IGFBP-4, specifically cross-linked to both IGF-I and II, although with a 20-fold lower affinity than intact IGFBP-4 (34, 35). Similarly, a carboxytruncated 23-kDa IGFBP-5 fragment from osteoblast-like cells demonstrated decreased IGF binding affinity (36, 37). Deletion mutagenesis of the carboxyterminal domains of IGFBP-1 and IGFBP-4 has resulted in a decrease in IGF affinity, thereby demonstrating the importance of the highly conserved Cys-Try-Cys-Val motif in the carboxyterminal region (38, 39). The present study is the first to clearly demonstrate the ability of the 28-kDa

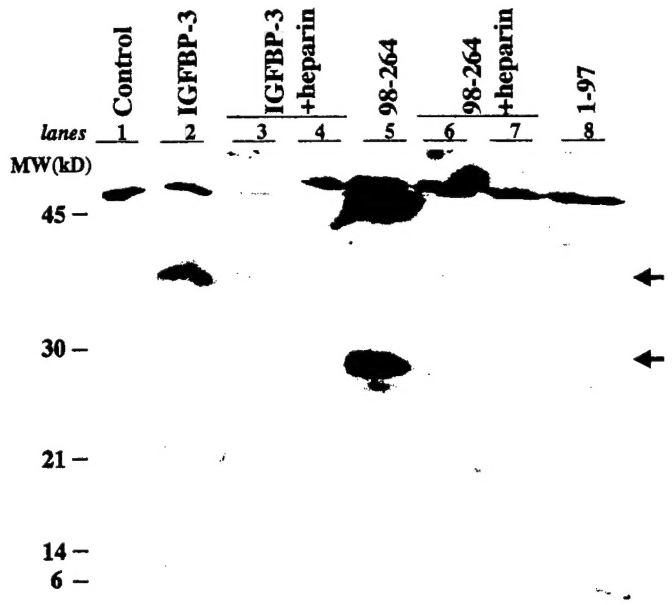

FIG. 6. Effect of heparin on cell surface association of IGFBP-3 and its fragments. Confluent NIH-3T3-IGFIR cells were treated with either peptides alone [lane 1, untreated cells; lane 2, IGFBP-3; lane 5, $^{(98-264)}$IGFBP-3; lane 8, $^{(1-97)}$IGFBP-3] or with peptides preincubated with heparin for 1 h at 4 C [lane 4, IGFBP-3+heparin; lane 7, $^{(98-264)}$IGFBP-3+heparin]; or the cells were first treated with heparin for 1 h, washed, and then the following peptides were added: lane 3, IGFBP-3; lane 6, $^{(98-264)}$IGFBP-3. All the treatments were carried out for 3 h at 15 C. After washing, the cells were cross-linked, and cell lysates were run on a 15% SDS-PAGE and immunoblotted with anti-IGFBP-3 monoclonal antibody. The *arrows* indicate the cell-surface-associated species.

$^{(98-264)}$, IGFBP-3 intermediate+COOH-terminal proteolytic fragment to bind both IGFs and insulin in two different procedures, affinity cross-linking and Western ligand blot. Interestingly, the binding of the $^{(98-264)}$IGFBP-3 fragment to ^{125}I-IGF-I or ^{125}I-insulin was competitively displaced by both IGF-I and insulin, though with different affinities, suggesting that the insulin and IGF binding sites are probably not identical but overlap or reside closely on the IGFBP-3 molecule. This is in contrast with the $^{(1-97)}$IGFBP-3 fragment, where insulin and IGF-I were approximately equipotent in displacing ^{125}I-IGF-I.

We have shown that IGFBP-3 causes a dose-dependent inhibition of IGF-I-induced IGFIR autophosphorylation in NIH-3T3 cells overexpressing the IGFIR. This inhibition occurs at an 1:1 molar ratio of IGFBP-3 to IGF-I, suggesting an IGF-dependent mechanism of modulation of receptor signaling. The $^{(1-97)}$ NH_2-terminal fragment retained the ability to modulate IGF-I binding and signaling via the IGFIR by inhibiting IGF-I-stimulated IGFIR autophosphorylation, albeit at 50-fold higher concentrations than intact IGFBP-3. That this inhibition of IGFIR signaling is largely attributable to sequestration of IGF-I is strongly supported by the observations that both intact IGFBP-3 and $^{(1-97)}$IGFBP-3 compete with ^{125}I-IGF-I binding/cross-linking to the receptor in monolayer affinity cross-linking experiments.

Interestingly, the $^{(98-264)}$ fragment unlike the $^{(1-97)}$IGFBP-3, failed to show any inhibition of IGFIR signaling, despite its ability to bind IGFs, as revealed by *in vitro* binding analysis. The COOH-terminal fragments $^{(98-264)}$ and $^{(184-264)}$ also failed to compete for ^{125}I-IGF-I binding and cross-linking to the IGFIR, compared with intact IGFBP-3 and the $^{(1-97)}$ NH_2-terminal IGFBP-3 fragment. We speculate that the inability of the fragments containing the COOH-terminal domain of IGFBP-3 to inhibit IGF-I binding to the IGFIR could be attributable to the following mechanisms: 1) the COOH-terminal fragment binds IGF-I, and the entire complex is still capable of binding to and autophosphorylating the IGFIR, implying that the binding site on IGF-I for the receptor and for the carboxyterminal region of IGFBP-3 are different; and 2) the COOH-terminal domain of IGFBP-3 possesses an extracellular matrix (ECM) binding region, and it is possible that in the cellular environment, the fragments containing the COOH-terminal domains are more prone to associate with the cell surface and are not available to sequester IGF-I, especially given their low affinity for IGF. To test these hypotheses, the ability of the FLAG-epitope tagged fragments to associate with the cell surface was studied in the presence of IGF-I, with subsequent cross-linking and by analysis of cell lysates on immunoblots probed with anti-IGFBP-3 or M2 anti-FLAG antibody. Our data indicate that the COOH-terminal fragments $^{(98-264)}$ and $^{(184-264)}$ have the ability to associate to the cell surface in the presence of IGF-I, unlike the NH_2 fragment $^{(1-97)}$IGFBP-3, which showed no cell-surface association. Further, there was no shift in molecular weight of the cell-surface associated bands, and heparin blocked the binding of both intact and the $^{(98-264)}$IGFBP-3 fragment to the cell surface, ruling out the possibility of interaction of the fragments with any receptor molecule and thereby supporting the second hypothesis. This is in agreement with an earlier study (40), which reported that an IGFBP-3 deletion fragment, lacking the 184–264 region, failed to show any cell-surface association. There are two putative heparin-binding motifs in IGFBP-3, located at amino acids 148–153 and 219–226 in the central and carboxylterminal regions, respectively, and the carboxylterminal motif has been shown to have 4-fold higher affinity for heparin (41). Recently, Bramani *et al.*, 1999 (42), have identified two nonbasic residues (Gly203 and Gln209) within the ECM binding region (201–218) in the carboxyterminal region of IGFBP-5, mutations of which cause 8- to10-fold reduction in affinity for human IGF-I. This region is a highly conserved domain in IGFBP-5, -3, and -6 and is known to contain the heparin-binding domain. The authors have proposed that the IGF-I and ECM binding sites partially overlap, and heparin binding to the basic amino acids might interfere with IGF-I interaction *in vivo*.

Previous studies with mini-receptor constructs and with isolated domains or proteolytic fragments of the IGF2R (43) urokinase receptor (44), GH receptor (45), talin (46), to name a few, have confirmed the involvement of two or more ligand contact regions. Similarly, in the case of IGFBP-3, it seems that the IGF- and insulin-binding domains are bipartite and possibly overlapping. In our biological system, the stoichiometry of IGFBP-3 binding to IGF-I seems to be 1:1. We postulate that both NH_2- and COOH-terminal domains have residues that are capable of binding IGF-I and insulin with low affinity. However, there is simultaneous interaction of the two so-called half sites, in intact IGFBP-3, which creates a high-affinity IGF binding site on the molecule. Simultaneously, this interaction leads to a markedly reduced ability of intact IGFBP-3 to bind insulin, possibly because of mask-

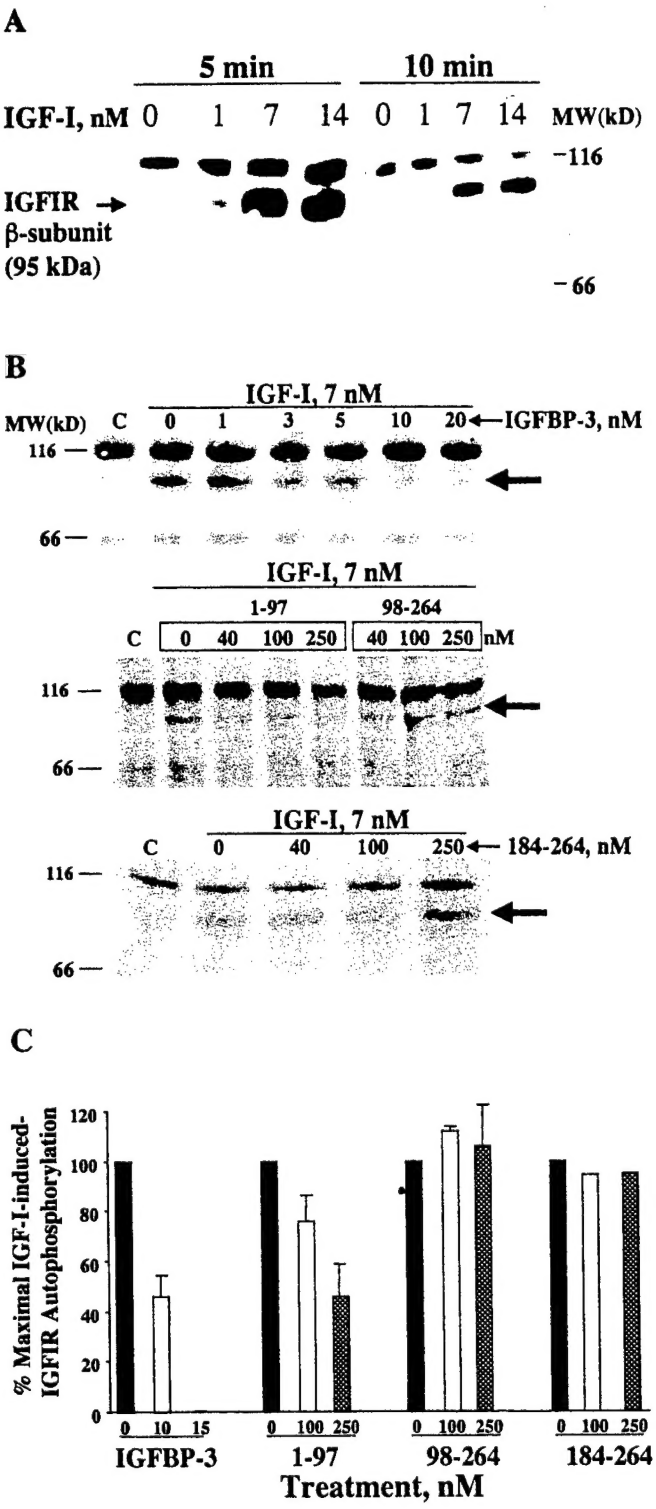

FIG. 7. IGFIR autophosphorylation assay. A, Confluent NIH-3T3-IGFIR cells stably transfected with the human IGFIR cDNA were exposed for either 5 min or 10 min to 1, 7, and 14 nM IGF-I peptide. The reaction was quenched by solubilization buffer, and the solubilized proteins were separated by 7.5% SDS-PAGE, under reducing conditions, and visualized by immunoblot analysis using antiphosphotyrosine monoclonal antibody. The *arrow* indicates the 95-kDa β-subunit of IGFIR. B, Confluent NIH-3T3-IGFIR cells were exposed for 5 min to 50 ng/ml IGF-I, which had been preincubated with IGFBP-3, 1–97, or 98–264 proteolytic fragment for 2 h at 4 C. The solubilized proteins were separated by 7.5% SDS-PAGE, under reducing conditions, and visualized by immunoblot analysis using antiphosphotyrosine monoclonal antibody. The *arrows* indicate the 95-kDa β-subunit of IGFIR in each immunoblot. C, The specific 95-kDa bands representing the phosphorylated β-subunit of the IGFIR and the 116-kDa nonspecific bands in the gels shown in B and in other replicate experiments (n = 2–4) were densitometrically analyzed. The ratio of the two band intensities was used to normalize and quantify the percentage of maximal IGF-I-induced IGFIR autophosphorylation detected in the presence of intact IGFBP-3 and its fragments.

ing of the residues that interact with insulin, as a result of tertiary conformational change (21). With respect to IGF binding to IGFBP-3, it is unclear whether the NH_2- and COOH-terminal domains contribute equally. We predict the presence of functional residues in the NH_2-terminus $^{(1-97)}$ and COOH-terminus (149–264) that confer high affinity by cooperative or conformational changes; the structural residues that mediate the necessary noncovalent interactions may reside in the NH_2-, intermediate or COOH-terminus of the IGFBP-3 molecule. Alternatively, given the striking similarity of the NH_2-terminal domains and the fact that this region is encoded by a single exon in all of the classical IGFBPs and the IGFBP-rPs (low-affinity IGF binders), it is possible that the NH_2-terminus is the critical functional component involved in binding IGFs, and that conformational effects imposed on the NH_2-terminus by the COOH-terminal domain are required for high-affinity binding.

In summary, the present study, along with previous work from our and other laboratories, clearly demonstrates the ability of the IGFBP-3 aminoterminal fragment to bind IGF and insulin and to inhibit IGFIR and insulin receptor autophosphorylation (21, 22), revealing that this 16-kDa fragment may be capable of both IGF-I-dependent and IGF-independent roles in modulating cell growth. However, the carboxylterminal fragments, which also have the ability to bind both IGF-I and insulin *in vitro*, fail to prevent binding of either IGF-I or insulin (data not shown) to their respective receptors, because of the tendency of these fragments for cell surface association via the heparin-binding domain. Also intriguing is the identification of a thyroglobulin-like motif in the COOH-terminal regions of IGFBP superfamily, which has also been found in the superfamily of protein inhibitors of cysteine proteinases (47, 48). Whether this highly conserved thyroglobulin type-I element indeed acts as an inhibitor of cysteine proteinases in these proteins, remains to be established. The intermediate region of IGFBP-3 does not seem to bind IGFs or insulin, and its role in high-affinity binding to IGFs is probably related to its ability to promote proper tertiary structure and optimal interactions between the amino- and carboxyterminal residues. Further, it has been demonstrated that the intermediate region of IGFBP-3 is involved in the specific interaction between IGFBP-3 and its putative cell-surface receptor (26). Taken together, it is tempting to speculate that various forms of IGFBP-3 fragments resulting from proteolysis by IGFBP-3 specific proteases will have different effects on the IGF-IGFIR axis, as well as potential IGF-independent actions.

Acknowledgments

We are grateful to Donna Graham and Elizabeth Wilson for technical support and to Drs. Vivian Hwa and Stephen M. Twiggs for helpful

discussions. We thank Diagnostic Systems Laboratories, Inc. for providing radiolabeled IGF-I.

References

1. **Jones JI, Clemmons DR** 1995 Insulin-like growth factors and their binding proteins: biological actions. Endocr Rev 16:3–34
2. **Rosenfeld RG, Hwa V, Wilson L, Lopez-Bermejo A, Buckway C, Burren C, Choi WK, Devi G, Ingermann A, Graham D** 1999 The insulin-like growth factor binding protein superfamily: new perspectives. Pediatrics 104:1018–1021
3. **Oh Y, Muller HL, Lamson G, Rosenfeld RG** 1993 Insulin-like growth factor (IGF)-independent action of IGF-binding protein-3 in Hs578T human breast cancer cells. J Biol Chem 268:14964–14971
4. **Cohen P, Lamson G, Okajima T, Rosenfeld R** 1993 Transfection of the human IGFBP-3 gene into Balb/c fibroblasts: a model for the cellular functions of IGFBPs. Growth Regul 3:23–26
5. **Valentinis B, Bhala A, DeAngelis T, Baserga R, Cohen P** 1995 The human insulin-like growth factor (IGF) binding protein-3 inhibits the growth of fibroblasts with a targeted disruption of the IGF-I receptor gene. Mol Endocrinol 9:361–367
6. **Oh Y, Muller HL, Pham H, Rosenfeld RG** 1993 Demonstration of receptors for insulin-like growth factor binding protein-3 on Hs578T human breast cancer cells. J Biol Chem 268:26045–26048
7. **Rajah R, Valentinis B, Cohen P** 1997 Insulin-like growth factor (IGF)-binding protein-3 induces apoptosis and mediates the effects of transforming growth factor-b1 on programmed cell death through a p53- and IGF-independent mechanism. J Biol Chem 272:12181–12188
8. **Leal SM, Liu Q, Huang SS, Huang JS** 1997 The Type V transforming growth factor b receptor is the putative insulin-like growth factor-binding protein 3 receptor. J Biol Chem 272:20572–20576
9. **Rajah R, Katz L, Nunn S, Solberg P, Beers T, Cohen P** 1995 Insulin-like growth factor binding protein (IGFBP) proteases: functional regulators of cell growth. Prog Growth Factor Res 6:273–284
10. **Booth BA, Boes M, Bar RS** 1996 IGFBP-3 proteolysis by plasmin, thrombin, serum: heparin binding, IGF binding, and structure of fragments. Am J Physiol 271:E465–E470
11. **Bang P, Brismar K, Rosenfeld RG** 1994 Increased proteolysis of insulin-like growth factor-binding protein-3 (IGFBP-3) in noninsulin-dependent diabetes mellitus serum, with elevation of a 29-kilodalton (kDa) glycosylated IGFBP-3 fragment contained in the approximately 130- to 150-kDa ternary complex. J Clin Endocrinol Metab 78:1119–1127
12. **Bereket A, Lang CH, Blethen SL, Fan J, Frost RA, Wilson TA** 1995 Insulin-like growth factor binding protein-3 proteolysis in children with insulin-dependent diabetes mellitus: a possible role for insulin in the regulation of IGFBP-3 protease activity. J Clin Endocrinol Metab 80:2282–2288
13. **Powell DR, Durham SK, Liu F, Baker BK, Lee PD, Watkins SL, Campbell PG, Brewer ED, Hintz RL, Hogg RJ** 1998 The insulin-like growth factor axis and growth in children with chronic renal failure: a report of the Southwest Pediatric Nephrology Study Group. J Clin Endocrinol Metab 83:1654–1661
14. **Bang P, Fielder PJ** 1997 Human pregnancy serum contains at least two distinct proteolytic activities with the ability to degrade insulin-like growth factor binding protein-3. Endocrinology 138:3912–3917
15. **Muller HL, Oh Y, Gargosky SE, Wilson KF, Lehrnbecher T, Rosenfeld RG** 1994 Insulin-like growth factor binding protein-3 concentrations and insulin-like growth factor binding protein-3 protease activity in sera of patients with malignant solid tumors or leukemia. Pediatr Res 35:720–724
16. **Baciuchka M, Remacle-Bonnet M, Garrouste F, Favre R, Sastre B, Pommier G** 1998 Insulin-like growth factor (IGF)-binding protein-3 (IGFBP-3) proteolysis in patients with colorectal cancer: possible association with the metastatic potential of the tumor. Int J Cancer 79:460–467
17. **Binoux M, Lalou C, Mohseni-Zadeh S** 1999 Biological actions of proteolytic fragments of the IGFBPs. In: Rosenfeld RG, Roberts Jr CT (eds) The IGF System-Molecular Biology, Physiology, and Clinical Applications. Humana Press, Totawa, NJ, pp 281–313
18. **Lalou C, Binoux M** 1993 Evidence that limited proteolysis of insulin-like growth factor binding protein-3 (IGFBP-3) occurs in the normal state outside of the bloodstream. Regul Pept. 48:179–188
19. **Maile LA, Xu S, Cwyfan-Hughes SC, Fernihough JK, Pell JM, Holly JM** 1998 Active and inhibitory components of the insulin-like growth factor binding protein-3 protease system in adult serum, interstitial, and synovial fluid. Endocrinology 139:4772–4781
20. **Lalou C, Lassarre C, Binoux M** 1996 A proteolytic fragment of insulin-like growth factor (IGF) binding protein-3 that fails to bind IGFs inhibits the mitogenic effects of IGF-I and insulin. Endocrinology 137:3206–3212
21. **Yamanaka Y, Wilson EM, Rosenfeld RG, Oh Y** 1997 Inhibition of insulin receptor activation by insulin-like growth factor binding proteins. J Biol Chem 272:30729–30734
22. **Vorwerk P, Yamanaka Y, Spagnoli A, Oh Y, Rosenfeld RG** 1998 Insulin and IGF binding by IGFBP-3 fragments derived from proteolysis, baculovirus expression and normal human urine. J Clin Endocrinol Metab 83:1392–1395
23. **Ho PJ, Baxter RC** 1997 Characterization of truncated insulin-like growth factor-binding protein-2 in human milk. Endocrinology 138:3811–3818
24. **Standker L, Wobst P, Mark S, Forsmann WG** 1998 Isolation and characterization of circulating 13-kDa C-terminal fragments of human insulin-like growth factor binding protein-5. FEBS Lett 441:281–286
25. **Vorwerk P, Oh Y, Lee PD, Khare A, Rosenfeld RG** 1997 Synthesis of IGFBP-3 fragments in a baculovirus system and characterization of monoclonal anti-IGFBP-3 antibodies. J Clin Endocrinol Metab 82:2368–2370
26. **Yamanaka Y, Fowlkes JL, Rosenfeld RG, Oh Y** 1999 Characterization of insulin-like growth factor binding protein-3 (IGFBP-3) binding to human breast cancer cells. Endocrinology 140:1319–1328
27. **Oh Y, Nagalla SR, Yamanaka Y, Kim H-S, Wilson E, Rosenfeld RG** 1996 Synthesis and characterization of insulin-like growth factor binding protein (IGFBP-7). J Biol Chem 271:30322–30325
28. **Hossenlopp P, Seurin D, Segovia-Quinson B, Hardouin S, Binoux M** 1986 Analysis of serum insulin-like growth factor binding proteins using western blotting: use of the method for titration of the binding proteins and competitive binding studies. Anal Biochem 154:138–143
29. **Zapf J, Born W, Chang JY, James P, Froesch ER, Fischer JA** 1988 Isolation and NH2-terminal amino acid sequences of rat serum carrier proteins for insulin-like growth factors. Biochem Biophys Res Commun 156:1187–1194
30. **Hwa V, Oh Y, Rosenfeld RG** 1999 Insulin-like growth factor binding proteins: a proposed superfamily. Acta Paediatr Suppl 428:37–45
31. **Baxter RC, Binoux M, Clemmons DR, Conover C, Drop SLS, Holly JMP, Mohan S, Oh Y, Rosenfeld RG** 1998 Recommendations for nomenclature for the insulin-like growth factor binding protein (IGFBP) superfamily. J Clin Endocrinol Metab 83:3213
32. **Hwa V, Oh Y, Rosenfeld RG** 1999 The insulin-like factor binding protein (IGFBP) superfamily. Endocr Rev 20:761–787
33. **Collett-Solberg PF, Cohen P** 1996 The role of the insulin-like growth factor binding proteins and the IGFBP proteases in modulating IGF action. Endocrinol Metab Clin North Am 25:591–614
34. **Cheung P-T, Wu J, Banach W, Chernausek SD** 1994 Glucocorticoid regulation of an insulin-like growth factor-binding protein-4 protease produced by a rat neuronal cell line. Endocrinology 135:1328–1335
35. **Chernausek SD, Smith CE, Duffin KL, Busby WH, Wright G, Clemmons DR** 1995 Proteolytic cleavage of insulin-like growth factor binding protein 4 (IGFBP-4): localization of cleavage sit to non-homologous region of native IGFBP-4. J Biol Chem 270:11377–11382
36. **Andress DL, Birnbaum RS** 1992 Human osteoblast-derived insulin-like growth factor (IGF) binding protein 5 stimulates osteoblast mitogenesis and potentiates IGF action. J Biol Chem 267:22467–22472
37. **Andress DL, Loop SM, Zapf J, Kiefer MC** 1993 Carboxy-truncated insulin-like growth factor binding protein-5 stimulates mitogenesis in osteoblast-like cells. Biochem Biophys Res Commun 195:25–30
38. **Qin X, Strong DD, Baylink DJ, Mohan S** 1998 Structure-function analysis of the human insulin-like growth factor binding protein-4. J Biol Chem 273:23509–23516
39. **Brinkman A, Groffen CA, Kortleve DJ, Kessel AGV, Drop SL** 1988 Isolation and characterization of a cDNA encoding the low molecular weight insulin-like growth factor binding protein (IGFBP-1). EMBO J 7:2417–2423
40. **Firth SM, Ganeshprasad U, Baxter RC** 1998 Structural determinants of ligand and cell surface binding of insulin-like growth factor-binding protein-3. J Biol Chem 273:2631–2638
41. **Fowlkes J, Serra D** 1996 Characterization of glycosaminoglycan-binding domains present in insulin-like growth factor-binding protein-3. J Biol Chem 271:14676–14679
42. **Bramani S, Song H, Beattie J, Tonner E, Flint DJ, Allan GJ** 1999 Amino acids within the extracellular matrix (ECM) binding region (201–218) of rat insulin-like growth factor binding protein (IGFBP-5) are important determinants in binding IGF-I. J Mol Endocrinol 23:117–123
43. **Devi GR, Byrd JC, Slentz DH, MacDonald RG** 1998 An insulin-like growth factor II (IGF-II) affinity-enhancing domain localized within extracytoplasmic repeat 13 of the IGF-II/mannose 6-phosphate receptor. Mol Endocrinol 11:1661–1672
44. **Behrendt N, Ronne E, Dano K** 1996 Domain interplay in the urokinase receptor. Requirement for the third domain in high affinity ligand binding and demonstration of ligand contact sites in distinct receptor domains. 271:22885–22894
45. **de Vos AM, Ultsch M, Kossiakoff AA** 1992 Human growth hormone and extracellular domain of its receptor: crystal structure of the complex. Science 255:306–312
46. **Gilmore AP, Wood C, Ohanian V, Jackson P, Patel B, Rees DJ, Hynes RO, Critchley DR** 1993 The cytoskeletal protein talin contains at least two distinct vinculin binding domains. J Cell Biol 122:337–347
47. **Lenarcic B, Turk V** 1999 Thyroglobulin type-1 domains in equistatin inhibit both papain-like cysteine proteinases and cathepsin D. J Biol Chem 272:563–566
48. **Fowlkes JL, Thrailkill KM, George-Nascimento C, Rosenberg CK, Serra DM** 1997 Heparin-binding, highly basic regions within the thyroglobulin type-I repeat of insulin-like growth factor (IGF)-binding proteins (IGFBPs) -3, -5, and -6 inhibit IGFBP-4 degradation. Endocrinology 138:2280–2285